INTERACTIONS BETWEEN CHLOROPHYLLS AND CAROTENOIDS IN LIGHT-HARVESTING COMPLEXES OF PHOTOSYSTEM II AND IN MODEL SYSTEMS

Ph.D. Thesis

Tamás Jávorfi

Dr. Győző Garab

Institute of Plant Biology
Biological Research Center
Hungarian Academy of Sciences
Szeged

Prof. K. Razi Naqvi

Department of Physics
Norwegian University of Science
and Technology
Trondheim

Szeged
2000

TABLE OF CONTENTS

ABBREVIATIONS

* (superscript)	shows singlet excitation on a given molecule
† (superscript)	shows triplet excitation on a given molecule
Car	carotenoid
CD	circular dichroism
C_C	characteristic detergent concentration
C_D	detergent concentration
Chl	chlorophyll
Chl*a*	chlorophyll *a*
Chl*b*	chlorophyll *b*
CMC	critical micelle concentration
DMSO	dimethyl sulfoxide
ET	energy transfer
LHCII	chlorophyll *a*/*b* binding light-harvesting pigment-protein complex associated with photosystem II
Lut	lutein
Neo	neoxanthin
n-OG	*n*-octyl-β, D-glucopyranoside
PSII	photosystem II
RC	reaction center
THF	tetrahydrofuran
TmS	triplet–minus–singlet (spectrum)
TX	Triton X-100
Vio	violaxanthin
Xan	xanthophyll
Zea	zeaxanthin

INTRODUCTION

Photosynthesis

The word 'photosynthesis' comes from Greek and literally means building up or assembly by light. It refers to the capability of plants, algae and certain bacteria to convert and store the solar radiation into the form of energy rich chemical compounds. Apart from using up these compounds for their own needs plants (or the products or fruits of them) can serve as a food (i.e. energy) supply for other kind of living organisms unable to perform the process of photosynthesis. For more than a century, industrial societies have relied solely on the energy source converted from the fossil remains of plants and algae throughout the past millions of years.

During the process of photosynthesis carbon-dioxide is withdrawn from the environment and molecular oxygen is released, as it is summarized in the following formula:

$$CO_2 + H_2O \xrightarrow{h\nu} CH_2O + O_2 .$$

This process has gradually turned the ambience on Earth from reducing to oxidizing, preparing the circumstances capable of sustaining other life-forms.

The whole course of photosynthesis can be divided into two distinct parts: the initial steps (also known as *light-reactions*) require the presence of light, while the rest of the process, involving mainly biochemical reactions, can be performed in the dark as well (*dark-reactions*). The term 'light-reaction' refers to a sequence of steps starting from the absorption of light to the production of ATP and NADPH, which are utilized during the conversion of carbon-dioxide into carbohydrates in the dark-reactions. The process is very complicated and involves several protein complexes, which are located in the thylakoid membranes in a highly organized manner.

The light reactions can be followed in Fig. 1. Upon absorption of a photon a pigment molecule in LHCII, the main light-harvesting antenna complex of photosystem II (PSII) gets into a higher excited state. The excitation from this molecule can migrate through several steps from pigment to pigment until it reaches the reaction center (RC) of

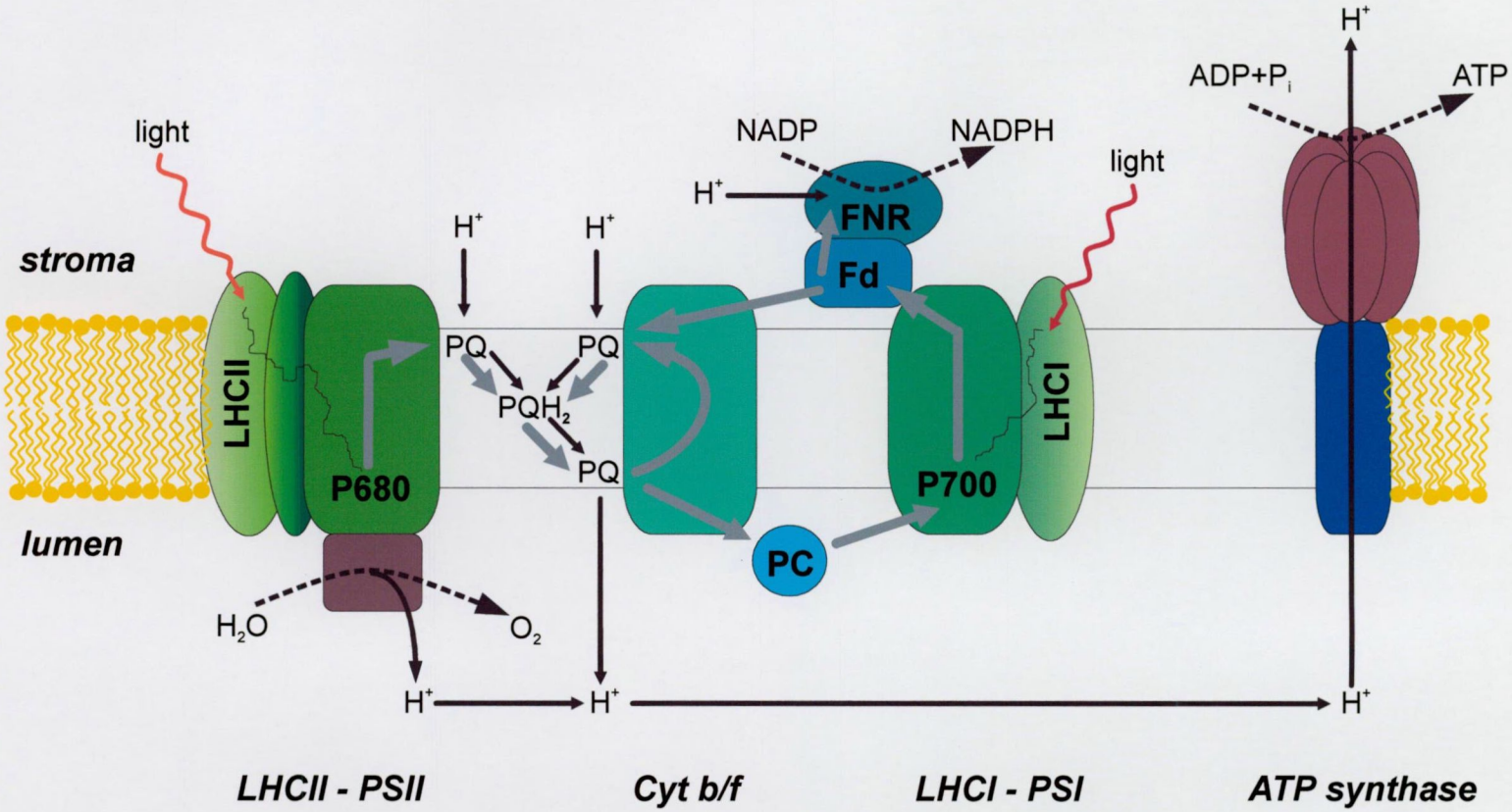

Fig. 1. *Schematic representation of the photosynthetic machinery in the thylakoid membrane of chloroplasts (redrawn after Salisbury & Ross, 1992). Excitation energy, followed by the capturing of light quanta in the antenna complexes (LHCII and LHCI) of the two photosystems (PSII and PSI), migrates (thin black line) to the reaction centers (P680 and P700) where the primary charge separation takes place. The electrons are then transferred along the path represented by the gray arrows, that is accompanied by the translocation of hydrogen ions (black arrows) resulting a proton gradient across the thylakoid membrane. This ΔpH drives the ATP synthase and has an important role in the mechanisms associated with the dissipation of excess excitation energy. (PQ: plastoquinone, PQH_2: plastoquinol, PC: plastocyanin, Cyt b/f cytochrome b/f complex, Fd: ferredoxin, FNR: ferredoxin-NADP reductase.)*

PSII, where it becomes trapped, and initial charge separation takes place. It should be noted here, that direct excitation of the reaction center molecules is also possible, although very rare. The antenna complex of a photosystem serves as a kind of a funnel, providing more frequent excitation of the RC, thus increasing the efficiency of photosynthesis. After the spatial separation of a positive and a negative charges the positive charge, sitting on the primary donor P680, is being neutralized by an electron, originating from the oxygen-evolving complex, where water splitting takes place. The electron is transported, through intersystem electron transport components (PQ, Cyt b/f, PC), to $P700^+$, the oxidized primary donor of photosystem I (PSI) and neutralizes its positive charge. (PSI is served by another light-harvesting antenna complex, LHCI.) The electron via this second charge separation process is transported to the ferredoxin-NADP reductase (FNR), where NADPH is formed from $NADP^+$ and H^+. Coupled to the electron transport from H_2O to $NADP^+$ a trans-membrane proton gradient, ΔpH, is formed, which drives the ATP synthase forming ATP from ADP + P_i. The products of the light-reactions (ATP and NADPH) are utilized in the subsequent biochemical processes, which involve carbon fixation.

The study of the whole process of photosynthesis gives limited information about the structure and function of the individual proteins. Thus each complex has been investigated separately. Since my work was devoted to the major light-harvesting antenna complex of PSII, I will give a more detailed description of this protein only.

Light-harvesting antenna complex

The chlorophyll *a/b* binding light-harvesting pigment-protein complex associated with PSII (LHCII) in the chloroplasts of higher plants is one of the most abundant proteins in the biosphere. The 25-27 kDa protein, which is located at the periphery of the PSII complex, is the product of the *Lhcb* gene family as well as some other minor antenna complexes such as CP26 (Lhcb5), CP29 (Lhcb4) or CP24 (Lhcb3) (Jansson, 1994). To be more specific, the term 'LHCII' usually refers to the mixture of the products of *Lhcb1* and *Lhcb2* genes. *Lhcb1* encodes the major LHCII protein (Lhcb1). In higher plants there are 3 to 16 copies of the *Lhcb1* gene. The Lhcb1 protein consists of 232

amino acids, but there might be some differences both between species and between the products of different genes within the same species. The Lhcb2 protein (product of *Lhcb2*) is very similar to Lhcb1, but it is slightly smaller (approximately 228 amino acids) and 14 distinctive amino acids have been identified. (Jansson & Gustaffson, 1990). The amount of Lhcb2 is about one third of that of Lhcb1, and the *Lhcb2* gene is present in fewer copies (1-4) than *Lhcb1* in the genome. In most cases (this work included) no distinction is made between Lhcb1 and Lhcb2. It is believed that they exist in mixed trimers and all four possible trimer combinations are present *in vivo* (Larsson *et al.*, 1987; Kühlbrandt, 1994).

LHCII shows a 3-fold symmetry in 2D crystals and it is also likely that the trimer is the basic LHCII unit *in vivo* (Kühlbrandt, 1994; Butler & Kühlbrandt, 1988), where they form large ordered aggregates (Garab *et al.*, 1988a; Barzda *et al.*, 1994). The structure of LHCII trimers has been resolved to 3.4 Å by Kühlbrandt and co-workers (1994). Electron crystallography data revealed that the LHCII monomer is composed of three trans-membrane α-helices, two of them are situated in symmetrically tilted position. They also succeeded in pinpointing 12 molecules of chlorophylls (Chl's) and two of luteins (Lut's), the precise identity, though, remained unresolved. The results indicate that Chl's are, more or less, located in two layers, parallel to the plane of the membrane, and oriented with their tetrapyrrol ring perpendicular to the membrane plane. The shortest interpigment distances (between atoms of the Lut polyene chain and Chl*a* tetrapyrrole or between the atoms of Chl tetrapyrrole rings) range from 4 to 5 Å, which allow fast transfer of excitation energy. Because of this proximity and the observed fast (less than 1 ps) singlet energy transfer (ET) from chlorophyll *b* (Chl*b*) to chlorophyll *a* (Chl*a*) (Trinkunas *et al.*, 1997) triplet formation is unique to Chl*a*. Triplet Chl*a*, however, can react with ground state (triplet, $^3\Sigma_g^-$) oxygen; since this results in the formation of potentially dangerous singlet form ($^1\Delta_g$) of oxygen (Fujimori *et al.*, 1957), triplet Chl*a* should be quenched. These considerations led Kühlbrandt and his co-workers to tentatively assign the 7 Chl's closest to the two central Lut's as Chl*a* molecules and the remaining 5 molecules as Chl*b*, as shown in Fig. 2. Although this explanation seems reasonable at first glance there is a constant debate in the literature (e.g. Peterman *et al.*, 1997). Moreover the position of an additional xanthophyll (Xan), neoxanthin (Neo),

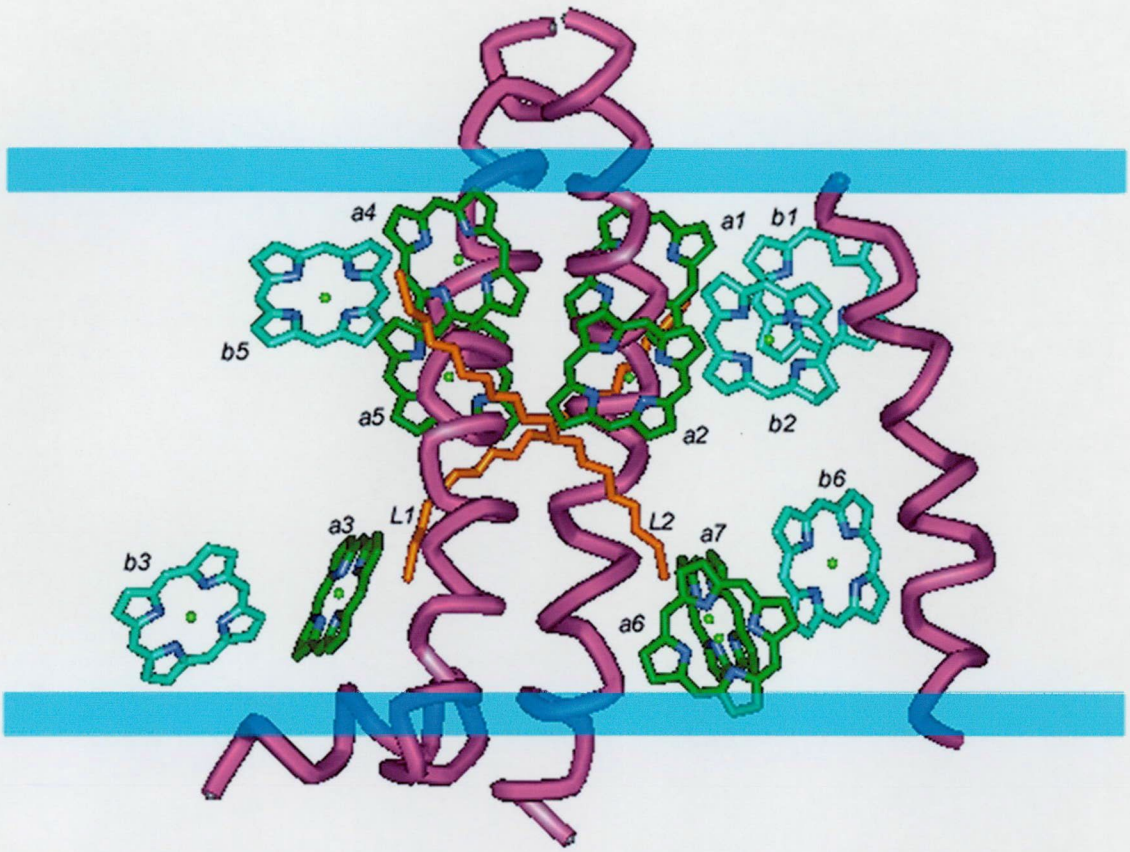

Fig. 2. *3.4 Å resolution model of LHCII, redrawn after Kühlbrandt et al. (1994). The colouring shows the tentative assignment of the molecules: dark green is for* Chl*a, light green for* Chl*b and orange for* Lut*. Purple helices represent the protein frame whereas the blue stripes show the membrane planes. Three* Chl*a molecules, a1-a3, and their symmetric complements, a4-a6, are in van der Waals contact with the luteins (L1 and L2, respectively). The seventh* Chl*a, a7, without a symmetry mate and positioned less close to L2, may in fact be* Chl*b. Each of the five* Chl*b molecules, numbered b1-b3, b5 and b6, is in van der Waals contact with its opposite number in the* Chl*a list, but b6 is also in contact with a7. This leaves a4 as the only* Chl *which is not in contact with another* Chl *and its role is not clear. The chromophore organisation within an* LHCII *monomer may therefore be described as a cluster of one diad and six triads, which may be represented by the symbols L2:a4, L2:a7:b6 and Lm:an:bn (m=1, n=1,2,3; m=2, n=5,6) with the understanding that the two pigments on either side of a colon are in van der Waals contact with each other.*

possibly one or two more Chl's per monomer and a sub-stoichiometric amount of violaxanthin (Vio), whose presence has been inferred on other grounds (Jansson, 1994; Siefermann-Harms, 1985; Bassi *et al.*, 1993), remained undetermined but probably loosely reside at the periphery of the complex. These peripheral Xan's, even if they are already in contact with one or more Chl's within a monomer, might well protrude from this monomer far enough to make contact with a Chl attached to a neighbouring monomer.

Pigments of LHCII

Chlorophylls

Chlorophylls belong to the family of porphyrin-type molecules, which have magnesium as their central atom. They are, more or less, planar molecules characterized by a long conjugated π-electron system along the porphyrin-ring, which results a rather strong absorption in the UV-visible region. Fig. 3 shows the chemical structures and the absorption spectra (in 95% ethanol) of both Chl*a* and Chl*b*.

Despite the tiny difference in their structure the absorption spectrum of Chl*a* and Chl*b*, dissolved in organic solvent, exhibit remarkable differences. Chl*a* has a strong absorption band at the shorter wavelength of the blue region (~ 435 nm, Soret band) and other two bands at the red region (~ 620 nm Q_x and ~ 670 nm Q_y bands), while Chl*b* absorbs at the greenish edge of the blue (~ 465 nm) and at the shorter wavelength of the red region (~ 600 nm and ~ 650 nm). Since they have complementary absorption spectrum, together they can absorb more light from wider range of the spectrum than any one of them alone. Of course, to make use of this, excitation energy should be efficiently transferred to the reaction centers where it can drive photosynthesis. In LHCII singlet ET from Chl*b* to Chl*a* or from Chl*a* to Chl*a* occurs on time scales of less than a ps to tens of ps. This fast ET competes efficiently with other, unimolecular processes. In organic solvents, the fluorescence lifetime of Chl*a* (Chl*b*) is in the order of 5 ns (6 ns). The fluorescence quantum yield, in organic solvents is 20-30% (6-10%), whereas the triplet yield is ~64% (~88%) (Kleima, 1999).

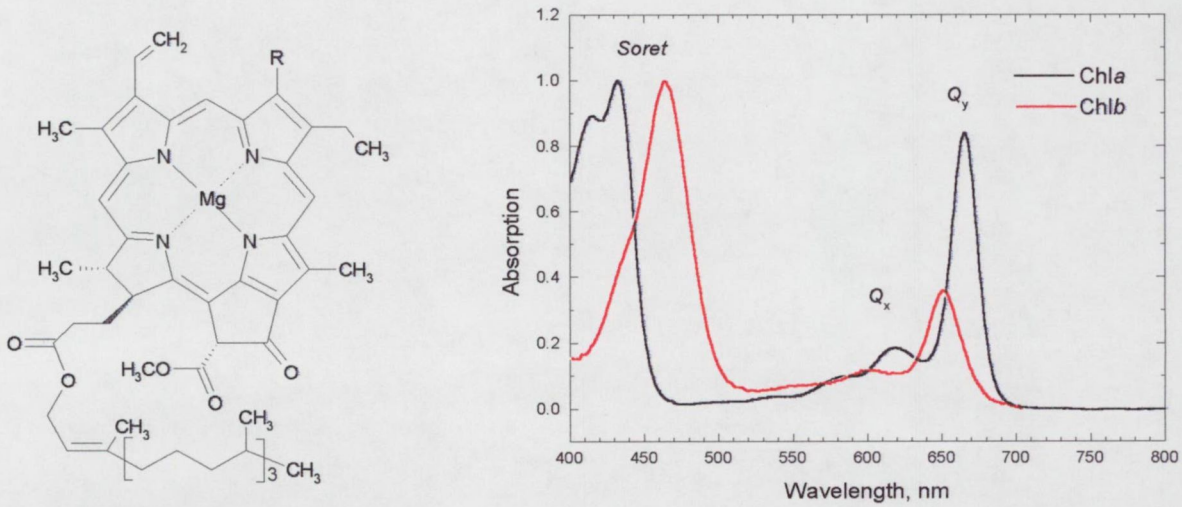

Fig. 3. *Chemical structure of* Chl*a (where R=CH₃) and* Chl*b (where R=CHO) and the corresponding absorption spectra, when dissolved in 95% ethanol. The absorption bands are also labelled.*

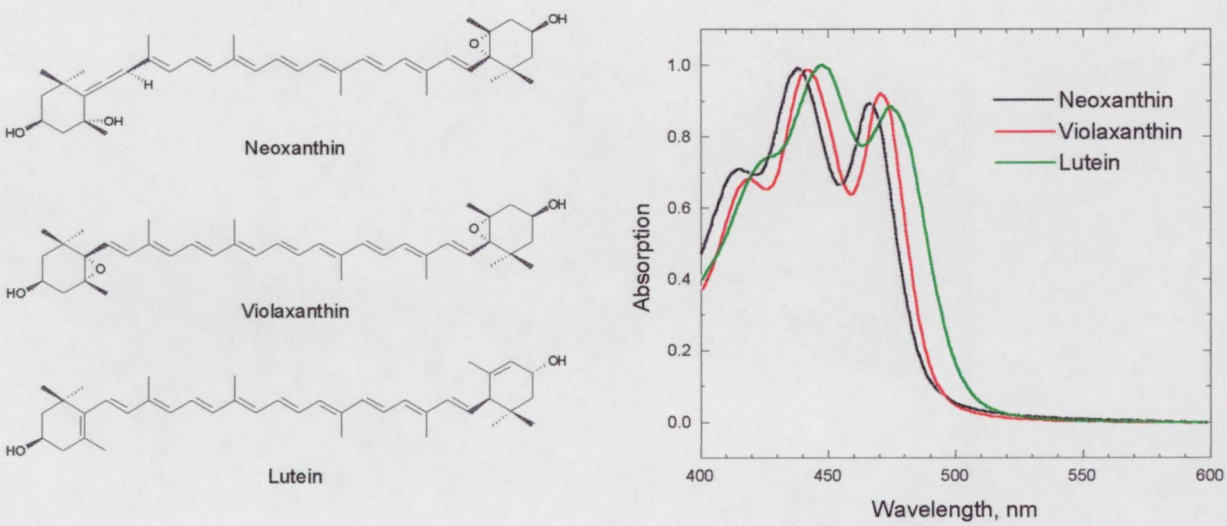

Fig. 4. *Chemical structure of the three LHCII xanthophylls (neoxanthin, violaxanthin and lutein) and the corresponding absorption spectra, when dissolved in acetone.*

Xanthophylls

Xan's are one class of the carotenoid (Car) family possessing oxygen-containing functional group(s). All Car's are characterized by a linear polyene chain, with approximately C_{2h} symmetry. The spectral characteristics of Car's, especially those Xan's associated with the antenna complexes, have been studied rather extensively *in vitro* (Frank *et al.*, 1994).

The absorption properties are determined by the length of the conjugated π-electron system along the polyene chain. It is generally true, however, that their yellowish colour is due to the strongly allowed electronic transition from the ground state ($1\ ^1A_g$) to S_2, the second excited singlet state ($1\ ^1B_u$), while the transition from the ground state to S_1, the lowest electronic singlet state ($2\ ^1A_g$) is dipole-forbidden and does not manifest itself in the spectrum. Since LHCII Xan's absorb in the region where Chl's have very low extinction, they can serve as accessory antenna pigments broadening the range of photosynthetically active radiation. The chemical structure and the absorption spectra of LHCII Xan's are displayed in Fig. 4.

Besides their role as light-harvesting pigments Car's are also efficient quenchers of singlet oxygen and Chl*a* triplets (Krinsky, 1979). Once a triplet Car is formed it is able to dissipate its excitation energy, rapidly and non-radiatively, through vibronic coupling predominantly to the C–C symmetric strech vibrations (Frank *et al.*, 1993). Car's were also credited with another function, namely the quenching of singlet excited state of Chl*a* although the underlying physical mechanism is not fully understood (e.g. Demmig *et al.*, 1987; Horton & Ruban, 1992). This process is very important in the dissipation of excess excitation energy under strong illumination and will be discussed later.

Xan's have a significant role in stabilizing the structure of the complexes, as it was shown from studies on reconstituted LHCII lacking the central Lut's (Paulsen *et al.*, 1990; Plumley & Schmidt, 1987).

The state of aggregation

The size of the aggregates of LHCII can be conveniently varied by adding non-ionic detergent to the sample, such as Triton X-100 (TX), *n*-octyl *β*-D-glucopyranoside (n-OG), *n*-dodecyl *β*-D-maltoside (DM) or digitonin (Ide *et al.*, 1987; Bassi *et al.*, 1991).

The effect of detergent on the state of aggregation of LHCII can be easily followed through the circular dichroism (CD) spectrum of the sample. The CD signal of a sample originates from different levels of molecular organizations. (For a review see e.g. Garab, 1996.) Intrinsic CD originates from the preferential absorption of the left and right circularly polarized light of an asymmetrical molecule. This signal is very weak and usually buried in the excitonic CD, which is induced when two or more molecules become juxtaposed. Large anomalous CD signals have been detected in various systems (e.g. in granal thylakoids by Garab *et al.*, 1988a and in isolated LHCII by Barzda *et al.*, 1994), with dimensions comparable to the wavelength of the measuring light (Keller & Bustamante, 1986), which is produced by the long-range chiral order of the chromophores. Since it was first observed in connection with DNA strands, such kind of CD signal has been referred to as polymerization and salt induced (psi) type CD. The admixture of detergent to LHCII aggregates results in the gradual loss of the psi-type CD bands (Barzda *et al.*, 1995).

A similar dependence of the fluorescence yield on the state of aggregation can also be observed, but in the opposite direction: the fluorescence yield increases significantly as one goes from large aggregates to trimers (Gregory & Raps, 1974; Ruban & Horton, 1992; Jennings *et al.*, 1994). The enhancement in the fluorescence yield of LHCII does not cease when the aggregates are dissociated into trimers but continues to increase upon further addition of detergent. It should be noted, however, that the average lifetime remains, even at the highest concentration (5% n-OG) used by Bassi *et al.* (1991), shorter than the lifetime of Chl*a* in organic solvents.

Comparative analysis of the CD and fluorescence yield of LHCII upon addition of detergent revealed that the transition from intact trimers into the state when the chromophoric organization of the complex becomes perturbed appears at a characteristic detergent concentration (C_C). In earlier publications (e.g. Barzda *et al.*, 1995; Barzda *et*

al., 1998; Naqvi *et al.*, 1997a) C_C was identified as the critical micelle concentration (CMC) but, as we will see later in the Results chapter, it is not always correct.

Thylakoid lipids also play a significant role in trimer formation. Eliminating a phospholipid (phosphatidyl-glycerol or PG for short) from the complex causes complete and irreversible dissociation of the trimer, while DGDG (digalactosyl-diacyl-glycerol) is essential for the formation of three-dimensional crystals and of large two-dimensional crystals but has no effect on the oligomerization of the complex (Nussberger *et al.*, 1993). MGDG (monogalactosyl-diacyl-glycerol), the major lipid component of the thylakoid membrane, which is a non-bilayer lipid, induces the formation of stacked lamellar aggregates of LHCII with long-range chiral order (Simidjiev *et al.*, 2000).

Fate of an excitation in LHCII

The process of photosynthesis starts with the absorption of a light quantum by one of the pigment molecules in the antenna system. Red and blue light is absorbed by the Chl's, while blue-green is absorbed by the Xan's, all the other colours are being reflected giving the usual green colour to the leaves.

The structure of LHCII ensures the optimal orientation and distances of the pigments for ultrafast ET. In such a protein frame a photoexcited Xan or Chl*b* molecule transfers its singlet excitation energy to Chl*a* with an efficiency close to 100% (Siefermann-Harms & Ninnemann, 1982), all the other, unimolecular processes (fluorescence, internal conversion or intersystem crossing) being too slow to compete. As for Chl*a*, it can transfer its excitation energy to another Chl*a* — eventually to the RC — or undergo any of the unimolecular decay processes, especially when the RC is occupied. Triplet Chl*a* molecules, however, can produce the sensitized form of singlet oxygen (Fujimori & Livingston, 1957), which cause damage to the photosynthetic apparatus. Xan's, on the other hand, can provide a two-fold protection against this degradation by quenching singlet oxygen or by taking over the triplet excitation directly from Chl*a* (Krinsky, 1979). Xan triplets then harmlessly and non-radiatively decay into the ground state (Frank *et al.*, 1993).

It was suggested that in LHCII, excitation energy from the lowest excited state of Chl*a* could be transferred to the S_1 level of a zeaxanthin (Owens *et al.*, 1992), although no such transfer has been observed so far. The possible pathways for the relaxation of excitation energy are depicted in Fig 5.

Later in the thesis a * or a † in the superscript of the symbol of a chromophore will denote a singlet or triplet excitation on the given molecule, respectively.

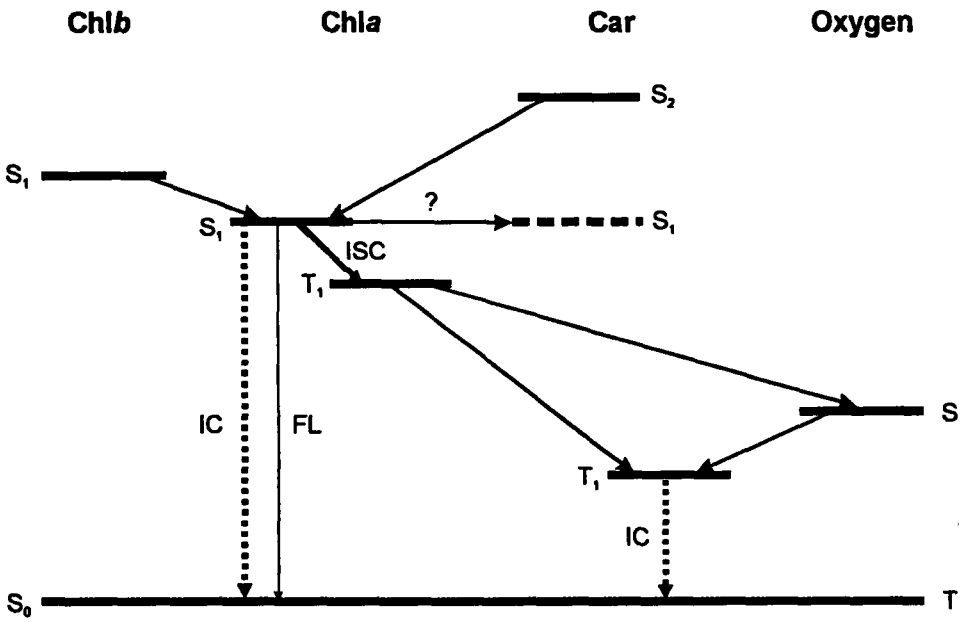

Fig. 5. *Schematic representation of the pathways of excitation energy relaxation. Unlabelled arrows represent energy transfer between chromophores. From the accessory pigments excitation energy is transferred with 100% efficiency to* Chl*a, thus fluorescence or triplet formation is unique to* Chl*a. Though energetically proved to be possible no back transfer from* Chl*a to* Car *(labelled with a question mark) has been observed so far. (IC stands for internal conversion, ISC for intersystem crossing and FL for fluorescence.)*

Regulation of the light-harvesting efficiency

LHCII has evolved to maximize the rate of delivery of excitation energy towards the reaction center by optimizing the orientation of its chromophores for efficient energy transfer and assuring a large cross-section for absorption. As a result of this, the photosynthetic electron transport chain can be saturated even at relatively low light

intensities. When plants are exposed to light intensities in excess of those that can be utilized for driving the electron transport, a non-photochemical energy-dissipating mechanism is induced in order to protect the photosynthetic apparatus (cf. Horton & Ruban, 1992). This process is called non-photochemical quenching (and abbreviated as q_N or NPQ) since it lowers the fluorescence yield of Chl*a* which is conveniently used for its determination. On the basis of the dark relaxation kinetics of Chl*a* fluorescence, q_N can be decomposed into a number of components (Walters & Horton, 1991.). One is relaxing with a halftime of 1-2 min and normally accounts for most of q_N. It has been associated with ΔpH and is called energy-dependent quenching (q_E). The second is relaxing over a time-scale of tens of minutes and labelled as q_I, referring to photoinhibition. The interpretation of this component can be difficult because it becomes increasingly important under strong light stress, when part of the quenching is due to the photodamaged RC. Sometimes a third component (q_T) is also distinguishable, which is associated with a state-transition (phosphorylation). Non-photochemical quenching has been a subject of extensive research in many aspects, but the underlying molecular mechanisms are still not fully understood (for a review see e.g Horton *et al.*, 1996). In thylakoids, excess light also induces reversible or irreversible changes in the macroorganization of complexes (Garab *et al.*, 1988b; Gussakovsky *et al.*, 1997). Similar rearrangements have been observed in lamellar aggregates of LHCII. These structural changes in thylakoids and also in LHCII have been shown to be associated with quenching of Chl*a* fluorescence (Jennings *et al.*, 1991; Barzda *et al.*, 1996, 1999; Gussakovsky *et al.*, 1997).

It was suggested that the xanthophyll cycle Car's play a major role in the regulation of light-harvesting (Demmig-Adams, 1990). As recapitulated in Fig. 6, exposure of the photosynthetic system to light intensities exceeding those that can be utilized for photosynthesis induces the enzymatic de-epoxidation of violaxanthin (Vio) to antheraxanthin and zeaxanthin (Zea); a reversible process which has been termed as xanthophyll-cycle (Yamamoto, 1979). As the length of the conjugated double-bond system increases from 9 (in Vio) to 11 (in Zea) the S_2 energy levels are shifted to the longer wavelengths. Little is known, however, about the S_1 level of these Xan's, whether it is higher or lower than that of Chl*a* (14 700 cm^{-1}, ~ 680 nm).

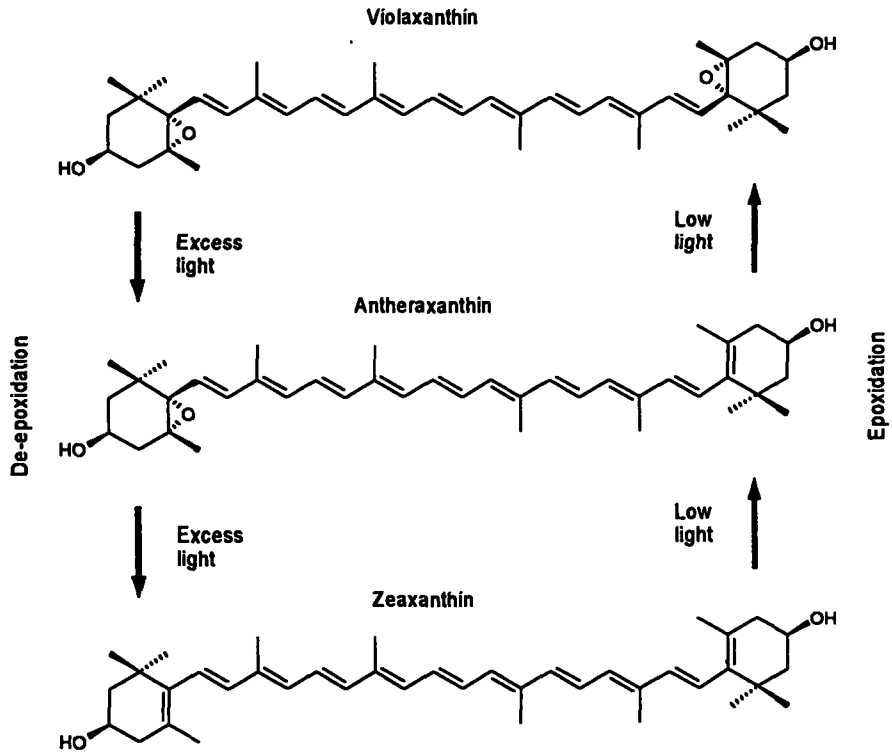

***Fig. 6.** Schematic representation of the xanthophyll-cycle. Under excess light-conditions the stepwise removal (de-epoxidation) of two oxygen functions (the epoxy groups) in violaxanthin results in a lengthening of the conjugated system of double-bounds from 9 to 11. De-epoxidation occurs within minutes, while the reverse process (epoxidation) may take minutes to hours. (Redrawn after Demmig-Adams & Adams, 1996.)*

Based on model calculations on polyenes, Owens and his co-workers suggested (1992) that the S_1 energy level of Vio can be as low as 16 600 cm^{-1} (~ 600 nm), while that of Zea is about 14 500 cm^{-1} (~ 690 nm). As a consequence of this, they proposed that Vio can act as an accessory light-harvesting pigment, transferring its singlet excitation to a neighbouring Chl, while the back transfer is limited by the poor spectral overlap and rapid ET among antenna Chl*a* molecules. Zea, on the other hand, has slightly lower S_1 energy level than that of Chl*a* opening a potential pathway for energy flow from Chl*a* to Zea. Since radiative and non-radiative transitions to the ground state are 2-3 orders of magnitude more rapid in Car's than in Chl*a*, permitting reverse ET from Chl*a* to Zea would result in the introduction of weak quenching centers in the antenna. This theory

would also explain the correlation found between the accumulation of Zea and the magnitude of fluorescence quenching (Demmig *et al.*, 1987). Further results supporting this 'molecular gear-shift' mechanism was published in 1994, when the application of femtosecond time-resolved transient absorption spectroscopy and the energy-gap law (Englman & Jortner, 1970) gave a more precise approximation of the S_1 level of Vio and Zea, placing them to 15 200 cm^{-1} (~ 660 nm) and 14 200 cm^{-1} (~ 705 nm), respectively (Frank *et al.*, 1994). However, the application of the energy gap law was failed to gain general acceptance (Naqvi K. R., personal communication).

In the meantime an alternative mechanism for excitation energy dissipation was proposed, which was based on structural alterations in the light-harvesting antenna system, brought about by the interconversion of Vio into Zea and/or by protonation upon excess illumination (indirect quenching) (Horton *et al.*, 1991; Horton *et al.*, 1996). According to this model, in the unquenched state, Vio prevents close Chl-Chl interaction (antiquenching), but in the presence of high ΔpH between the stroma and the lumen side of the thylakoid membrane (due to photosynthetic activity), antiquenching is overcome under the influence of protonation to give Chl-Chl quenching. Alternatively, if Vio is de-epoxidized to Zea and a moderate ΔpH is present, Chl-Zea complex is formed and quenching will occur by its ability to accept energy from Chl. This model would explain why Vio inhibits q_N while Zea enhances it (Phillip *et al.*, 1996), and the fact that high level of quenching can be observed in thylakoids lacking Zea (Noctor *et al.*, 1991). It is worth pointing out that, according to this hypothesis, (indirect) quenching would occur even if the S_1 energy level of the Xan was not favorable for back ET, although the underlying physical mechanism is still not understood.

Recently, another report was published, where the authors were able to measure the $S_2 \leftarrow S_1$ transition of Vio and Zea, by the aid of femtosecond spectroscopy, and found the S_1 level of Vio and Zea at 14 470 cm^{-1} (691 nm) and 14 030 cm^{-1} (713 nm), respectively (Polivka *et al.*, 1999). Since both of these S_1 levels below that of Chl*a*, this result support further the indirect effect of the xanthophyll cycle on non-photochemical quenching.

No consensus has been reached on the identification and whereabouts of the quencher itself. Li *et al.* (2000) identified a protein (PsbS), which seems to be directly responsible for the dissipation of excess excitation energy (see also Demmig-Adams, & Adams, 2000). The authors suggest that this protein, which has a very similar structure to LHCII, is not involved in the process of light-harvesting, but instead, it is specialized in energy dissipation. They also propose that this protein could be located somewhere in the antenna, or between the antenna and the PSII core complex. The physical mechanism of the quenching, though, remains to be elucidated.

Absorption spectra of LHCII

Macroscopic absorption is usually described according to the Beer-Lambert law. This law is valid for homogeneous suspensions when the size of the chromophores is negligible with respect to the wavelength of measuring light. However, deviations from Beer-Lambert law appear when the chromophores are assembled into aggregates. The two main reasons that can be accounted for these deviations are: (*i*) the increase in light scattering (which yields to an increase in the measured absorption) and (*ii*) decrease in the measured absorbance due to the shadowing effect of the particles, also called absorption flattening or sieving.

The problem was first studied by Duysens (1956) and later by Latimer and his co-workers (1959, 1962). It amounts to relating A_C — the true absorption of a suspension of randomly distributed, identical clusters of absorbing subunits — to A_D, the absorption that would be recorded if each cluster could be disrupted without affecting the absorption cross section of its constituents.

Closely related to clustering is also the phenomenon of selective light scattering, which, even if it is negligible in a sample containing isolated subunits, becomes significant when the size of the entire cluster approaches the wavelength of the monitoring light. A widely used method for reducing scattering effects is putting an opal-glass plate in front of the detector which collects the light scattered in forward direction. Nonetheless, light scattered at angles exceeding 90° cannot be brought back to the detector by the opal-glass. The ideal solution would be the collection of all the scattered

light (e.g. by an integrating sphere) and feeding it back to the detector, which is unfortunately rarely a realistic option[1]. If, however, the system under investigation fulfills some basic assumptions a numerical method can be applied to obtain scattering-free spectrum.

In the Materials and Methods chapter, I will describe a method, adopted from Latimer and Eubanks (1962), to correct the measured absorption spectrum of the aggregates for selective scattering and from Duysens (1956) for the mutual shadowing of trimers within a single aggregate.

Triplet states in LHCII

As one can see from the previous paragraphs interactions between Car's and neighbouring Chl molecules play a very important role in the photosynthetic functions. In my thesis I studied different systems, natural as well as man-made, where a Car is in close proximity of a Chl or a Chl-like tetrapyrrole pigment. The ordinary singlet-singlet ($S_n \leftarrow S_0$) absorption spectrum of such a system gives little indication of the interactions between the Car and its partner molecule, but other photophysical data — derived, for example, from fluorescence excitation or nanosecond laser photolysis studies — have shown that the two pigments do interact with each other.

Absorption-detected magnetic resonance (ADMR) experiments on aggregated LHCII revealed that the entire triplet-minus-singlet (TmS) spectrum is dominated by a broad band of Car triplets ($Car^{\dagger}$) with maxima at 505 and 523 nm (van der Vos *et al.*, 1991). However, there is also a noticeable bleaching signal, around 676 nm, decaying at the same rate as the $Car^{\dagger}$ (with a lifetime of 9 μs). Since Car's do not absorb in the red region van der Vos and his co-workers attributed the negative signal to the perturbation of the Q_y absorption band of a Chl*a* molecule by a proximate $Car^{\dagger}$. They also measured, with the same technique, the triplet–triplet ($T_n \leftarrow T_1$) absorption spectrum of $Lut^{\dagger}$ which gives rise to two peaks (at 507 nm and 525 nm), while they found only a single peak (at

[1] Investigations on the absorption spectra of diluted samples in a spherical cuvette with reflective coating, however, revealed new spectral distortions due to multiple reflections (Naqvi, K. R., Jávorfi, T. & Garab, G. unpublished results). Similar distortions have recently been observed using the integrating sphere (Merzlyak & Naqvi, in press).

525 nm) in the corresponding spectrum of $Neo^{\dagger}$ and $Vio^{\dagger}$ (van der Vos *et al.*, 1994). They also noticed that the relative contribution of the 525 nm signal rose with increasing the concentration of LHCII in the sample, and attributed the enhancement to preferential population of $Neo^{\dagger}/Vio^{\dagger}$, facilitated by trimer-to-trimer transport of electronic excitation energy within the aggregates. On the basis of these observations they concluded that all three Xan species contribute to the TmS spectrum of aggregated LHCII and associated the 505 nm peak to $Lut^{\dagger}$ (with a shoulder at 523 nm) and the 523 nm peak to $Neo^{\dagger}$ and $Vio^{\dagger}$.

Xan triplets in LHCII monomers and trimers have also been extensively studied with the aid of flash-induced transient absorption technique at room temperature (Nechustai *et al.*, 1988) and with laser kinetic spectrophotometry at room temperature as well as low temperatures (Peterman *et al.*, 1995). They confirmed that the lifetime of $Xan^{\dagger}$, at room temperature and under anaerobic conditions, is 9 μs and independent of the wavelength of observation (506 and 528 nm). They also found that the efficiency of triplet ET from Chl*a* to Xan is near unity at room temperature but drops down to 0.92 ± 0.02 at 77 K and to 0.82 ± 0.07 at 4 K. Peterman and his co-workers (1995) concluded that at least three Xan's contribute to the TmS spectrum of trimeric LHCII (from which it follows that at least one non-Lut Xan is in close proximity to at least one Chla). In a later publication they assigned the Xan triplet absorption band in the TmS spectrum of trimeric LHCII to Lut, at 506 nm, and to Vio, at 525 nm (Peterman *et al.*, 1997). They also reconstituted the singlet-singlet absorption spectrum and place the corresponding singlet peaks at 494 and 510 nm and at 486 nm for Neo. They found, however, that this latter Xan shows hardly any singlet transfer to Chl, nor does it accept a significant amount of triplets from Chl.

Bleaching signals in the Q_y region of Chl*a* have also been observed in the TmS spectra of thylakoids and the Chl *a/c* containing LHCII of the yellow-green alga *Pleurochloris meiringensis* (Büchel *et al.*, 1998), and analogous interactions have been reported in some bacterial systems (Angerhofer *et al.*, 1995) and in peridinin-Chl*a*-protein (PCP) complexes isolated from two dinoflagellates (Carbonera *et al.*, 1996). It seemed reasonable to assume then, that a negative signal in the Q_y region of Chl*a* is present in the TmS spectrum of all photosynthetic samples, where Car's are in close

contact with Chl molecules. However, Wolff and Witt (1969), who were the first to report the TmS spectrum of chloroplasts in the late sixties, emphasized the absence of such a signal. It would imply that the TmS signal in chloroplasts originates from a group of Car's whose photophysical properties are significantly different from the Car's which give rise to the TmS spectrum of LHCII.

AIMS AND OUTLINE OF THE THESIS

The present study was undertaken to investigate the disparate photophysical behaviour of LHCII at different levels of molecular organization, in suspensions of (*i*) isolated aggregates, (*ii*) intact trimers, and (*iii*) perturbed trimers, as well as (*iv*) in native thylakoid membranes. Aggregation of LHCII is known to be accompanied by a quenching of excitation energy although the underlying molecular mechanism is still not understood. It seems plausible that as monomers assemble into trimers, and these go on to form oligomers, additional interactions, intra-trimer as well as extra-trimer, come into play. Our main goal was to find a connection between the extent of quenching and the changing interactions between the chromophores in LHCII and to find clues for the physical mechanism of quenching. The importance of our investigations derives from the fact that, *in vivo*, LHCII occurs in the form of oligomers, and the process of non-photochemical quenching plays an important role in protecting plants against excess illumination.

Since one of the most prominent features of aggregation is a noticeable change in the absorption spectrum compared to that of the trimers, we started our investigations with a thorough analysis of the absorption spectra of aggregates and trimers of LHCII. In order to counteract with the severe spectral distortions, due to the effects of selective scattering and the non-random distribution of trimers in the aggregates, we applied numerical correction methods to obtain the true absorption spectrum of the aggregates.

Carrying out nanosecond laser photolysis experiments on aggregated and trimeric forms of LHCII, as well as on detergent perturbed complexes, we found that the triplet formation yield of Chl*a* decreases in parallel to its fluorescence yield. Similar results were observed earlier in artificial caroteno-porphyrin dyads, which was explained by suggesting that Car's are able to enhance the internal conversion rate of a nearby Chl-like molecule. Based on this similarity, we hypothesize that the same process, which has been termed as 'catalysed internal conversion' (CIC), also operates in natural antenna complexes. The influence of a Car on a nearby Chl*a* molecule can be detected as a bleaching signal in the Q_y region of Chl*a*, which is associated with the triplet state of its

Car neighbour. We demonstrate that, in LHCII, as pigments are torn apart from each other and the influence of a nearby Car weakens, Chl*a* suffers less quenching.

We also recorded the triplet absorption spectra of a few Car's in various organic solvents in order to find a clue for the locations of their singlet and triplet absorption peaks in LHCII. It also helped us to rationalize the differences in the triplet-minus-singlet (TmS) spectrum of trimers and aggregates.

As a possible explanation for the dissipation of excitation energy of Chl*a*, reverse energy transfer from Chl*a* to Xan — which has been proposed though not yet observed — cannot be ruled out on the basis of the energy levels of the chromophores. Similarly, in the first generation caroteno-porphyrin dyads the S_1 energy level of the Car moiety was lower than that of its (Chl-like) partner molecule, thus allowing a direct quenching via the transfer of excitation energy from the partner molecule back to the Car. In order to show the generality of catalysed internal conversion, we investigated the photophysical properties of two caroteno-pyropheophorbide dyads, where the energy levels were unfavourable for draining away excitation from the pyropheophorbide molecule by the Car moiety. A Car-induced decrease in the fluorescence of its partner molecule must entail a process other than energy transfer.

The bleaching signal in the Q_y region of Chl*a* (or a Chl-like) molecule has been observed in a wide range of natural as well as man-made systems, where Car's are in close proximity to their partner molecule. The absence of a bleaching signal in the TmS spectrum of chloroplasts, as it was reported earlier, would imply that a prerequisite of catalysed internal conversion does not hold in green plants. This peculiarity urged us to reinvestigate this vexed issue.

The rest of the thesis is structured along the following lines: after assembling the theoretical wherewithal and describing the experimental details I will present our results in the order as it was invoked in the previous paragraphs. The interpretation of our data and a discussion follows each section.

MATERIALS AND METHODS

In this chapter I will describe the isolation procedures of different plant materials used in this study. A detailed description of applied spectroscopic techniques as well as the experimental conditions and the theoretical background of the numerical methods for the correction of the absorption spectrum will also be summarized.

Isolation of chloroplasts and thylakoid membranes

Chloroplasts were isolated from fresh spinach obtained from the local market. The isolation procedure was described by Garab *et al.* (1988a), which was based on the method used by Slovacek & Hind (1977). Leaves were homogenized in a buffer containing 0.35 M sorbitol, 20 mM Tricine/NaOH, pH 7.6 and 0.2 mM $MgCl_2$. The suspension was filtered through 4 layers of cheesecloth and centrifuged 20-30 sec at 2000 g. The supernatant was centrifuged for 4 min at 4000 g. The pellet was resuspended in a medium containing 1 mM Tricine/NaOH, pH 7.6 and 0.35 M sorbitol and centrifuged again at 4000 g for 4 min. Finally the pellet was resuspended in 20 mM Tricine/NaOH, pH 7.6 supplemented with 0.35 M sorbitol, 5 mM $MgCl_2$ and 10 mM KCl, and was stored at 4°C.

For thylakoid isolation the chloroplast pellet was resuspended in hypotonic buffer, containing 10 mM Tricine/NaOH, pH 7.6, 2 mM Na-EDTA and centrifuged at 27000 g for 5 min. The thylakoid pellet was resuspended and stored in the same buffer as the chloroplasts.

Isolation of LHCII

In our lab LHCII was isolated according to a method described by Simidjiev *et al.* (1997). This isolation procedure is, in turn, an improved version of the method developed by Krupa *et al.* (1987). Leaves of two week old pea (*Pisum sativum*, L.) grown in the greenhouse or fresh spinach from a local market were used for isolation of LHCII. During the entire procedure the sample was kept on ice, except for the solubilization of

thylakoid membranes, which was carried out at room temperature. The isolation was performed in normal light conditions. The basic procedure consists of the following steps.

Leaves were homogenized in a cold buffer containing 50 mM Tricine/NaOH, pH 7.8, 0.4 mM sorbitol and the brei was filtered through 4 layers of cheesechloth. The suspension was spun down at 5000 g for 5 min. The pellet was resuspended in a cold buffer containing 15 mM Tricine/NaOH, pH 7.8, 5 mM EDTA and 50 mM sorbitol. The suspension was homogenized in a Potter homogenizer and centrifuged at 10000 g for 10 min. The pellet of thylakoid membranes was resuspended in a cold 15 mM Tricine/NaOH, pH 7.8 buffer, and homogenized again, as above. The density of the suspension was adjusted to an absorbance of 0.8 at 680 nm in a cuvette with an optical pathlength of 0.2 mm; the baseline was set to zero at 720 nm and the sample was placed close to the opal glass–detector combination in order to reduce scattering effects. Triton X-100 from a 10% (v/v) stock solution buffered with 15 mM Tricine/NaOH, pH 7.8, was added to obtain a detergent concentration between 0.5 and 1.2% (v/v). The suspension was stirred at room temperature for 30 min followed by a centrifugation at 30000 g for 40 min. The pellets containing unsolubilized material and starch were discarded. LHCII was aggregated by adding 1 M $MgCl_2$ and 2 M KCl stock solutions to the supernatant to obtain final concentrations of 20 mM and 100 mM, respectively. The suspension was stirred gently for about 10 min and layered on a 0.5 M sucrose cushion equilibrated with 15 mM Tricine/NaOH, pH 7.8, and centrifuged at 10000 g for 10 min. (The volume of the sucrose layer should exceed three times of that of the LHCII suspension.) The pellet was resuspended in a buffer containing 50 mM Tricine/NaOH, pH 7.8, and 100 mM sorbitol. The absorbance of the LHCII suspension at 680 nm was adjusted to 0.8 in a cuvette with an optical pathlength of 0.2, as before. The LHCII macroaggregates were disaggregated by adding Triton X-100, as above, to obtain a final concentration of 0.7% (v/v). After stirring for 5 min, LHCII was aggregated by adding 1 M $MgCl_2$ and 2 M KCl stock solutions to achieve final concentrations of 20 and 100 mM, respectively. The suspension was stirred for about 10 min and then fractionated on a 0.5 M sucrose cushion, as earlier. The pellet containing LHCII macroaggregates was washed 3-4 times in 15 mM Tricine/NaOH, pH 7.8, and centrifuged for 5 min at 5000 g. The preparation was finally suspended in the same buffer. The sample could be stored in the dark at 4°C

for about 2 weeks without degradation. Freezing and thawing, however, leads to a complete destruction of its macrostructure.

This basic procedure, depending on the concentration of detergent used for the solubilization of thylakoid membranes, yields four different types of LHCII. These products differ from each other in their macrostructure, lipid content and composition, content of minor antenna complexes as well as in their spectroscopic features. (A detailed analysis can be found in Simidjiev, 1998.) In our investigations we used samples of loosely stacked lamellar aggregates (type II) or large three-dimensional aggregates with long-range chiral order (type IV).

The pigment composition of the LHCII preparations used in this study was determined by applying the spectrum-reconstruction method as it was described by Naqvi *et al.* (1997b). We found that each LHCII monomer in our samples contains 7 molecules of Chl*a*, 6 of Chl*b*, 2 of Lut, 1 Neo and a sub-stoichiometric amount (1/4–1/3) of Vio.

Caroteno–pyropheophorbide

In order to study the basic energy transfer processes between chromophores, we performed experiments on two caroteno–pyropheophorbide dyads which served as model systems of the light-harvesting antenna complexes and were synthesized and kindly provided to us by the group of Prof. A. Osuka (Kyoto University). **F-Φ** and **P-Φ**, the two caroteno–pyropheophorbide dyads (where **Φ** stands for methyl pheophorbide-*a* and the Car moiety being fucoxanthin in **F-Φ** and peridinin in **P-Φ**) were synthesized recently by transesterification at the 13^2 methoxycarbonyl group of methyl pheophorbide-*a* (Osuka & Kume, 1998). The chemical structure of the compounds can be seen in Fig. 7.

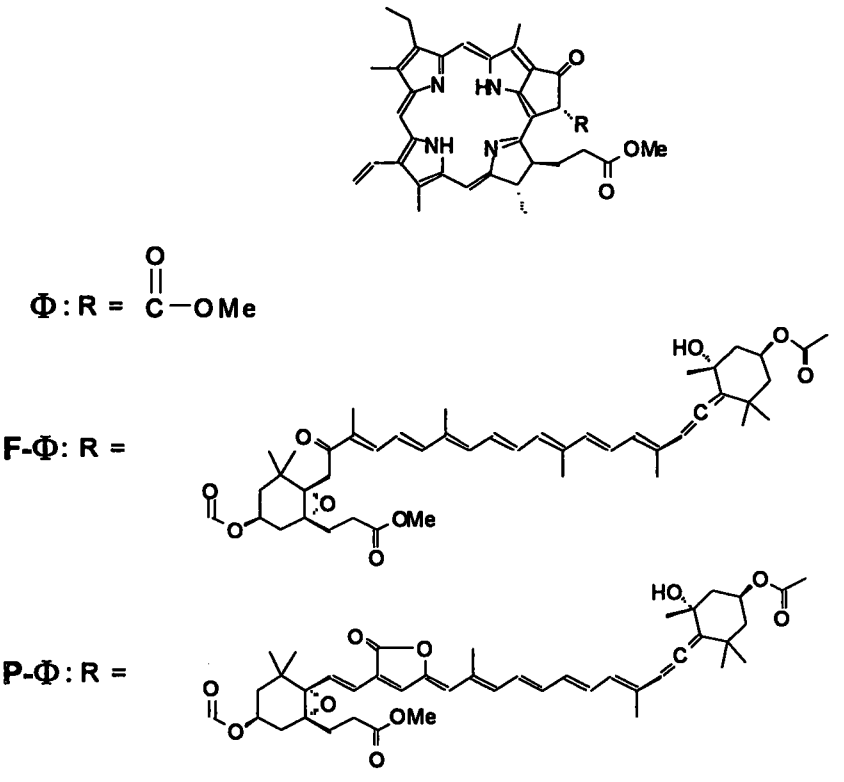

***Fig. 7. The chemical structures of methyl-pheophorbide a and the two dyads. The carotenoid component of the dyad is fucoxanthin in* F-Φ *and peridinin in* P-Φ.**

Carotenoid isolation

Lycopene and β-carotene were obtained from tomato (*Lycopersicon esculentum Mill.*) fruits. Aggregated LHCII from spinach or petals of daffodil (*Narcissus* L.) served as the source of lutein, neoxanthin, and violaxanthin.

The pigments were extracted from plant tissues with ethanol, and the extract saponified with potassium hydroxide at 65° C for 10 min in the presence of pyrogallol as an antioxidant (Merzlyak *et al.*, 1983). After that ca. 20% of water was added to the extracts and unsaponified lipids were extracted several times with n-hexane. The solvent was evaporated by a stream of nitrogen and the dry residue containing the carotenoid was redissolved in a small volume of chloroform before separation by thin-layer chromatography (TLC).

TLC was performed on precoated 20×20 cm^2 silica gel plates (Merk) using n-hexane-acetone-benzene (in 1:1:1 volume ratio) for separation of xanthophylls (Tosic & Moore, 1945) and n-hexane-chloroform (2:1 volume ratio) for purification of lycopene. The parameters of the carotenoid absorption spectra recorded in different solvents were close to those reported in the literature (Britton, 1995).

In some experiments, commercial samples (supplied by Fluka) of β-carotene, lutein (from alfalfa) and lycopene (Sigma, from tomato) were used. Chl*a* was purchased from Fluka. All the solvents used were at least 99% pure.

Absorption spectroscopy

Two different spectrophotometers were used in this study for recording absorption spectra. One was a commercial double-beam instrument (Shimadzu 160A), which was connected to a PC for data processing. The other instrument was a single-beam fiber-optic spectrometer with an optical multichannel analyzer where at the detection side we used two different disperser-sensor systems. In one case it was a Zeiss M CS 224 instrument with an identical pair of a concave holographic grating and a 512-element diode array (one of which covered the spectral range 200-610 nm, the other 600-1010 nm). In the other case the disperser was a triple-grating monochromator (Acton Research Corporation Model 275) with a gated and intensified diode array attached to it (Princeton Instruments model IRY-512G/RB detector head, ST-120 controller and PG-200 pulser). This disperser-sensor system covered a slightly more than 300 nm spectral range, which could be shifted by changing the setting of the grating. A 450 W Xenon arc lamp (Osram) and a chopper or a medium pressure pulsed lamp (EG&G) served as a light source.

The spectral resolution of Shimadzu 160A depends on the range of the scan (R). It was 0.2, 0.5 or 1 nm when $R \leq 200$ nm, $200 < R \leq 400$ nm or $R > 400$ nm, respectively. The spectral resolution of the Zeiss and Princeton detectors was approximately 0.8 and 0.6 nm, respectively. Samples were put as close to the detector as it was possible (~ 2 cm) in order to reduce absorption loss due to scattering. In the case of large aggregates, where scattering and absorption flattening ('sieving') effects were significant, a numerical correction method was applied to counteract with these spectral distortions.

Correction for scattering

Let $E(\lambda;\gamma)$ denote the apparent absorption spectrum of a sample, containing C absorbing-and-scattering particle per unit volume, recorded by an on-axis detector with an acceptance angle of 2γ. It is clear that $E(\lambda;\gamma)$ differs from $A(\lambda)$, the true absorption spectrum, because the detector does not receive the light scattered between the angles γ and π radians. It is also obvious that $E_\pi(\lambda) \equiv \lim_{\gamma\to\pi} E(\lambda;\gamma)$ equals the true absorption at wavelength λ. Latimer and Eubanks (1962) realized that, if two apparent absorbance curves, $E_1(\lambda) \equiv E(\lambda;\gamma_1)$ and $E_2(\lambda) \equiv E(\lambda;\gamma_2)$, can be recorded, it is possible to extract $E_\pi(\lambda)$ provided that the scattered intensity shows no angular dependence in the range $\gamma_1 \le \gamma \le \pi$, where γ_1 is the smaller of the two collection angles. Nonetheless, a different approach is shown here to derive the relation linking E_π to E_1 and E_2.

Let us begin with the algebraic identity

$$\begin{aligned} E_\pi(\lambda) &= E_1(\lambda) + \frac{E_\pi(\lambda) - E_1(\lambda)}{E_2(\lambda) - E_1(\lambda)}[E_2(\lambda) - E_1(\lambda)] \\ &= E_1(\lambda) + L(\lambda;\gamma_1,\gamma_2)[E_2(\lambda) - E_1(\lambda)] \end{aligned} \tag{1}$$

From Eq. 1, one can see that, in order to extract the true absorption spectrum $E_\pi(\lambda)$ from the measured, scattering-contaminated absorption curves $E_1(\lambda)$ and $E_2(\lambda)$, one needs to know the quotient

$$L(\lambda;\gamma_1,\gamma_2) = \frac{E_\pi(\lambda) - E_1(\lambda)}{E_2(\lambda) - E_1(\lambda)}, \tag{2}$$

which requires, in turn, the knowledge of $E_\pi(\lambda)$. The only way to overcome on this problem is if $L(\lambda;\gamma_1,\gamma_2)$ can be found or estimated directly from the experimental curves $E_1(\lambda)$ and $E_2(\lambda)$. To show that, lets write the measured extinction, $E(\lambda;\gamma)$ in the form of the sum of $A(\lambda)$ and $S(\lambda;\gamma)$, the true absorption and the scattering, respectively:

$$E(\lambda;\gamma) = A(\lambda) + S(\lambda;\gamma) = E_\pi(\lambda) + S(\lambda;\gamma). \tag{3}$$

Eq. 2 now reads

$$L(\lambda;\gamma_1,\gamma_2) = \frac{S_1(\lambda)}{S_1(\lambda) - S_2(\lambda)}, \tag{4}$$

where $S_k(\lambda) = S(\lambda;\gamma_k)$ and $k = 1$ or 2. We now make the simplifying assumption that, for $\gamma_1 \leq \gamma \leq \pi$, the scattering contribution can be expressed as

$$S(\lambda;\gamma) = g(\gamma)\sigma(\lambda)Cl, \tag{5}$$

where $g(\gamma)$ is a purely geometrical factor, $\sigma(\lambda)$ is the total scattering cross section of the absorbing-and-scattering particles, and l is the optical pathlength. The meaning of Eq. 5 is that the spectrum of the scattered light shows no angular dependence in the range of $\gamma_1 \leq \gamma \leq \pi$. With this assumption, after inserting Eq. 5 into Eq. 4, we can find that L becomes independent of λ. Hence, choosing a wavelength λ_0 where there is no absorption, one can replace $S_k(\lambda_0)$ by $E_k(\lambda_0)$ and get an expression for L in terms of $E_1(\lambda_0)$ and $E_2(\lambda_0)$. Consequently Eq. 1 now reads

$$\widetilde{E}_\pi(\lambda) = E_1(\lambda) - \frac{E_1(\lambda_0)}{E_1(\lambda_0) - E_2(\lambda_0)}[E_1(\lambda) - E_2(\lambda)], \tag{6}$$

where a tilde has been added to the left-hand side to emphasize the fact that $\widetilde{E}_\pi(\lambda)$ is an approximation to $E_\pi(\lambda) \equiv A(\lambda)$. Hereafter $\widetilde{E}_\pi(\lambda)$ is called *scattering-compensated extinction spectrum*.

Correction for absorption flattening

When we study the absorption spectrum of a suspension of randomly distributed clusters of subunits we can find that it is flattened in comparison with the absorption spectrum of a sample containing the same number of randomly distributed but isolated subunits. This phenomenon was first discussed by Duysens (1956) and more recently by Berberan-Santos (1990). It can be explained by the fact that the subunits shade one another more effectively when they are assembled into clusters than when they are in isolation.

In order to derive an analytical correction formula let us start with a sample with a pathlength l containing N isolated subunits per unit volume, each of them is characterized by an extinction coefficient $\epsilon(\lambda)$. According to the Beer-Lambert law the absorbance of such a sample is $A_I(\lambda) = \epsilon(\lambda)Nl$. Suppose now that, by manipulating the conditions, the subunits can be made to form spherical clusters, each of diameter d, and that the new

absorbance of the sample becomes $A_C(\lambda)$. If we assume that Beer's law applies not only to the overall sample, but also to each individual cluster, then we can write that the absorbance of a cluster along its diameter is:

$$a(\lambda) = \varepsilon(\lambda)nd, \tag{7}$$

where n denotes the concentration of the subunits in a single cluster and $\varepsilon(\lambda)$ is their extinction coefficient. If we now further assume that cluster formation does not modify the spectral properties of the subunits and set, accordingly, $\varepsilon(\lambda) = \epsilon(\lambda)$, then the quotient $q(\lambda) \equiv a(\lambda)/A_I(\lambda)$ becomes independent of λ, and yields the relation

$$a(\lambda) = qA_I(\lambda) = \frac{nd}{Nl} A_I(\lambda). \tag{8}$$

Since $a(\lambda)$ is not a measurable quantity, it can only be determined indirectly: one chooses q and calculate the Duysens spectrum $A_D(\lambda)$ from a knowledge of $A_I(\lambda)$ and the relation (Duysens, 1956)

$$A_D(\lambda) = \frac{2\alpha(\lambda)}{3[1-\beta(\lambda)]} A_C(\lambda), \tag{9}$$

where $\alpha \equiv a \ln 10$, and β, the average transmission of a spherical cluster, is related as follows:

$$\beta(\lambda) = \frac{2[1-[1+\alpha(\lambda)]\exp[-\alpha(\lambda)]]}{\alpha^2(\lambda)}. \tag{10}$$

The most appropriate value of q can be determined by comparing the calculated absorbance A_D with A_I, the actual absorbance of isolated subunits, and minimizing the mean-square deviation. Once the best value has been chosen, Eq. 8 provides the absorbance of a spherical cluster (along its diameter).

Flash spectroscopy

Flash photolysis is a powerful spectroscopic technique to follow the relaxation of a sample after a short flash of excitation. The flash will introduce a concentration-jump which is monitored by means of absorption spectroscopy. The measured quantity is the change in the absorbance of the sample,

$$\Delta A(\lambda;t) \equiv \tilde{A}(\lambda;t) - A(\lambda), \tag{11}$$

where $A(\lambda)$ is the absorbance of the pre-irradiated sample at wavelength λ, and $\tilde{A}(\lambda;t)$ is the absorbance at time t after the flash excitation. When $\Delta A(\lambda;t)$ is plotted against λ, while the other variable, t, is being held fixed, the curve is called time-resolved spectrum. Such a plot is also frequently referred as a difference or transient spectrum. Another possibility of representing $\Delta A(\lambda;t)$ when the wavelength λ is kept fixed and the time is the independent variable in which case the plot is called decay curve. A set of transient spectra, recorded at different delays, can give us some coarse-grained information of the decay process of the intermediate states produced by the flash excitation.

Let us now consider a single-chromophore system, the absorbance of which can be expressed, like before, as

$$A(\lambda) = \varepsilon(\lambda)Cl. \tag{12}$$

As a result of a flash of excitation a small fraction (f) of the molecules will be converted into an unstable intermediate state with a lifetime τ. The concentration of this intermediate state, $C^\dagger$, will decay according to the equation $C^\dagger = C^\dagger(0)\exp(-t/\tau)$, where $C^\dagger(0) \equiv fC$. The absorbance of the sample at time t after the flash excitation can be written as:

$$\begin{aligned} \tilde{A}(\lambda;t) &= \varepsilon(\lambda)[C - C^\dagger(t)]l + \varepsilon^\dagger(\lambda)C^\dagger(t)l \\ &= \varepsilon(\lambda)Cl + [\varepsilon^\dagger(\lambda) - \varepsilon(\lambda)]C^\dagger(t)l, \end{aligned} \tag{13}$$

where we took into account that the extinction coefficient of the intermediate state, $\varepsilon^\dagger(\lambda)$, is usually different from that of the ground state, $\varepsilon(\lambda)$. By using Eqs. 12 and 13, Eq. 11 now can be written as follows:

$$\Delta A(\lambda;t) = [\varepsilon^\dagger(\lambda) - \varepsilon(\lambda)]C^\dagger l, \tag{14}$$

which shows that $\Delta A(\lambda;t)$ can be positive, negative or zero, depending on the relation between the extinction coefficients of the two states involved.

When the actinic flash excites more than one type of chromophore, the above relation can be easily extended. For instance, in some of our experiments the Xan and the Chl*a* population of LHCII were both excited, in which case we can write:

$$\begin{aligned}\Delta A(\lambda;t) &\equiv \tilde{A}(\lambda;t) - A(\lambda) \\ &= [\varepsilon_x^\dagger(\lambda) - \varepsilon_x(\lambda)]C_x^\dagger(t)l + [\varepsilon_a^\dagger(\lambda) - \varepsilon_a(\lambda)]C_a^\dagger(t)l\end{aligned} \tag{15}$$

where the subscripts *x* and *a* denote Xan and Chl*a*, respectively. We shall note here that $Xan^\dagger$ is generated through triplet ET from Chl*a*, which requires intimate contact between the chromophores. It also means that the extinction coefficient of Chl*a* which is in contact with a Xan is not necessarily identical with that of a Chl*a* which is in contact with a $Xan^\dagger$ (Peterman *et al.*, 1995).

Triplet-minus-singlet spectrum

If, in the above example, the intermediate is a triplet state then the difference spectrum of the sample is referred as a triplet-minus-singlet spectrum, and frequently abbreviated by the term TmS. A typical experimental set-up for recording difference spectra is shown in Fig. 8, which is essentially a pump-probe system. In the probe beam a 250 W low-pressure Xenon-arc lamp was used as a light source, which was focussed, through a ca. 4×4 mm entrance slit, to the sample. On the pump side the output of an optical parametric oscillator, abbreviated as OPO, (OP 901.355, B.M. Industries, France) provided the excitation beam, which was pumped by the third harmonic of a Nd:YAG laser (B.M. Industries, France) at a repetition rate of 10 Hz. The OPO had a tunable output over the range of 410-700 nm, which was aligned, by the aid of a cylindrical lens, to overlap with the probe beam throughout the sample. The approximate duration of each pulse was 7 ns, and the energy was in the range of 10 mJ, depending on the wavelength chosen.

In practice obtaining a TmS spectrum entails two measurements of intensities *versus* the wavelength of the probe beam, $I(\lambda)$ and $\tilde{I}(\lambda;\ t)$, which refer to the light intensities leaving the sample before or at time t delay after the laser-excitation,

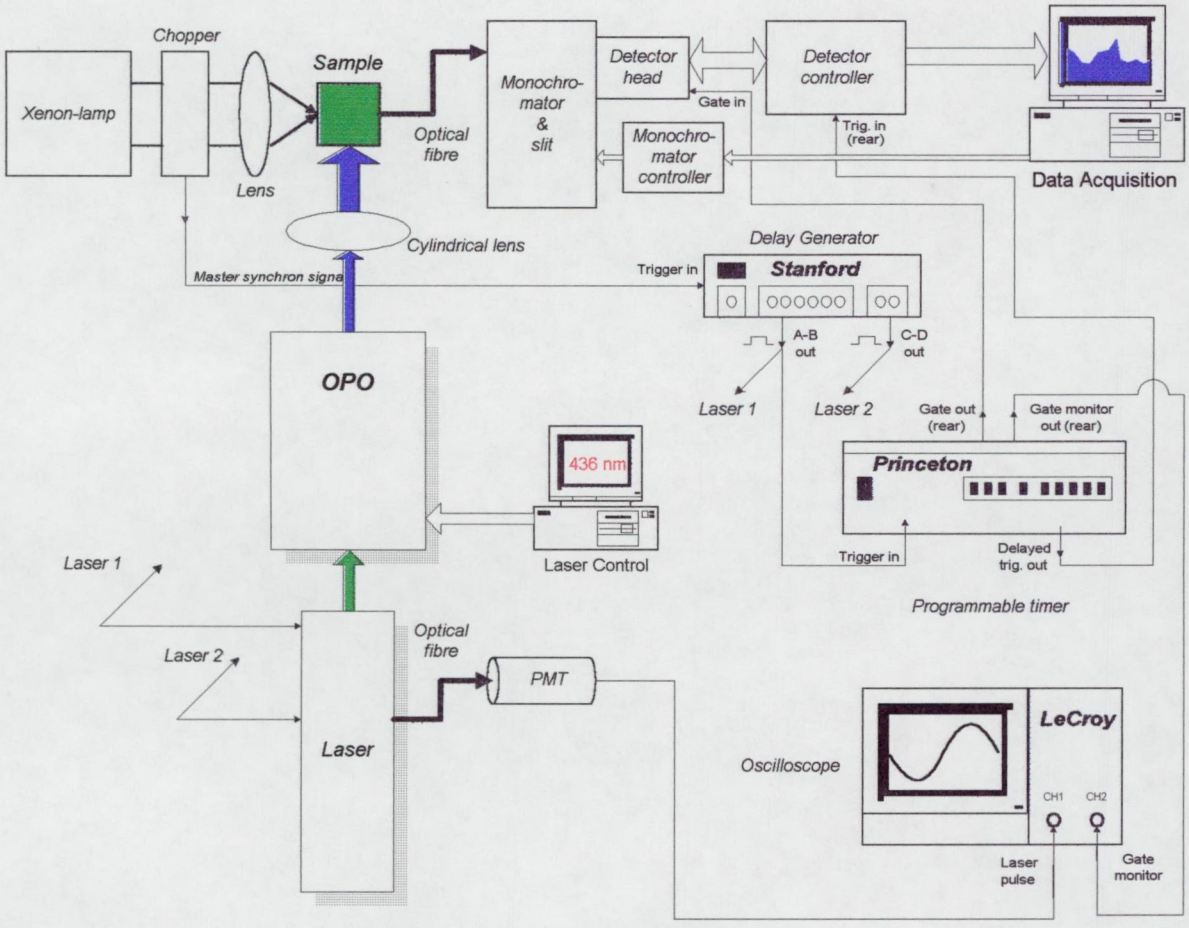

Fig. 8. *The laser-flash setup used in the Biophysics Lab of NTNU. Apart from the optical layout the picture shows the controlling instruments as well. A mechanical chopper in the probe beam provided the trigger signal for the other instruments. A delay generator (Stanford, DG535) was used to produce the necessary electronic pulses for firing the laser, and it also triggered a programmable timer (Princeton, PG 200) which provided the delayed gating signal for the detector. A photomultiplier tube (PMT) and a 2 GHz double-beam digital oscilloscope (LeCroy 9001) were used solely for checking the delay between the laser excitation and the moment of data acquisition.*

respectively. If $I_0(\lambda)$ would represent the intensity of the incident light before entering the sample then the corresponding absorbances could be written as follows:

$$A(\lambda) = \lg \frac{I_0(\lambda)}{I(\lambda)}, \qquad \tilde{A}(\lambda) = \lg \frac{I_0(\lambda)}{\tilde{I}(\lambda;t)}. \tag{16}$$

The change in absorbance introduced by the laser excitation is then given by the equation

$$\Delta A(\lambda;t) \equiv \tilde{A}(\lambda;t) - A(\lambda) = \lg \frac{I(\lambda)}{\tilde{I}(\lambda;t)}, \tag{17}$$

from which the reader can see that measuring $I_0(\lambda)$ is redundant, and $I(\lambda)$ will play the role of the reference signal.

The acquisition was performed by one of the two multichannel detector systems, mentioned previously, and the data was immediately transferred to the controlling computer for calculating and plotting the absorbance against wavelength. For the TmS spectra reported here, the triple-grating monochromator with a gated and intensified diode array served as the spectrophotometer. The gate width was held at 20 ns, and the delay between the excitation pulse and the opening of the observation window was varied between 20 ns and 40 μs.

Fluorescence spectroscopy

We could also record the laser-excited fluorescence emission spectra with the same multichannel arrangement, which was employed for obtaining the TmS spectra, by blocking the monitoring beam. This method has the advantage that one can record the TmS and the emission spectra under the same experimental condition.

Fluorescence excitation spectra, corrected for the spectral distribution of the excitation light source, were recorded by using a commercial Spex Fluorolog 2 spectrofluorimeter, which uses double monochromators both for isolating the excitation bandpass and for analyzing the fluorescence emitted by the sample. The apparent fluorescence spectrum of a sample must be corrected, if one is intended to compare it

with the corresponding spectrum recorded on a different instrument, by dividing $F(\lambda)$, the output of the detector used for monitoring the fluorescence emitted by the sample within a given solid angle, by a reference signal, whose amplitude is proportional to $E(\lambda)$ or $I_0(\lambda) \equiv E(\lambda)\lambda$, the energy or the intensity (respectively) of the beam used for exciting the specimen. Originally our spectrofluorimeter employed a dual-beam arrangement, using a beamsplitter and a quantum counter, for recording $F(\lambda)$ and $I_0(\lambda)$ in parallel, and the software supplied with the instrument provided their ratio, $X(\lambda) \equiv NF(\lambda)/I_0(\lambda)$, which is referred as the corrected fluorescence excitation spectrum (where N is a multiplicative constant). However, we used a different approach and operated the instrument in single beam mode by discarding the beamsplitter, as it was described by Naqvi (1998a).

First we measured $F(\lambda)$, then replaced the cuvette holder with a Golay detector (Oriel Corp., Model 7500), whose output is proportional with the incident energy, and measured *in situ* $E(\lambda)$. For this purpose the exciting light (a 250 W quartz-halogen lamp) was modulated at 10 Hz with a slotted disk chopper (EG&G Model 9479) and the output of the detector was fed to a lock-in amplifier (EG&G Ortholoc-SC 9505) whose output was sampled with a data acquisition board of a PC. Subsequent data handling was done with a commercial spreadsheet program. Although our Golay cell was designed for infrared detection its response proved to be nonselective down to 430 nm. The spectral bandpass of the excitation monochromator was 1.8 nm, and that of the analyzing monochromator 6 nm. The fluorescence signal was acquired using a sampling interval of 0.5 nm. The spectra were recorded at room temperature using a 2 mm quartz cuvette. The sample was diluted so as to have a peak absorption around 0.5 in a 1 cm cuvette.

Photodegradation

The cheapest way to increase the signal-to-noise ratio is the repetitive signal averaging, which is the simplest approach and does not distort the data. However, there is a serious drawback of this method when the sample is likely to undergo a degradation process after strong irradiation.

To avoid photo-damage of the sample one can reduce the light intensity falling to the sample. In order to maintain the signal-to-noise ratio this means shorten the laser

pulses on the pump side, and/or by shadowing the probe light when the laser is idle by applying a chopper or a pulsed lamp instead of continuous illumination of the sample.

When studying photosynthetic systems the main source of photodegradation is that triplet Chl's, when not completely quenched by Car, can react with the surrounding oxygen molecules, which have a triplet ground state. The only way to prevent this free radical formation is to remove the oxygen from the environment. For approaching oxygen-free conditions, we bubbled high-purity argon through the sample for 10 min prior to the measurements. During the data acquisition the tip of the hypodermic needle bringing the argon to the sample was kept near the top of the sample to make sure that bubble formation would not disturb the measurement.

If none of these preventive methods is feasible (or proved to be satisfactory) a frequent change of the sample and the ground averaging of the spectra, obtained with a fresh sample, might be the only solution.

RESULTS AND DISCUSSION

Comparison of the absorption spectra of trimers and aggregates of LHCII

The absorption spectrum of aggregated LHCII looks, at first sight, very different from that of a trimer. The decrease in the amplitudes in the Soret region (and, to somewhat lesser extent, also in the Q_y region) is due to the flattening effect (Duysens, 1956). Scattering contribution to the absorption spectra becomes more and more pronounced as the size of the aggregates increases. Fig. 9 shows the absorption spectrum of aggregates at different detergent (TX) concentrations. Similar results were obtained when n-OG was used instead of TX. When the detergent concentration (C_D) exceeds a threshold, C_C, (around 0.015% for TX and 0.67% for n-OG) the 436 nm peak practically ceases to increase and the shape of the Q_y band becomes distorted. Since at C_C the scattering contribution becomes negligible, as one can see from the data pertaining to the 700-800 nm region, the differences in extinction seen after further addition of detergent must therefore be attributed to changes in the chromophoric organization of the complex. The absorption spectrum obtained at C_C will be taken as the true absorption spectrum of the trimers and labelled as $A_T(\lambda)$.

An interesting feature of the spectra presented at Fig. 9 is the occurrence of two isosbestic points, at which total extinction (i.e. scattering-contaminated experimental absorbance) stays constant over a wide range of C_D (Fig. 10). The exact position of the isosbestic points will vary depending on the scattering contribution to the apparent absorption spectrum, which in turn, depends on the optical layout. For a given experimental arrangement it will be determined by the physical dimensions of the aggregates in the detergent-free sample.

The characteristic detergent concentration, C_C, at which the aggregates disassemble into trimers, was found to be almost identical with the critical micelle concentration (CMC), but proved to be dependent not only on the detergent but also on the LHCII concentration in the sample. Fig. 11 shows the absorption spectra of two samples, in which the peak absorption in the Soret-region of Chl*a* (436 nm) was nearly 1

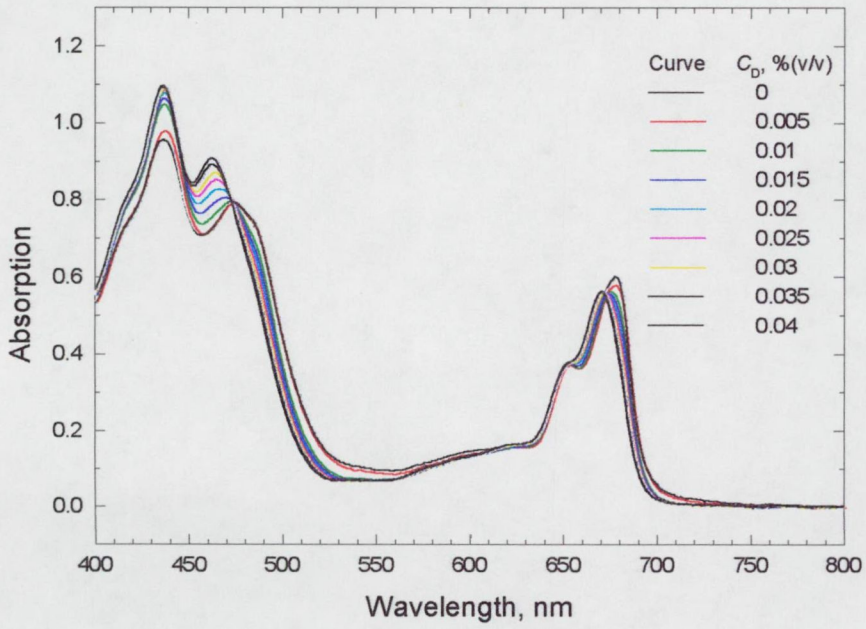

Fig. 9. *Absorption spectra of LHCII containing detergent (TX) in different concentrations (C_D). The spectra were recorded using a Shimadzu 160A spectrophotometer with a built-in opal glass plate for reducing scattering.*

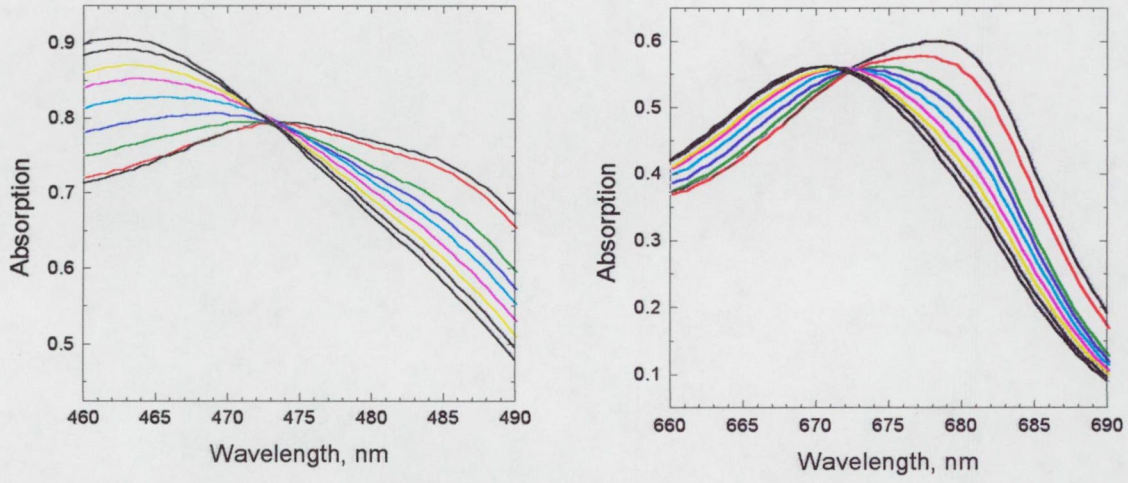

Fig. 10. *A magnified view of the two spectral regions embracing the isosbestic points. The experimental absorption stays constant over a wide range of detergent. The colour code on Fig. 9 also applies here.*

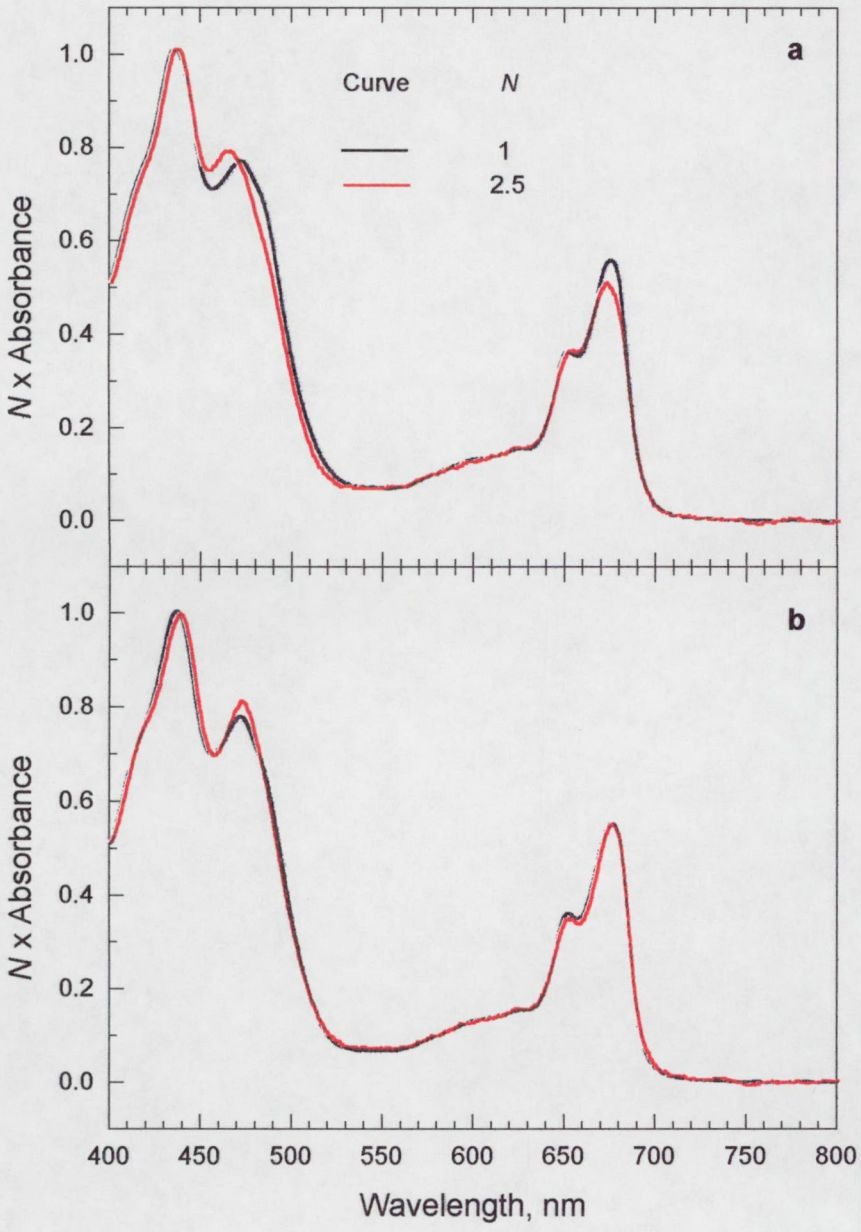

Fig. 11. *Absorption spectra of LHCII in the presence of detergent at a concentration close to its CMC value. The detergent is TX in panel* ***a*** *and n-OG in panel* ***b****. In each frame the absorption spectra of two samples are shown. The red curves represent samples where the total Chl concentration was 40% of that in samples portrayed by the black lines. In order to counteract with the difference in Chl concentration the absorption spectra of the more dilute sample was multiplied by N(=2.5).*

and 0.4, after adding detergent at its CMC. The detergent was TX on Fig. 11a and n-OG on Fig. 11b. It is evident from the spectra presented here, that in case of n-OG, C_C is rather insensitive to the LHCII concentration, while in case of TX the detergent concentration, which disrupts the aggregates into trimers, should be lower in the diluted sample. As for the TX-containing samples, we can say, without undertaking a thorough investigation, that the more diluted the sample the lower the value of C_C. For samples with a peak absorption (in the Soret-region) around 1 C_C is close to, but slightly higher than, the CMC. Therefore all the results presented in this thesis was obtained using samples with peak absorbance close to 1 for easier comparison with other results. The values of CMC are 23±3 mM and 0.24 mM for n-OG and for TX, respectively, or 0.67% (w/v) and 0.015% (v/v).

In order to compare the absorption spectrum of trimers and aggregates one has to take into account the distortions introduced by selective light scattering and absorption flattening by the aggregates. The correction method consists of three steps: (*i*) one must first obtain the scattering free absorption spectrum $A_C(\lambda)$, (*ii*) one must record—after applying some chemical and/or physical process for rupturing the clusters—the absorption spectrum of isolated subunits $A_I(\lambda)$, finally (*iii*) one must transform, with the aid of $A_I(\lambda)$ and Duysens' formula (Eq. 9), $A_C(\lambda)$ into the corresponding Duysens spectrum $A_D(\lambda)$.

In order to correct for selective light scattering we adopted a method from Latimer and Eubanks (1962), as it was described in the previous chapter. It entails two measurements of the absorption spectrum in the two extreme position of the sample compartment of the spectrophotometer. These two spectra have different contributions from light scattering, which gives us the opportunity to calculate the scattering-compensated absorption spectrum.

Fig. 12 shows $E_1(\lambda)$ and $E_2(\lambda)$, the two experimental absorption spectra of suspension of LHCII aggregates recorded in two different positions: for $E_1(\lambda)$ the sample was put as far from the detector as the sample compartment allowed us to place it (~10 cm), while $E_2(\lambda)$ was recorded in the opposite extreme (~2 cm). Also shown in Fig. 12 is the calculated scattering-compensated extinction spectrum, $\tilde{E}_x(\lambda)$. The quality of the baseline shows that, at least in the 700-800 nm region, our scattering-compensated

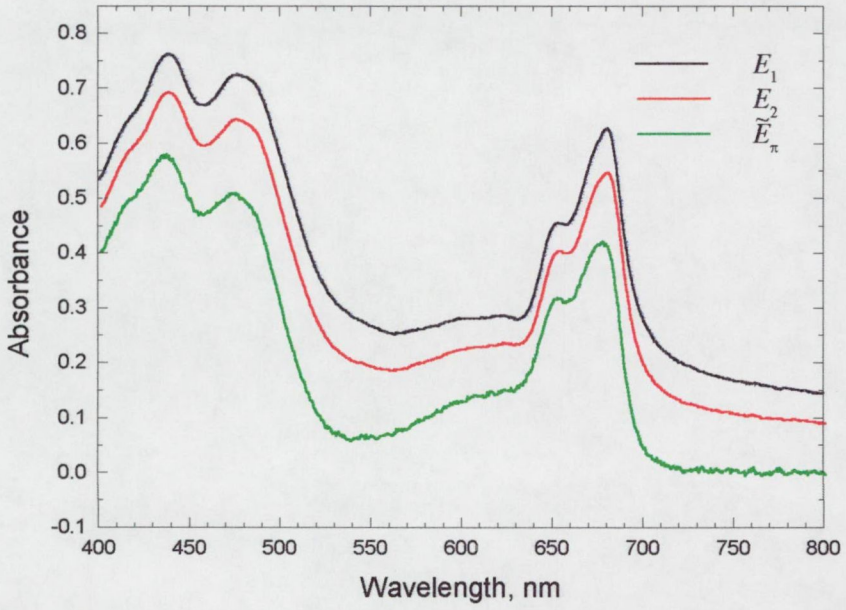

Fig. 12. *The experimental absorption spectra of detergent-free LHCII recorded when the sample was placed to the two extreme positions of the sample compartment. (E_1 belongs to the farthest and E_2 to the nearest position of the sample with respect to the detector.) The calculated scattering-compensated extinction spectrum ($\tilde{E}_\pi$) is also plotted.*

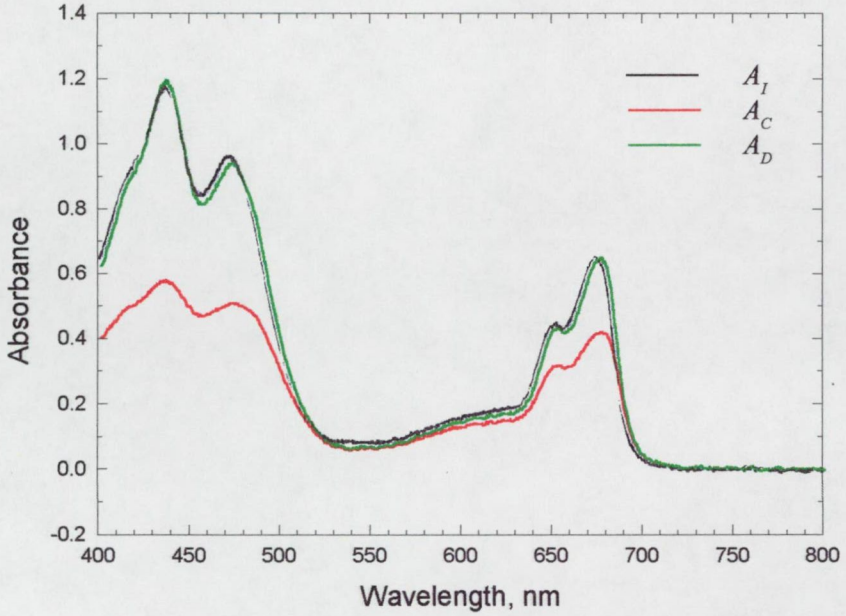

Fig. 13. *The scattering-free absorption spectrum of LHCII aggregates containing no additional detergent (A_C), and the experimental absorption spectrum of LHCII suspension containing 0.7% n-OG (A_I). The latter is identified with the absorption spectrum of the trimers. The calculated Duysens spectrum (A_D) is also plotted.*

spectrum can be regarded as scattering-free hence, we will take as $A_C(\lambda)$ when calculating the Duysens spectrum. The assumption concerning the γ-independence of scattering in the $\gamma_1 \leq \gamma \leq \pi$ angular region can be judged from the difference spectrum, $\Delta E(\lambda) \equiv E_1(\lambda) - E_2(\lambda)$, which shape appeared to be rather insensitive to the relative positions of the samples.

The mutual shadowing of trimers within a single aggregate is taken into account with the Duysens formula (Eq. 9), as it was described in the Materials and Methods chapter. The calculated Duysens spectrum of LHCII aggregates is plotted in Fig. 13. One can see that the absorption spectrum of the aggregates, when corrected for distortions introduced by scattering and absorption flattening, is almost superposable to the absorption spectrum recorded after disrupting the aggregates into trimers by the addition of detergent at C_C. The scattering-corrected absorption spectrum of the aggregates is also shown in Fig. 13 for better comparison.

Since earlier attempts on unicellular organisms were handicapped by the fact that disintegration of the scattering sample, using organic solvents, destroyed the pigment–protein interactions (Duysens, 1956) or by the failure of rupturing the cells into fragments by mechanical agitation (Das *et al.*, 1967), our results on the trimer–aggregate system provides the first experimental evidence for the applicability of Duysens' method.

If a reliable estimates for ε and n can be made then the average value of d, the effective diameter of the clusters, can be evaluated. Knowing the crystal structure of LHCII (Kühlbrandt, 1994) we can approximate the volume of a trimer by a cylinder about 70 Å across and 50 Å in height. If we take 50 as the number of chromophores per trimer, we can get the value of 0.34 M for the chromophore concentration. The corresponding figure in the aggregates may even be lower. From the spectral reconstruction of the absorption spectrum of LHCII aggregates (Siefermann-Harms, 1985) we can get the rough estimate of the average extinction coefficient of the chromophores at the wavelength of peak absorption (436 nm) and arrive at a value of 5×10^4 M^{-1} cm^{-1}. From Eqs. 7 and 8 we can get the expression for the diameter of a cluster:

$$d = \frac{qA_1(\lambda)}{n\varepsilon(\lambda)}. \tag{18}$$

Using our estimates for ε and n, the effective diameters of the aggregates come out to be commensurate with the wavelength of visible light (220 – 690 nm for different preparations). This approximation is in good agreement with earlier results, where the estimation was made on the basis of the CD spectra of LHCII (Barzda *et al.*, 1994), and is similar to the estimated sizes (d ~ 200 – 400 nm) in granal thylakoid membranes (Garab *et al.*, 1988c; Finzi *et al.*, 1989).

On the basis of our results we can conclude that the absorption spectrum of aggregated LHCII—when corrected for spectral distortions due to selective scattering and absorption flattening—turns out to be similar to the absorption spectrum of the trimers. This implies that intertrimer interactions due to aggregation, though they may have other observable consequences, have little influence on the absorption spectrum of the trimers.

The similarity of the absorption spectra of trimers and aggregates has another important consequence. As it was derived from theory (Strickler & Berg, 1962) the radiative lifetime, τ_r, of a transition between the electronically excited upper state n and the lower state m can be expressed like:

$$\tau_r = \frac{1}{A_{nm}} \approx \frac{3.417 \times 10^8}{\tilde{\nu}_{nm}^2 \, n^2 \mathscr{A}}, \tag{19}$$

where A_{nm} is the Einstein-coefficient for spontaneous emission, $\tilde{\nu}_{nm}$ is the wavenumber of the transition in cm^{-1} (which we may approximate with $\tilde{\nu}_{max}$, the wavenumber of the maximum absorption) and $\mathscr{A}$ is the integrated extinction coefficient:

$$\mathscr{A} = \int_{band} \varepsilon(\tilde{\nu}) d\tilde{\nu}, \tag{20}$$

where the integration is carried over the whole absorption band (Gilbert & Baggot, 1991). This implies that aggregation does not change the radiative lifetime of Chl*a**. Our result does not support the earlier proposal of Ruban & Horton (1992), who associated the aggregation induced quenching of Chl*a* fluorescence with changes in the absorption spectrum.

Quenching of chlorophyll *a* singlet and triplet states by carotenoids in LHCII

Comparison of aggregates and trimers

The time-dependence of the TmS spectra of a suspension of LHCII aggregates are displayed in Fig. 14, which shows plots of $N \times \Delta A(\lambda;t)$ for three values of t (0.1, 4.1 and 7.1 μs). The multiplication factor N (≥1) was used to normalize these curves to the one obtained with the shortest delay time. The values of the normalization factor (N=1, N=1.5 and N=2.1) are consistent with the decay curves representing plots of $\Delta A(\lambda;t)$ against t, where three values of λ were used for each sample (508, 515 and 525 nm). All of the decay curves were found to follow monoexponential decay, $\Delta A(\lambda;t)=\Delta A(\lambda;0)\exp(-t/\tau)$, with τ=9.3±0.3 μs. Since no difference was found in the kinetics, only results obtained at 508 nm are plotted on Fig. 15 for trimers and aggregates of LHCII.

The TmS spectra of aggregates and trimers of LHCII are compared in Fig. 16 at t=0.1 μs. The difference spectra of aggregates differ from the corresponding spectra of trimers on two counts: (*i*) in the aggregates, the Car triplet-triplet absorption band (ΔA>0) is red-shifted and broader; and (*ii*) the features attributable to the perturbation of the Q_y band of Chl*a* by a nearby Car triplet are more pronounced, than in trimers. The trimer spectrum appeared to have, like the aggregate spectrum, a single decay time but the signal in the Chl*a* Q_y region is much too weak to allow an unequivocal statement about its rate of decay. Based on the dissimilarity between low-temperature TmS spectra of LHCII trimers (Peterman *et al.*, 1995) and aggregates (van der Vos *et al.*, 1991) we can compare the room-temperature TmS spectra of trimers and aggregates, which are displayed in Fig. 16. In the spectral region between 500 and 530 nm, where ΔA>0 and absorption by ground state Xan molecules are negligible, the observed difference in the TmS spectrum, particularly the larger width of the aggregate spectrum, arises from the difference in the shapes of the $T_n \leftarrow T_1$ absorption bands of Xan's, similar to those reported for the low temperature spectra. We can conclude that disruption of the aggregates puts an end to the interaction between trimers, and thereby changes the relative population of $Neo^{\dagger}/Vio^{\dagger}$, whose $T_n \leftarrow T_1$ spectra are characterized by a single peak at 525 nm. Detergent-induced disaggregation would also slacken the opportunity to

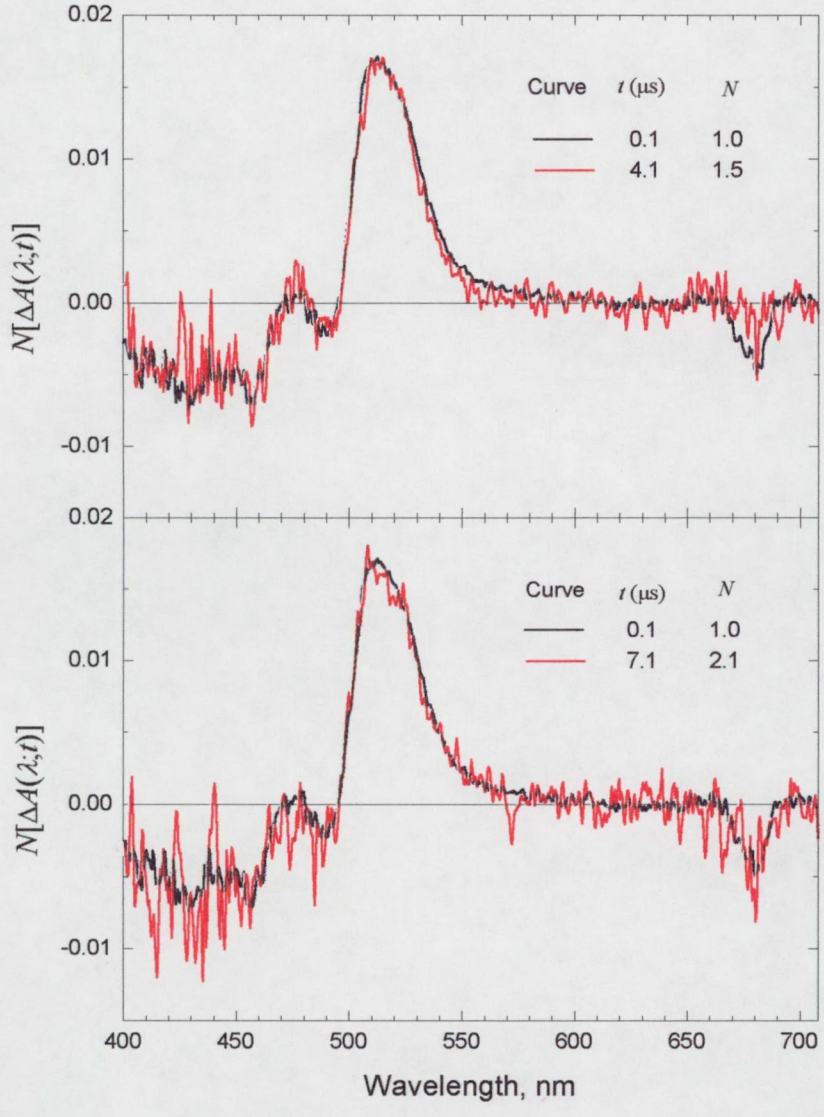

Fig. 14. *TmS spectra of LHCII aggregates at three different delays. The curves procured at the two longer delays are compared with the one obtained at 100 ns after the laser excitation. The former traces have been multiplied by N(> 1) for better comparison.*

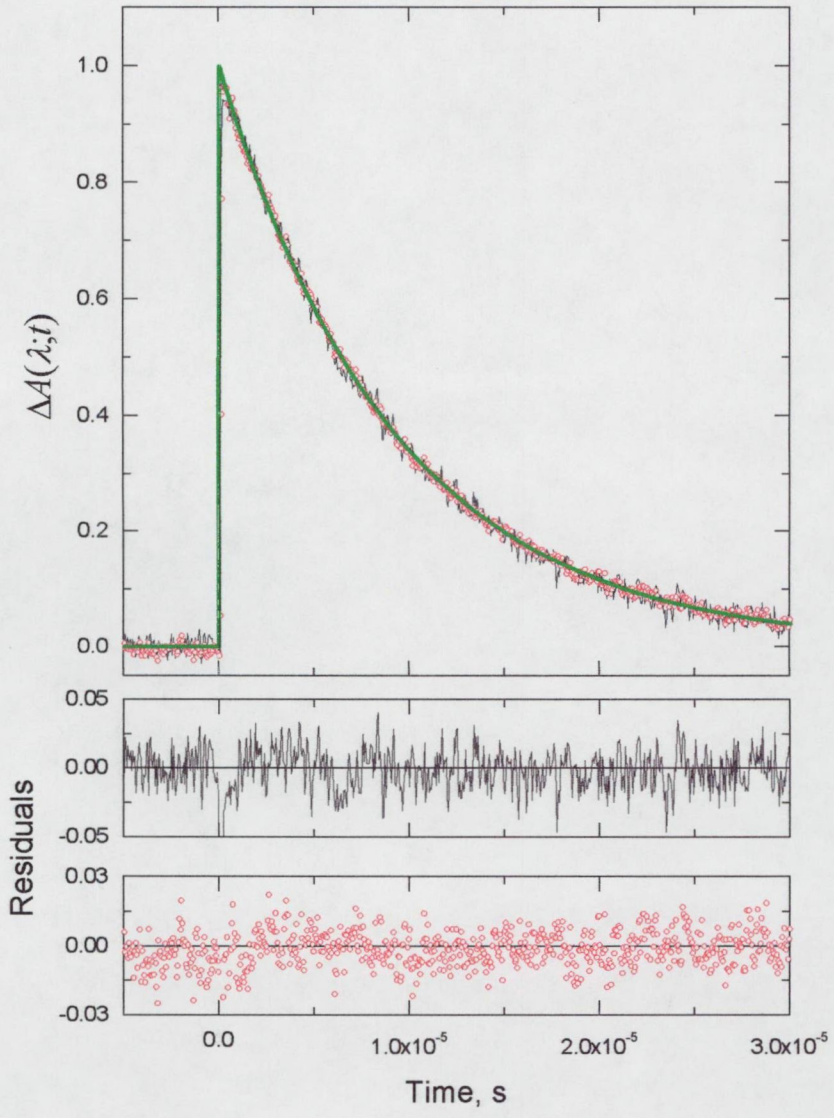

Fig. 15. *Normalized decay curves displaying the decrease of the carotenoid triplet peak (monitored by recording the laser-induced change in the absorbance at 508 nm with the aid of a LeCroy 9001 digital storage oscilloscope) and the corresponding residuals. The green curve is a plot of* $H(t)\exp(-t/\tau)$*, where* $H(t)$ *is the unit step function and* $\tau = 9.3 \times 10^{-6}$ *s. The thin black trace and the red circles refer to the aggregates and trimers, respectively.*

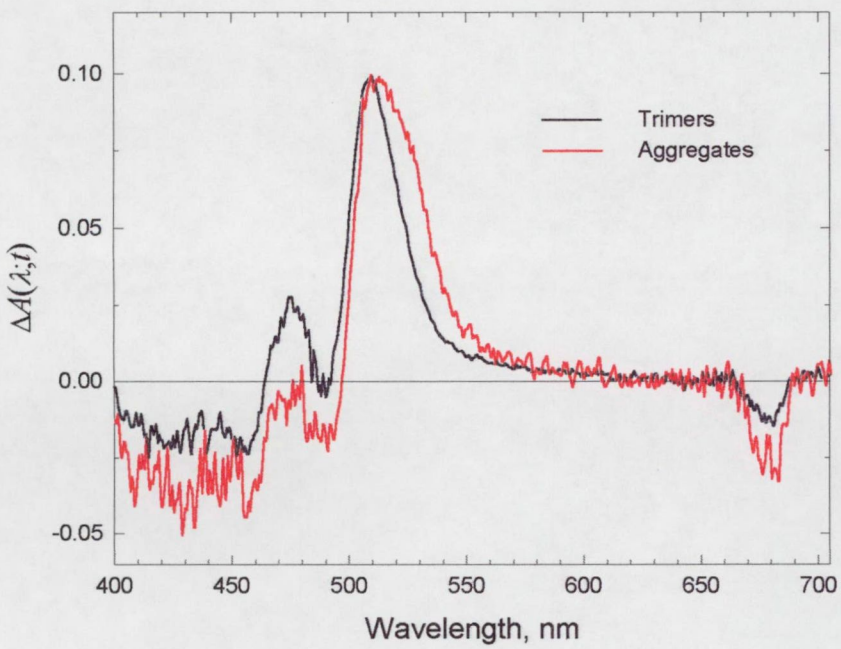

Fig. 16. *TmS spectra of LHCII trimers and aggregates at 100 ns after the laser excitation. The spectra have been normalized to the same peak absorbance for better comparison.*

perturb the Q_y transition of a peripheral Chl*a* by a Xan belonging to a different trimer. As a consequence, the Q_y bleaching signal in the trimers should become smaller which concurs with our observation.

The influence of C_D on the fluorescence and TmS spectra is shown in Fig. 17. The spectra of samples containing 0.3 and 0.6% n-OG in each set have been normalized to the corresponding sample without (additional) detergent. Since the two sets of measurements were recorded under identical conditions of illumination, the change in absorbance (resulting from the addition of n-OG to the sample) affects the fluorescence spectrum and the TmS spectrum equally. One can see from these spectra that the population of $Xan^{\dagger}$ increases, so does the fluorescence intensity (Table 1), upon the addition of n-OG, though the determination of the triplet yield is handicapped by the fact that one is dealing with a heterogeneous assembly of chromophores. Inasmuch as the efficiency of triplet energy transfer from Chl*a* to Xan stays constant (close to 100%) at all three values of C_D, it is reasonable to conclude that the triplet formation yield is approximately proportional to that for fluorescence emission.

Table 1.
Relative fluorescence intensities (Fl.) and the population of xanthophyll triplets ($Xan^{\dagger}$) at different concentrations (C_D) of detergent (n-OG)

C_D (%)[a]	Fl.	$Xan^{\dagger}$
0	1	1
0.3	1.4	1.5
0.6	2.3	2.4

[a] w/v

As we saw from our results on the comparison of the absorption spectrum of trimers and aggregates of LHCII, the radiative lifetime of Chl*a* does not depend on the extent of aggregation. Therefore a parallel decline of the fluorescence and triplet formation yields implies an increase in the rate constant for internal conversion of Chl*a* as trimers are assembled into aggregates. Similar results were observed earlier in artificial caroteno-porphyrin dyads (Bensasson *et al.*, 1981; Moore *et al.*, 1982; Gust *et al.*, 1992), which was explained by suggesting that Car's are able to quench the fluorescence and

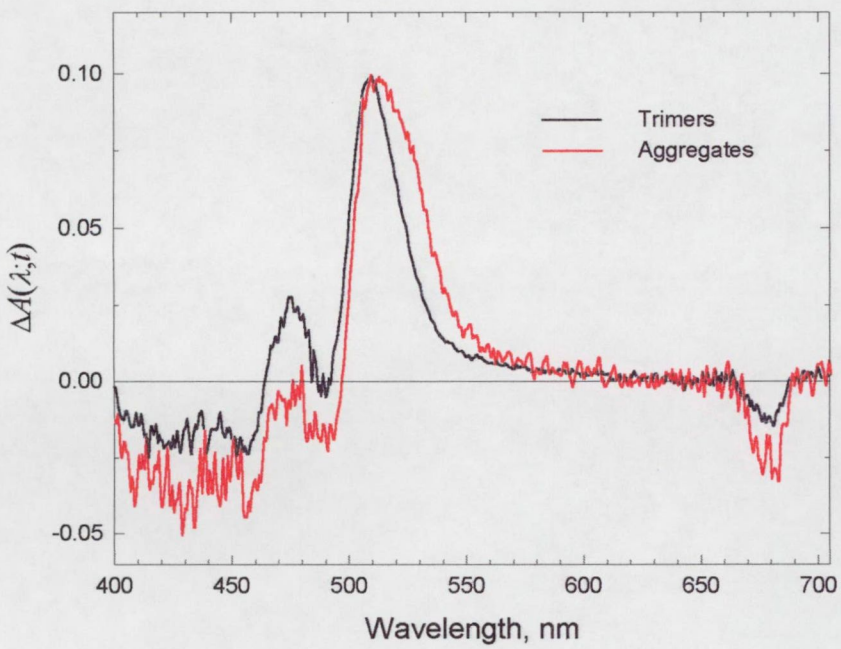

Fig. 16. *TmS spectra of LHCII trimers and aggregates at 100 ns after the laser excitation. The spectra have been normalized to the same peak absorbance for better comparison.*

triplet formation yields of a nearby Chl-like molecule via a process, which has been termed as 'catalysed internal conversion' (CIC). Based on this similarity, we put forward the hypothesis that CIC operates also in natural antenna complexes. The quenching in the fluorescence yield of Chl*a* (or a Chl-like molecule in the dyads) and the observed bleaching signal in the Q_y region of Chl*a* — which reveals the influence of a nearby Car — imply that a proper description of the electronic states of a Chl*a*:Car pair (where the colon represents van der Waals contact between the chromophores) cannot be obtained without allowing the mixing of the zero-order states of the pair (Naqvi, 1998b). Such treatment takes into account $i \rightarrow k \rightarrow f$ indirect transitions from the initial state i to the final state f via an intermediate state k. Quenching of Chl*a* *can* be explained by introducing, through the use of second-order perturbation theory, virtual transition to and from a charge-transfer state, $Chla^{-}:Car^{+}$, or a 'non-ionic' intermediate state, for instance $Chla:Car^{**}$ (Fig. 18).

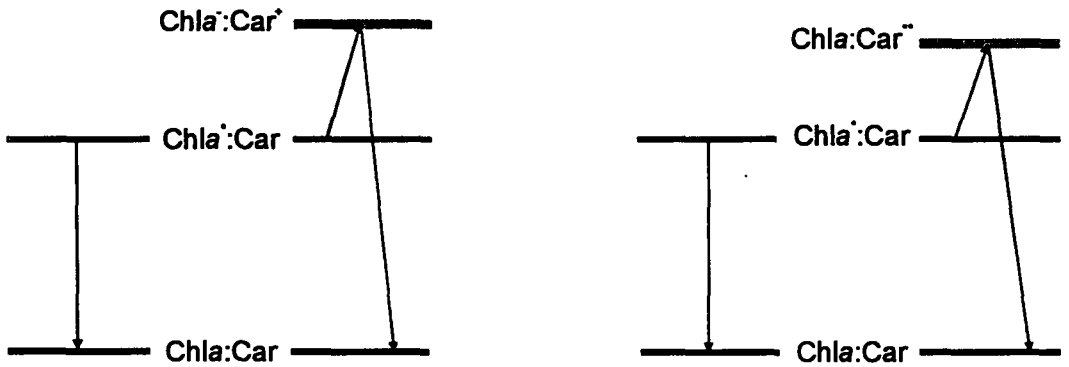

Fig. 18. *Schematic representation of the quenching of* Chl*a** *in a* Chl*a*:Car *pair via virtual transitions to and from an intermediate state. These indirect transitions are taken into account by allowing the admixture of zero-order states. (Reproduced after the conference talk of Naqvi, 1998b.)*

Our initial working hypothesis, namely that the formation of Chl*a*† might have some bearing on the dissipation of excess excitation energy, has been ruled out on the basis of our conclusion that the triplet formation yield decreases parallel with the quantum yield for fluorescence. Therefore it seems unlikely that triplet states of Chl*a* are directly engaged with the dissipation of excess energy.

Perturbed trimers

The TmS spectra of LHCII samples containing n-OG at a concentration higher than C_C are plotted in Figs. 19 and 20. In Fig. 19a the wavelength of excitation was 680 nm, where only Chl*a* absorbs, while that in Fig. 19b was 462 nm, where absorption by Chl*a* is negligible. One can see from these figures that the shape of the spectra changes when different types of chromophores are excited.

The overall TmS signal can be decomposed into two contributions whose shapes are time-invariant and amplitudes decrease with time. One can write $\Delta A(\lambda;t)=\Delta A_x(\lambda;t)+\Delta A_c(\lambda;t)$, where $\Delta A_x(\lambda;t)$, the signal originating from Xan, becomes negligible at $t = 40$ μs, and $\Delta A_c(\lambda;t)$, which persists for several hundred microseconds, is contributed by those Chl molecules which fail to transfer their triplet excitation to an adjacent acceptor. Using the symbols t_0 and t_1 to denote a delay of 0.1 μs and 40 μs, respectively, one can summarize the behaviour of the two components as follows: while $\Delta A_x(\lambda;t_1)$ is negligible in comparison with $\Delta A_x(\lambda;t_0)$, $\Delta A_c(\lambda;t_1)\approx\Delta A_c(\lambda;t_0)$. For $t_0\le t\le t_1$, one may set $\Delta A_x(\lambda;t)=\Delta A(\lambda;t)-\Delta A_c(\lambda;t_1)$. Fig. 20 shows plots of $\Delta A(\lambda;t_0)$, $\Delta A_x(\lambda;t_0)$ and $\Delta A_c(\lambda;t_1)$ at two different C_D. The spectral decomposition of the TmS spectrum provides an opportunity to estimate the total triplet concentration. We will use the symbols $\hat{\lambda}_x$ and $\hat{\lambda}_a$ to denote the wavelengths (around 508 and 674 nm, respectively) at which signals representing absorption by Xan† and depopulation of Chl*a* reach their peak values, and set $\hat{\varepsilon}_x^\dagger \equiv \varepsilon_x^\dagger(\hat{\lambda}_x)$, and $\hat{\varepsilon}_a^\dagger \equiv \varepsilon_a^\dagger(\hat{\lambda}_a)$. Since absorption by Xan is negligible at $\hat{\lambda}_x$ and absorption by Chl*a*† negligible at $\hat{\lambda}_a$, we can write, using Eq. 15, the expression for $\Delta A(\lambda;t)$ in case of the two-chromophore system, $\Delta A_x(\hat{\lambda}_x;t)=\hat{\varepsilon}_x^\dagger C_x^\dagger(t)l$ and $\Delta A_a(\hat{\lambda}_a;t)=-\hat{\varepsilon}_a^\dagger C_a^\dagger(t)l$. If one now introduces the symbols

$$\Delta A_x(\hat{\lambda}_x;t)=\varepsilon_x^\dagger C_x^\dagger(t)l\equiv\hat{\Delta}_x(t) \text{ and } \Delta A_a(\hat{\lambda}_a;t)=-\varepsilon_a^\dagger C_a^\dagger(t)l\equiv\hat{\Delta}_a(t),$$

the total triplet concentration, $C^\dagger$, can be expressed as

$$\begin{aligned} C^\dagger(t) &\equiv C_a^\dagger(t)+C_x^\dagger(t)=[\hat{\Delta}_x(t)/\hat{\varepsilon}_x^\dagger]-[\hat{\Delta}_a(t)/\hat{\varepsilon}_a^\dagger] \\ &=[\hat{\Delta}_x(t)-(\hat{\varepsilon}_x^\dagger/\hat{\varepsilon}_a)\hat{\Delta}_a(t)]/\hat{\varepsilon}_x^\dagger=Y(t)/\hat{\varepsilon}_x^\dagger \end{aligned} \qquad (18)$$

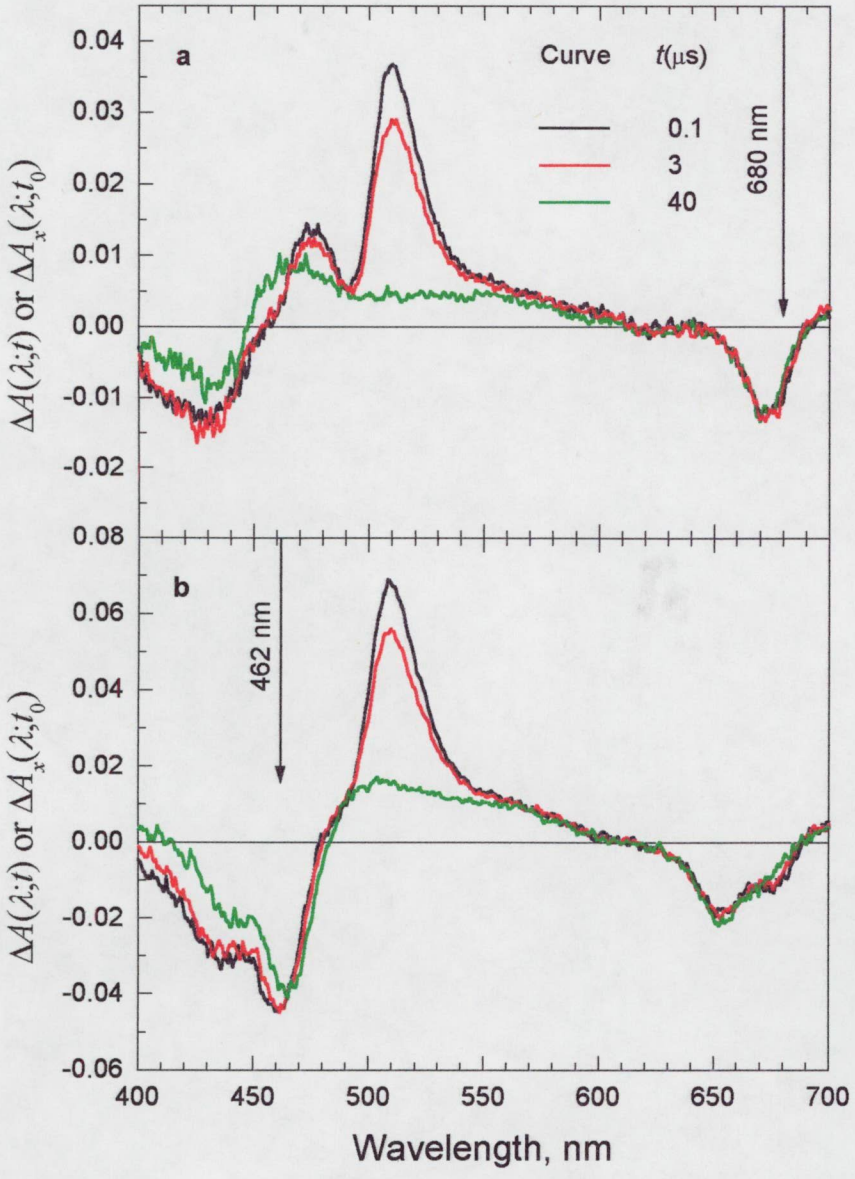

Fig. 19. *TmS spectra of LHCII suspension, at different delays, after the addition of 0.9% (w/v) n-OG. The vertical arrows show the wavelength of excitation. Only* Chla *molecules were excited by the laser flash at 680 nm (panel* ***a)****, while laser excitation of* Chla *was negligible at 462 nm (panel* ***b)****.*

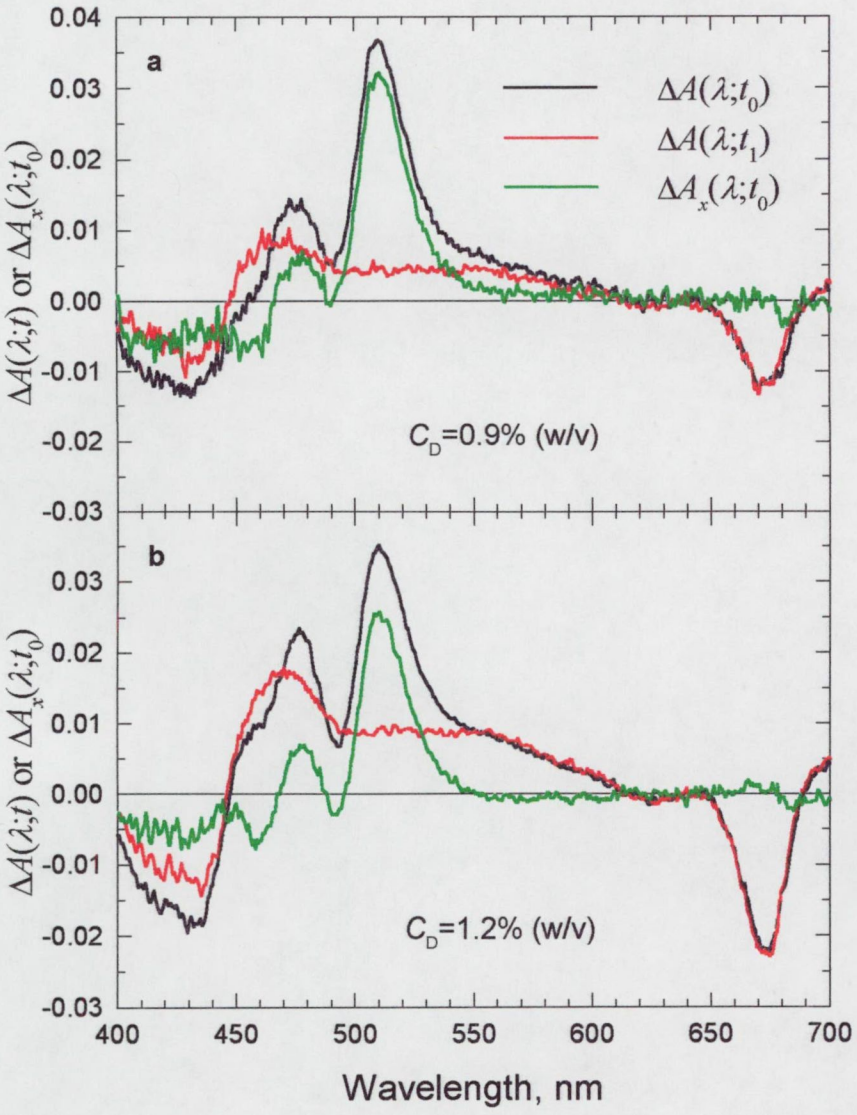

Fig. 20. *TmS spectra of LHCII at different detergent (n-OG) concentrations (C_D). The black and red curves represent spectra recorded at t_0=0.1 and t_1=40 μs delay, respectively, while the green ones display the contribution made by the xanthophylls.*

The relative magnitudes of the triplet yield (at different values of C_D), can be expressed, if the ratio $\hat{\rho}_a^x \equiv \hat{\varepsilon}_x^\dagger / \hat{\varepsilon}_a$ is known, by ratios of the function $Y(t)$ introduced above. Now, the values of $\hat{\varepsilon}_a$ in various organic solvents lie in the range 6–8×10^4 M^{-1} cm^{-1} (Lichtenthaler, 1987), but those of $\hat{\varepsilon}_x^\dagger$ show a much wider scatter, covering the range 1.3–2.4×10^5 M^{-1} cm^{-1} (Carmichael & Hug, 1986). Here we adopt the choice, namely $\hat{\rho}_a^x = 2.4$, made by Peterman and co-workers (1995) in a previous research dealing with LHCII, and add that our own investigations (of the triplet-triplet spectra of several Car's in organic solvents), concur with this choice.

When TX is used as the detergent, the behaviour of the TmS spectra differs from that seen in samples containing n-OG in two important respects: (*i*) a small fraction of the Chl triplets hand over their excitation to a Xan (within a few microseconds), which leads to a slight growth of the Xan signal and a concomitant decline in the Chl signal (Fig. 21), (*ii*) the shape of $\Delta A(\lambda;t_1)$ in the blue region (around 450 nm) is not independent of C_D (Fig. 22). If we ignore these noticeable but minor complications, and compensate for the loss of Chl*a* signal between t_0 and t_1 by multiplying $\Delta A(\lambda;t_1)$ with a numerical factor K so that $K\Delta A(\lambda;t_1)$ becomes indistinguishable, in the Q_y region of Chl*a*, from $\Delta A(\lambda;t_0)$, we may set $K\Delta A(\lambda;t_1) \equiv \Delta A_a(\lambda;t_0)$, and proceed as before. The contribution $\Delta A_x(\lambda;t_0)$ made by Xan to $\Delta A(\lambda;t_0)$ can be isolated by forming the difference $\Delta A_x(\lambda;t_0) \equiv \Delta A(\lambda;t_0) - K\Delta A(\lambda;t_1)$, and the relative values of the total initial concentration of Chl*a*† may be found by calculating $Y(t_0) \equiv \Delta A_x(\hat{\lambda}_x;t_0) - \hat{\rho}_a^x \Delta A_a(\hat{\lambda}_a;t_0)$.

The relative values of the triplet yields using n-OG or TX are presented in Table 2. These values show that the total yield of Chl*a* triplets increases with the concentration of detergent. That a growth in the triplet yield of Chl*a* accompanies the detergent-induced decrease in the efficiency of triplet transfer from Chl*a* to Car can be explained if we assume, as we did before when dealing with intact trimers, that internal conversion in Chl*a** is faster in the presence of a Car neighbour than that in the absence.

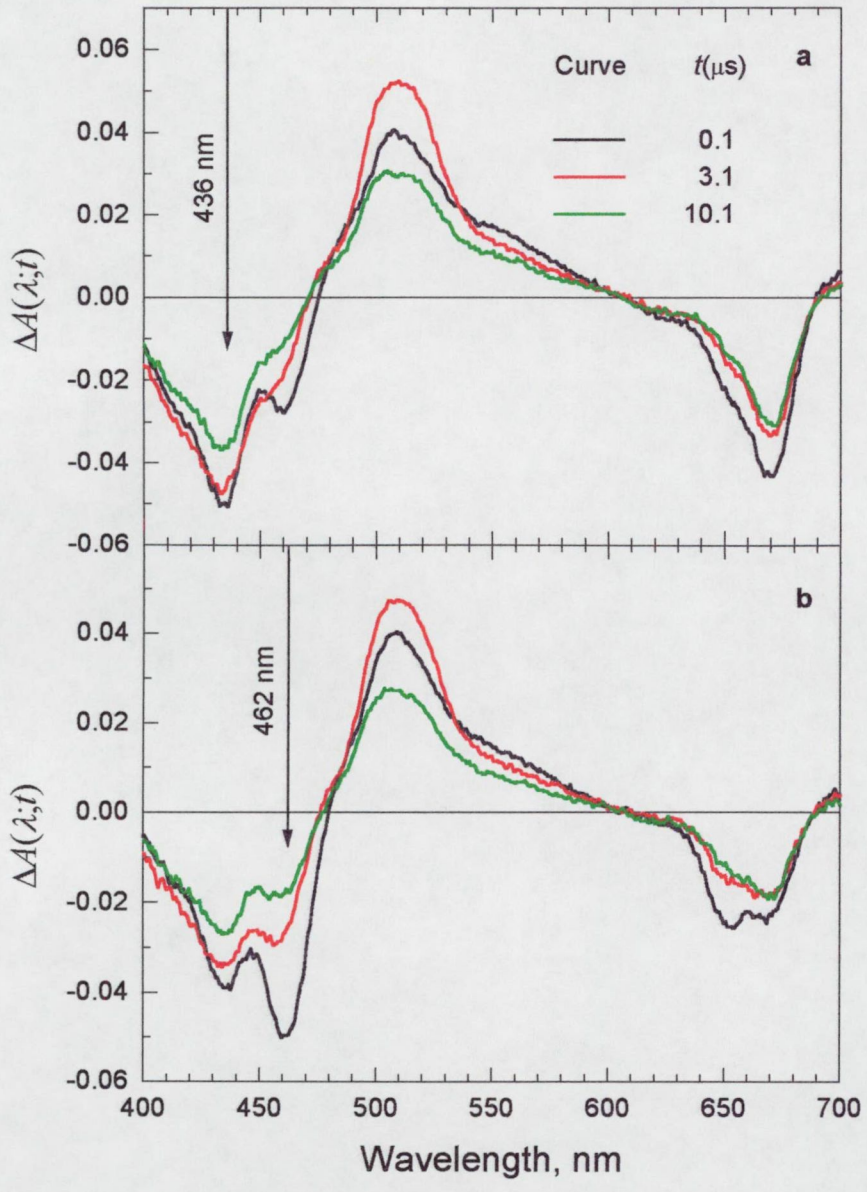

Fig. 21. *TmS spectra of LHCII suspension, at different delays, after the addition of 0.03% (v/v) TX showing a rise in the Xan peak and a concomitant decrease in the Q_y bleaching signal. The vertical arrows show the wavelength of excitation. At 462 nm laser excitation of* Chla *is negligible.*

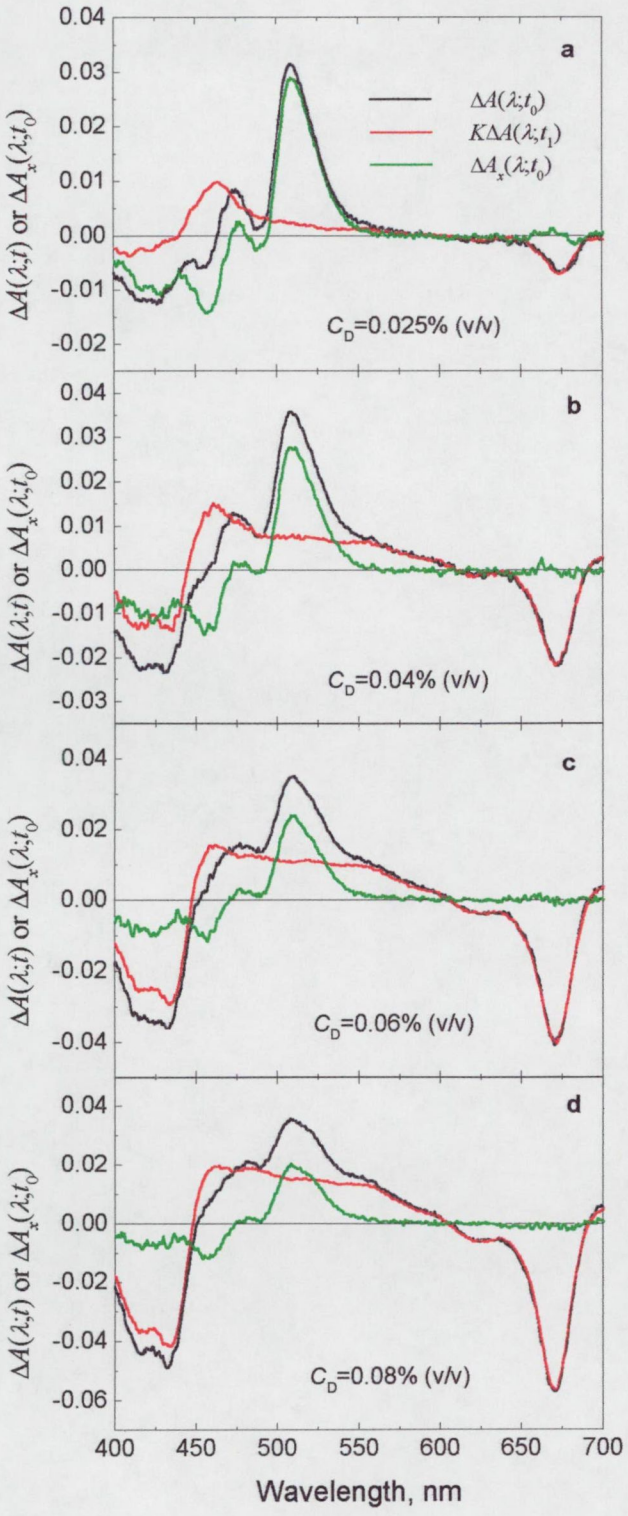

Fig. 22. *TmS spectra of LHCII suspension in the presence of different amounts of TX. The black and red curves represent spectra recorded at* t_0*=0.1 and* t_1*=40 μs delay, respectively, while the green ones display the contribution made by the xanthophylls. K is a normalization factor introduced to compensate for the loss of* Chl*a signal between* t_0 *and* t_1*. The wavelength of excitation is 672 nm.*

Table 2.
Dependence of the (relative) triplet yield on the concentration (C_D) of detergent (n-OG or TX)

Detergent	C_D (%)	Triplet yield (relative)
n-OG[a]	0.9	1
	1.2	1.3
TX[b]	0.025	1
	0.04	1.8
	0.06	2.6
	0.08	3.4

[a] w/v, [b] v/v

As one can see from Figs. 19b and 21b, Chl$b^{\dagger}$ makes a sizeable contribution to the TmS spectrum, which implies that singlet ET from Chl*b* to Chl*a* slackens to such extent that unimolecular processes become competitive with ET. Since we assess these spectral changes to the detergent-induced perturbation in the chromophoral organization of the trimer it would serve useful to introduce a new notation: two chromophores which are out of van der Waals contact will be represented by interposing a wedge (^) between their symbols. In intact trimers, where the pigments are in intimate contact, we can write the process of singlet ET from Chl*b* to Chl*a* like:

$$\text{Chl}a\text{:Chl}b^{*} \rightarrow \text{Chl}a^{*}\text{:Chl}b, \qquad (21)$$

which is known to occur on the (sub)ps time scale (Trinkunas *et al.*, 1997), thus preventing any unimolecular decay process for Chlb^{*}. The occurrence of Chl$b^{\dagger}$ in the TmS spectrum of perturbed aggregates leads us to conclude that the transfer efficiency from Chl*b* to Chl*a* drops down as a consequence of the change in the distance (and probably orientation) between the interacting chromophores. In this case process (21) can be written as:

$$\text{Chl}a \text{ ^ Chl}b^{*} \rightarrow \text{Chl}a^{*} \text{ ^ Chl}b. \qquad (22)$$

The separation between Chl*a* and Chlb^{*} to allow unimolecular decay of the latter cannot be calculated solely on the basis of Förster's formula (1965). More likely, electron exchange mechanism (Naqvi, 1980) gives a significant contribution to the observed fast

energy transfer rates in intact trimers, but this process becomes less and less important when the chromophores are torn apart by the detergent.

In intact trimers triplet excitation from Chl*a* is immediately (at least within 20 ns) transferred to Lut, where it is safely dissipated via internal conversion (Fig. 16). This process can be summarized as follows:

$$\text{Lut:Chl}a^{\dagger} \rightarrow \text{Lut}^{\dagger}\text{:Chl}a. \qquad (23)$$

However, in TX perturbed trimers one can see a rise in the population of $\text{Xan}^{\dagger}$ (on the time scale of μs) and a concomitant decline in the population of $\text{Chl}a^{\dagger}$ (Fig. 21). Since transfer of triplet energy occurs via electron exchange mechanism (Gilbert & Baggott, 1991), the chromophores, separated by the detergent, must first get into contact in order to participate in the process. This diffusion-mediated transfer of triplet energy can be depicted as:

$$\begin{array}{ccc} \text{Xan} \wedge \text{Chl}a^{\dagger} & & \text{Xan}^{\dagger} \wedge \text{Chl}a \\ \downarrow & & \uparrow \\ \text{Xan:Chl}a^{\dagger} & \rightarrow & \text{Xan}^{\dagger}\text{:Chl}a. \end{array} \qquad (24)$$

Whether the acceptor is a Lut or any other Xan in this process is not possible to decide. The reason why process (24) cannot be seen when n-OG was used as the detergent maybe due to the fact that the concentration of n-OG is almost two orders of magnitude higher than that of TX, and the average separation between the detached chromophores is too large to allow a momentary encounter between a $\text{Chl}a^{\dagger}$ and a Xan.

As we increase the concentration of detergent in the sample and the van der Waals contact between the chromophores in the triads Chl*b*:Chl*a*:Lut of the intact trimer are torn apart, transformation of process (21) into (22) and process (23) into (24) takes place, resulting a decline in the corresponding singlet and triplet transfer efficiencies. As a consequence, $\text{Chl}a^{*}$ suffers less quenching than before, resulting an increase in the quantum yields of fluorescence emission and intersystem crossing.

Triplet spectra of some photosynthetic carotenoids

The singlet-singlet ($S_2 \leftarrow S_0$) absorption spectra and extinction coefficient for more than 100 Car is well documented (Britton, 1995). The location of the band as well as the extinction coefficient is sensitive to the polarizability of the medium surrounding the chromophore, i.e. the position of the band can be shifted significantly by changing the solvent (Andersson *et al.*, 1991). Much less is known, however, about the triplet absorption properties of these Car's. Apart from very few exceptions (Carmichael & Hug, 1986), the extinction coefficients of the triplet peak have not been determined, nor has there been a systematic investigation of the influence of the solvent on the location of this peak. Accordingly, we decided to record the triplet-triplet spectra of some Car's, including the three Xan's (Lut, Neo and Vio) which are bound to LHCII.

Three different solvents, acetone, 95% ethanol (EtOH) and dimethyl sulfoxide (DMSO) were used. The reason for choosing these solvents was the availability of sufficient purity, the good solubility of the pigment molecules and the relatively wide range of polarizability and viscosity.

Since the triplet state of the Car's cannot be directly populated we used Chl*a* molecules as triplet energy donors. The concentrations of the chromophores were chosen so as to obtain efficient energy transfer, while at the same time minimize Chl*a* triplet-triplet annihilation. Typical values were 8 μM for Lut and 4 μM for Chl*a*.

The triplet-triplet ($T_n \leftarrow T_1$) absorption spectra ($A_T(\lambda)$) were recorded in two steps. First we obtained the TmS spectrum of the sample at two delays: at t_0=50 ns and at t_1=25 μs (Fig. 23). The short delay spectrum is essentially the TmS spectrum of Chl*a*, ($\Delta A_a(\lambda;t_0)$) since hardly any ET could take place in such a short time, while the long delay spectrum is the superposition of TmS spectra of Chl*a* and Car ($\Delta A(\lambda;t_1)$). The TmS spectrum of Car ($\Delta A_c(\lambda;t_1)$) can be extracted by normalizing the long delay spectrum so as to coincide with the short delay one in the Q_y region of Chl*a*, than subtract the short delay spectrum from the normalized one:

$$\begin{aligned} \Delta A(\lambda;t_1) &= \Delta A_c(\lambda;t_1) + \Delta A_a(\lambda;t_1) \\ \Delta A_c(\lambda;t_1) &= \Delta A(\lambda;t_1) - \Delta A_a(\lambda;t_1) \\ N\Delta A_c(\lambda;t_1) &= N\Delta A(\lambda;t_1) - \Delta A_a(\lambda;t_0), \end{aligned} \tag{25}$$

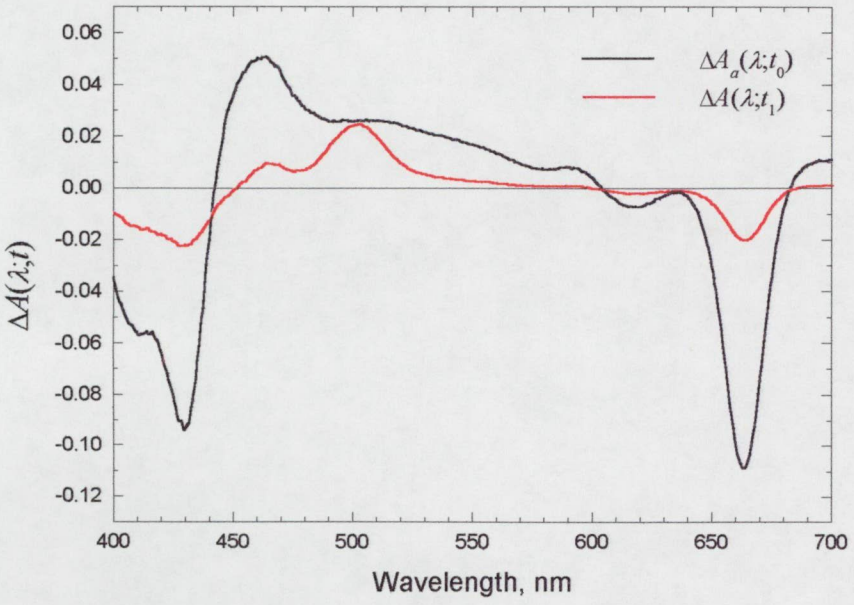

Fig. 23. *TmS spectra of the admixture of* Chl*a and* Lut *at two different delays (t_0=50 ns and t_1=25 μs). The solvent is acetone.*

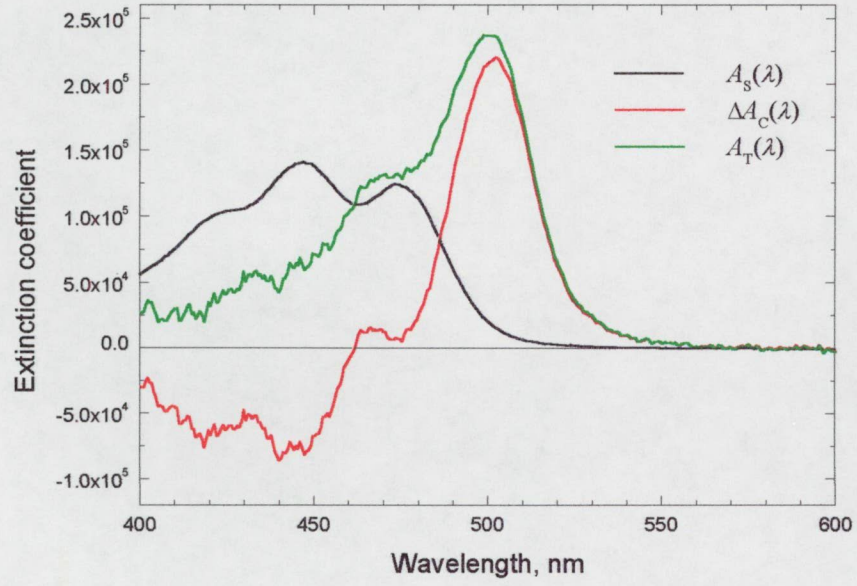

Fig. 24. *Singlet absorption (black), triplet absorption (green) and TmS spectra (red) of* Lut *in acetone.*

where N was chosen so to satisfy:

$$N\Delta A(\lambda;t_1) = \Delta A_a(\lambda;t_0) \tag{26}$$

in the Q_y region of Chl*a* ($\lambda \geq 590$ nm).

Since the TmS spectrum is a superposition of $A_T(\lambda)$ and the singlet absorption spectrum ($A_S(\lambda)$), forming a linear combination of $\Delta A_c(\lambda;t_1)$ and $A_S(\lambda)$ of the Car, recorded at the same spectrophotometer, will result $A_T(\lambda)$:

$$A_T(\lambda) = N\Delta A_c(\lambda;t_1) + nA_S(\lambda). \tag{27}$$

One has to choose n by using common sense keeping in mind that it should be large enough to bring $A_T(\lambda)$ to the positive region without giving too much feature from $A_S(\lambda)$.

Fig. 24 shows a typical set of $A_S(\lambda)$, $\Delta A_c(\lambda;t_1)$ and $A_T(\lambda)$. Instead of presenting a multitude of similar spectra, we can summarize our results in the following: Only one vibronic progression (with a vibrational spacing of ca. 1300 cm^{-1}) could be observed in the 250-900 nm spectral region. It overlaps, but is red-shifted ($\leq 10^3$ cm^{-1}) with respect to the $S_2 \leftarrow S_0$ absorption progression, which has a similar vibrational spacing. In the triplet spectrum the 0-0 peak (T_{00}-peak) is the most intense one, in contrast with the singlet spectrum, where the 1-0 peak is always larger than the 0-0 peak (S_{00}-peak). The location of the peaks in the singlet and triplet spectrum moves, as the solvent changes, by almost the same amount, as one can see from Table 3.

Table 3.
The location of the most intense singlet and triplet peaks of carotenoids in different solvents: acetone, 95% ethanol (EtOH) and dimethyl sulfoxide (DMSO)

	$\lambda(S_{10})$			$\lambda(T_{00})$		
	Acetone	**EtOH**	**DMSO**	**Acetone**	**EtOH**	**DMSO**
Neoxanthin	440	439	449	487	487	501
Violaxanthin	441	440	453	486	484	499
Lutein	447	445	458	501	498	517
Lycopene	473	472	–	526	524	–
β-carotene	453	451	–	513	511	–

Identifying the triplet peaks in LHCII

The previously covered solvatochromism of singlet and triplet absorption spectra of Lut, Neo and Vio might give us a clue to the location of the singlet and triplet peaks of these Xan's in LHCII. The location of the 0-0 peaks (depicted in Fig. 25 as a stick spectrum) moves, as the solvent changes, in this case from acetone to DMSO, by almost the same amount. Since this pattern was observed in a variety of solvents, we assume that the same holds for the protein environment as well.

The spectral assignments due to Peterman *et al.* (1997), as it was recalled in the Introduction, are recapitulated in Fig. 26. They attribute the triplet peaks at 506 and 525 nm to Lut and Vio (Fig. 26b), and place the corresponding singlet peaks at 494 and 510 nm (Fig. 26a); this is consistent with our data on the separation between the T_{00}-peak and the S_{00}-peak of a Xan in different solvents. Had Neo, whose S_{00}-peak lies, according to them, at 486 nm, made a sizeable contribution to the TmS spectrum, its T_{00}-peak would have been manifested around 500 nm. The absence of such a peak in the spectrum of LHCII (monomers and trimers) implies that Neo triplets, if formed, hand over their excitation to Lut or Vio.

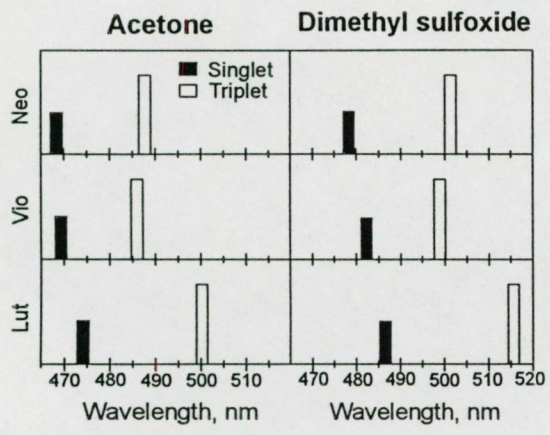

Fig. 25. *A schematic representation of the solvent-induced shift in the position of the xanthophyll absorption bands. Only the 0-0 peaks are shown here; the relative heights of the singlet and triplet peaks are only rough guides to the actual intensities.*

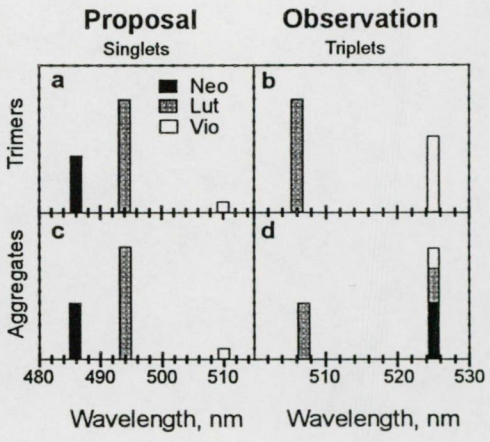

Fig. 26. *The proposed locations and heights of the S_{00}-peaks in the trimers (a, Peterman et al., 1997) and in the aggregates (c); the observed values (positions and total heights of the two T_{00}-peaks) and assignments in the trimers (b, Peterman et al., 1997) and in the aggregates (d, van der Vos et al., 1994).*

We have shown recently, that when allowance is made for scattering and sieving, the absorption spectrum of LHCII aggregates turns out to be almost identical with that of the trimers (Naqvi, K. R. *et al.*, 1997a). On the basis of this finding we can conclude that the spectral assignments for triplets, shown in Fig. 26a, should hold for aggregates too, as it is depicted in Fig. 26c. One is led to infer then, if all three Xan's contribute to the TmS spectrum of the aggregates, peaks would be seen around 500, 506 and 525 nm. Upon examining the TmS data on aggregated LHCII (van der Vos *et al.*, 1991 and 1994), as it was recalled in the Introduction, one finds two peaks (at 507 and 525 nm). The authors have attributed the 507 nm peak to Lut, and the 525 nm peak to all three Xan's (Fig. 26d). Our results on the solvent induced shifts of the singlet and triplet absorption bands of LHCII Xan's, however, does not support the presumed location of the S_{00}-peak of Neo in LHCII aggregates and trimers.

Photophysical characterization of two model antenna systems

In the past two decades, caroteno-porphyrin and caroteno-pyropheophorbide molecular dyads were studied as models of natural antenna systems (Bensasson *et al.*, 1981; Moore *et al.*, 1982; Gust *et al.*, 1992). In these dyads a Car moiety is attached covalently to a tetrapyrrole pigment (Pyr). Such a bichromophoric system performs, if its structure permits close contact between Car and Pyr, two important tasks of a photosynthetic antenna complex (Frank & Cogdell, 1996), namely light-harvesting and quenching of Pyr triplets. An additional process, the quenching of Pyr fluorescence, takes place in the dyad even if its structure is not suited to the above functions (Bensasson *et al.*, 1981). However, the S_1 state of the particular Car (7'-apo-7'aryl-β-carotene) used in the first-generation dyads is believed to be lower than that of Pyr (Young & Frank, 1996), and the observed quenching of Pyr fluorescence might well have been caused by singlet ET from Pyr to Car. The two dyads used in our investigations (Osuka & Kume, 1998) circumvent this decay channel, being the S_1 state of the Car moiety (fucoxanthin or peridinine) higher than that of the Pyr moiety, a methyl pheophorbide *a*.

The interaction between the two chromophores in each dyad is so weak that the absorption spectrum of the dyad, can be well approximated by the sum $S(\lambda)=A_P(\lambda)+A_C(\lambda)$, where $A_P(\lambda)$ is the absorbance of Pyr, and $A_C(\lambda)$ the absorbance of the unattached Car. Since the absorption spectra of **Φ**, **F-Φ** and **P-Φ** in the 590–690 nm region (when dissolved in the same solvent) are nearly identical, as are their fluorescence emission spectra, the determination of the fluorescence yield (denoted by ϕ_F) of **F-Φ** or **P-Φ** (relative to that of **Φ**) can therefore be carried out with ease and confidence if one is using an excitation wavelength lying in the above spectral region. If the relative yield of **F-Φ** or **P-Φ** comes out to be lower than unity, the reduction would imply quenching of Pyr fluorescence by the adjoining Car.

The conclusion that both fucoxanthin and peridinin are capable of such quenching, was arrived at by measuring the relative quantum yields of the Pyr emission under photostationary conditions. The data are shown in Table 4. I have to point out, that our results were confirmed by the fluorescence life-time measurements of two of our co-

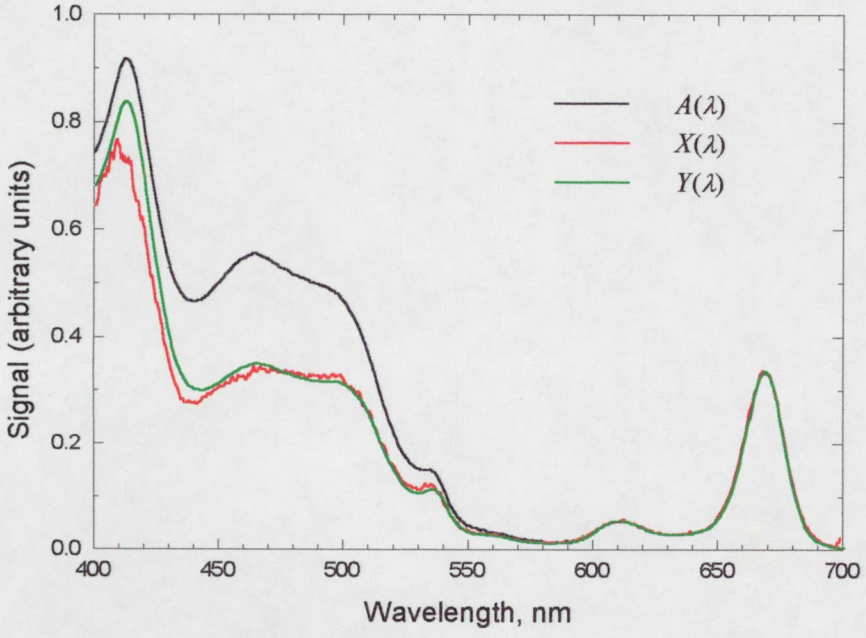

*Fig. 27. The absorption (black) and corrected fluorescence excitation (red) spectra of one of our dyads, peri-pheophorbide (**P-Φ**), when dissolved in tetrahydrofuran. The green curve shows the linear combination of the absorption spectra of the individual compounds. The spectral region below 430 nm should be disregarded because the response of the Golay cell used for measuring the excitation intensity is not flat in this region.*

Table 4.

The (relative) fluorescence yield (ϕ_F) and light-harvesting efficiency (ϕ_{LH}) of the two caroteno-pyropheophorbide dyads in two different solvents: tetrahydrofuran (THF) and dimethyl sulfoxide (DMSO).

	in **THF**			*in* **DMSO**	
	ϕ_F	ϕ_{LH}		ϕ_F	ϕ_{LH}
Φ	1	n.a.		1	n.a.
F-Φ	0.90±0.05	0.20±0.01		0.82±0.05	0.13±0.01
P-Φ	0.90±0.05	0.62±0.03		0.61±0.05	0.18±0.01

workers, João Carlos Lima and Eurico Melo (Osuka *et al.*, 1999), whose data are not shown here.

The light-harvesting efficiency, ϕ_{LH}, of each dyad was determined by recording $X(\lambda)$, the fluorescence excitation spectrum, and fitting it to the function $Y(\lambda)\equiv N\times[A_P(\lambda)+\phi_{LH}\,A_C(\lambda)]$. The value of N is fixed by making $X(\lambda)$ agree with $Y(\lambda)$ in the 590–690 nm region, where $A_C(\lambda)$ is negligible. ϕ_{LH} is found by adjusting its value so as to bring the two curves into near coincidence in the 430–600 nm region, where $A_C(\lambda)$ is not negligible. The region between 400 and 430 nm should be disregarded because the response of our Golay cell used for measuring the excitation intensity is not flat in this region. A typical set of the measured and simulated extinction spectra, together with the absorption spectrum, is shown in Fig. 27. The results are arranged in Table 4.

The TmS spectra of the two dyads, when dissolved in tetrahydrofuran (THF), are presented in Fig. 28. In **F-Φ**, (Fig. 28a) the difference spectrum at a delay of 20 ns is essentially the TmS spectrum of **Φ**, hence we call it a Pyr-type spectrum. Within 1 μs, nearly half of the initially generated Pyr triplets transfer their excitation energy to the Car, while the other half decay at a significantly slower rate. The behaviour of **P-Φ**, displayed in Fig. 28b, is rather different. In this case, the triplet ET from Pyr to Car is so fast that even the shortest delay spectrum is dominated by features identifiable with the Car triplet, and the few Pyr triplets which escape the fast transfer are quenched within 200 ns. Therefore we refer the spectrum as Car-type. For delays larger than 200 ns, the entire spectrum (including the residual negative signal around 670 nm) decays at the same rate, a trait observed in natural light-harvesting complexes (van der Vos *et al.*, 1991; Angerhofer *et al.*, 1995; Peterman *et al.*, 1995; Naqvi *et al.*, 1997b; Büchel *et al.*, 1998). Since the Car's do not absorb around 670 nm, the negative signal in the TmS spectrum can be explained if one assumes that the extinction coefficient of Pyr depends on the electronic state of its Car neighbour (van der Vos *et al.*, 1991).

Similar results were obtained when we changed the solvent to acetone, 95% EtOH or 2-propanol. In each of these solvents the TmS spectrum, recorded at the shortest delay (20 ns), of **F-Φ** was Pyr-type, while that of **P-Φ** was Car-type. When DMSO was used as the solvent, the shortest delay spectrum of **P-Φ** changed to a hybrid, with roughly equal

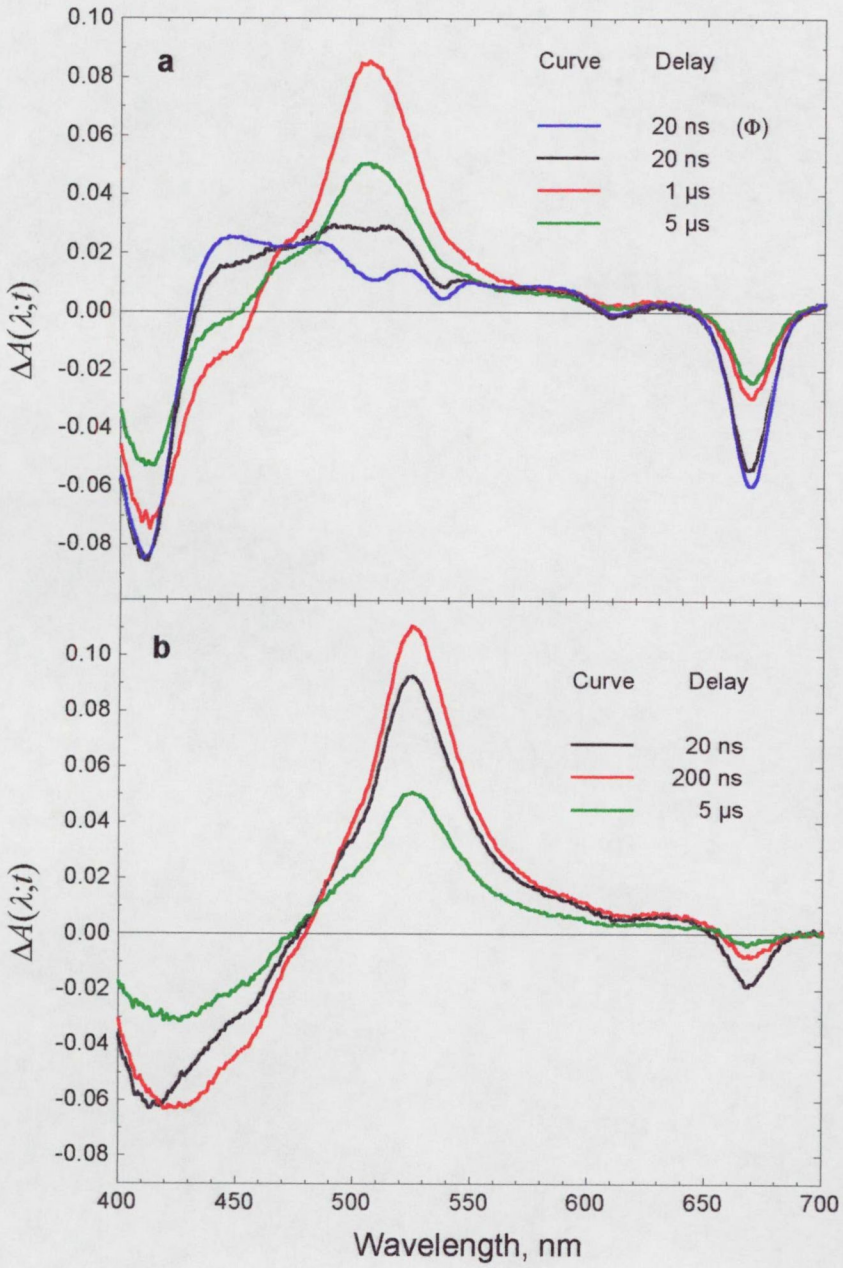

Fig. 28. *TmS spectra, at different delays, of the two dyads (***F-Φ** *in panel* ***a*** *and* **P-Φ** *in panel* ***b****) when dissolved in tetrahydrofuran. The TmS spectrum of pyropheophorbide-a (Φ) obtained at the shortest delay time (20 ns) is also plotted in panel* ***a*** *(blue curve).*

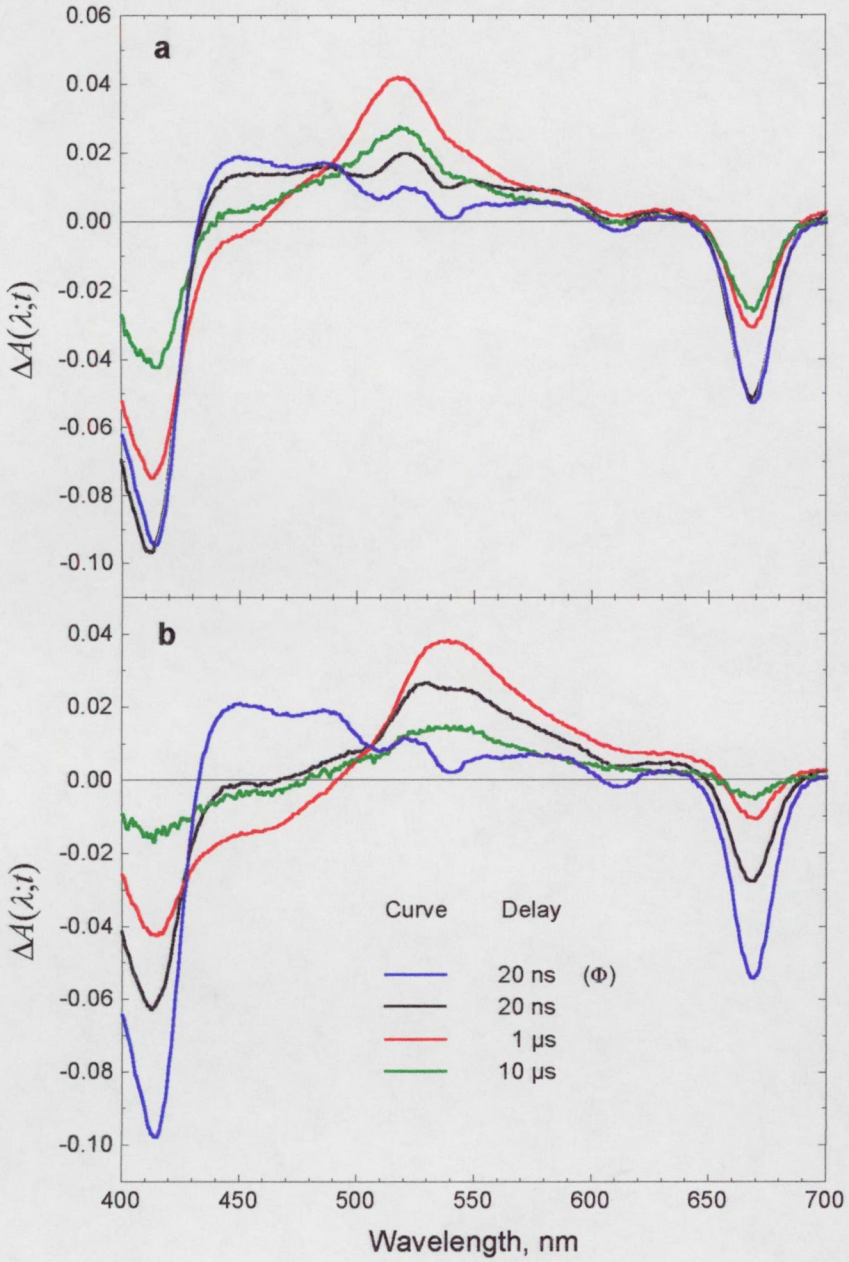

Fig. 29. *TmS spectra, at different delays, of the two dyads (***F-Φ** *in panel* ***a*** *and* **P-Φ** *in panel* ***b****) when dissolved in dimethyl sulfoxide. The TmS spectrum of pyropheophorbide-a (Φ) obtained at the shortest delay time (20 ns) is also plotted (blue curve). The same legend applies for both panels.*

contributions from Pyr and Car triplets, whereas that of **F-Φ** remained a Pyr-type spectrum. These results are plotted in Fig. 29.

On the basis of our TmS data we can conclude that, apart from the spectral similarity of fucoxanthin and peridinin, **F-Φ** and **P-Φ** adopt different conformations in a given solvent. Apparently **F-Φ** is having conformations (in all the solvents mentioned above) most of which are unfavourable for rapid electron exchange, while as for **P-Φ**, we must divide the solvents into two groups. In DMSO only about half of the conformations are suited for rapid electron exchange, while in the other solvents, the vast majority of conformations allow electron exchange within 20 ns. It is worth mentioning that these conclusions are supported by computer simulation data of one of our co-workers, Greg Haggquist (Osuka *et al.*, 1999). The optimal folded conformations of both dyads, as a result of molecular modelling, are shown in Fig. 30. According to Fig. 30, the π-orbitals of the Car-Pyr moieties are parallel in **P-Φ**, allowing significant overlap, but tilted in **F-Φ**.

Another interesting feature of **P-Φ** is worth pointing out. Table 4 shows that **P-Φ**, when dissolved in THF, has high values of ϕ_F and ϕ_{LH}, and that both yield fall when the solvent is changed to DMSO. This observation implies that a conformation well suited for quenching need not be favourable for light-harvesting. Indeed, if the goal is to switch over from light-harvesting to energy dissipation, a parallel decline in both yields, as seen here, offers a more effective means of achieving the goal.

The exact locations of the S_1 states of fucoxanthin and peridinin are not known with certainty. The published fluorescence spectra of these Car's (Mimuro *et al.*, 1992) place them around 16200 cm^{-1}, which is higher than the S_1 state of Chl*a* or **Φ**. From a quantum mechanical point of view, the bleaching signal in the TmS spectra and the quenching of Pyr fluorescence by an adjacent fucoxanthin or peridinin may be grasped if (but only if) one goes beyond the traditional, first-order description of energy transfer, and allows for an admixture of the wave functions of the interacting partners (Naqvi, 1998b). When allowance is made for such mixing, indirect quenching (via virtual transitions involving one or more intermediate states), in which Car acts as an energy sink, is predicted. It is worth adding here that in a recent publication a sizeable mixing of the electronic states of carotenoid and bacteriochlorophyll was predicted in the LH2

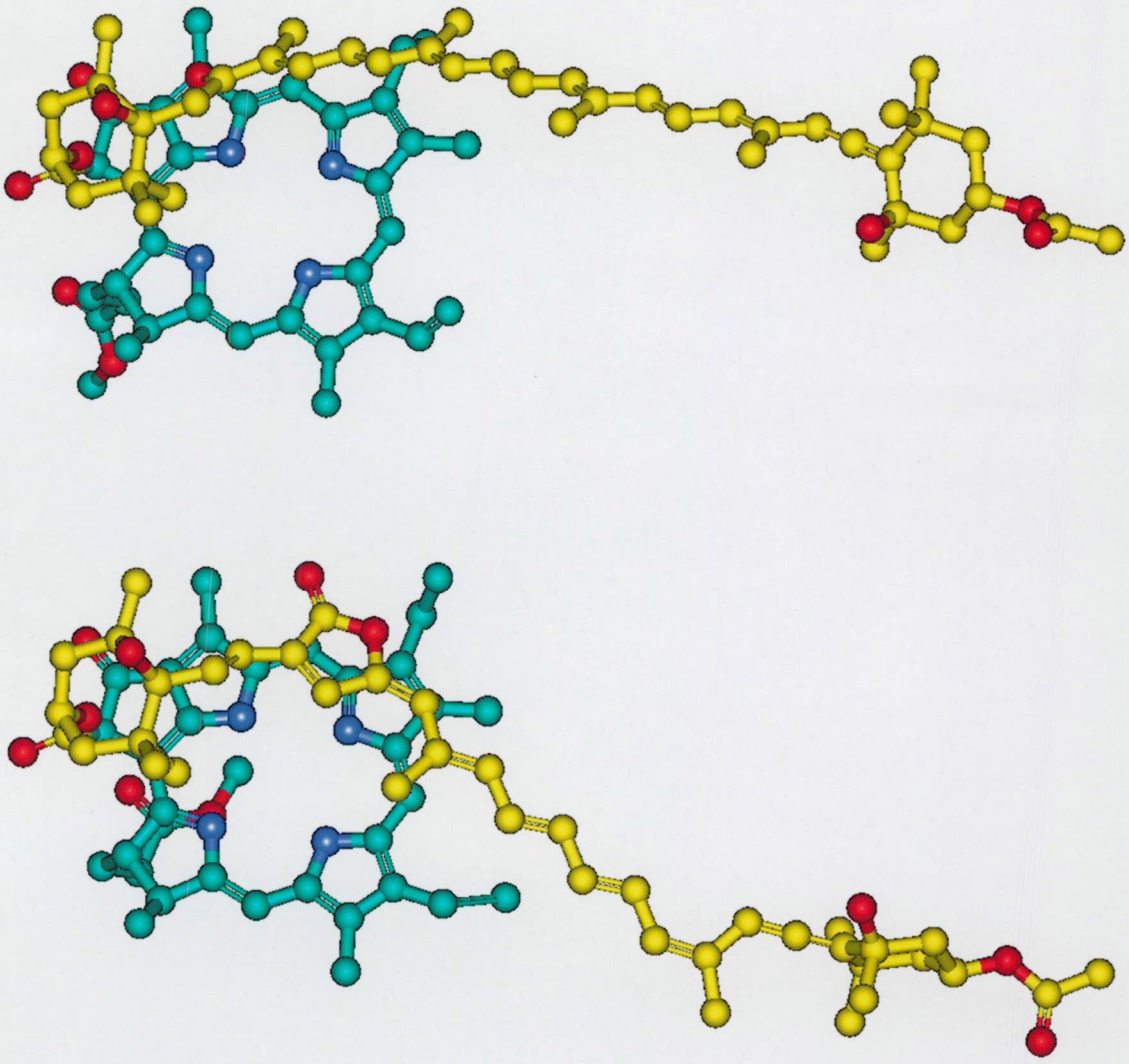

Fig. 30. *Minimum energy folded structures of the two dyads,* **F-Φ** *(top) and* **P-Φ** *(bottom), found by molecular dynamics calculations, as it was reported in (Osuka et al., 1999). Visualization was done by the software VebLab ViewerPro from Molecular Simulations Inc. Green colour shows the pyropheophorbide-a molecule, while yelow represents the attached carotenoid (fucoxanthin in* **F-Φ**, *and peridinin in* **P-Φ**). *Red and cyan atoms are oxygen and nitrogen. One can see from this picture that the π-orbitals (along the double-bonds) are considerably overlapping in* **F-Φ**, *but tilted in* **F-Φ**.

complex (the bacterial light-harvesting antenna system) by means of *ab initio* quantum chemical calculations (Krueger *et al.*, 1999).

The hypothesis that Car's in a natural antenna system, where they are usually in van der Waals contact with Chl's, drain energy away from the S_1 state of Chl pigments (Owens *et al.*, 1992; Frank & Cogdell, 1996) has failed to gain general acceptance. A Car can evidently act as an acceptor of electronic excitation if energy flows downhill from Chl, as is the case when Chl triplets are quenched, or when the S_1 state of the Car happens to be lower than that of Chl (Polivka *et al.*, 1999). Our data show that a Car which is unable to function as an energy acceptor can still bring about the quenching of Chl fluorescence. It supports our hypothesis, that the mechanism of catalysed internal conversion — which we have shown to operate regardless of the relative energy levels of the compounds — should not be disregarded when one is about to interpret the quenching in natural antenna complexes.

Metastable states in chloroplasts and in thylakoid membranes

The absence of a Q_y bleaching signal in the TmS spectrum of isolated chloroplasts, as it was reported by Wolff and Witt (1969), and a presence of such a signal in LHCII, an integral protein of thylakoid membranes (van der Vos *et al.*, 1991; Peterman *et al.*, 1995; Naqvi *et al.*, 1997b), led us to the urge to reinvestigate the situation. The difference in the behaviours of chloroplasts and LHCII, if reproducible, would imply that the Car triplets, which give rise to the TmS spectrum of chloroplasts, do not influence the absorption spectra of their Chl*a* neighbour. With a view to reaching a firm conclusion on this issue we reinvestigated the TmS spectrum of spinach chloroplasts and thylakoid membranes under the same experimental conditions which were used to examine LHCII.

Fig. 31 shows the TmS spectra obtained by irradiating a suspension of chloroplasts under anaerobic conditions. It is apparent that the half-life of the triplets is close to 5 μs. The spectra obtained by using aerated samples (not shown), though very similar, showed signs of contamination from free Chl triplets (probably released as a result of photodamage in the presence of oxygen). The half-life of the triplets in this case was estimated to be 2.2 μs. The TmS spectra of argon-bubbled suspensions of thylakoid membranes are displayed in Fig. 32.

All the spectra shown in Figs. 31 and 32 contain a negative signal centered at 680 nm, and their overall shape bears a great resemblance to the recently published TmS spectra of the following systems: Chl *a/b*-LHCII (van der Vos *et al.*, 1991; Peterman *et al.*, 1995; Naqvi *et al.*, 1997b), PCP complexes isolated from dinoflagellates (Carbonera *et al.*, 1996), Chl *a/c*-LHCII and thylakoids of *P. meirengensis* (Büchel *et al.*, 1998), bacterial antenna complexes (Angerhofer *et al.*, 1995) and chlorosomes (Melø *et al.*, 2000) and synthetic bichromophoric systems (Osuka *et al.*, 1999). Furthermore, our estimates of the half-life of Car triplets in chloroplasts (ca. 2.2 μs in aerobic conditions and ca. 5 μs in argon-bubbled samples) are in excellent agreement with those reported by Mathis *et al.* (1979). The half-life of Car triplets in deoxygenated suspensions of thylakoid membranes, estimated from an examination of the two spectra in Fig. 32, is slightly longer than 5 μs. Since no attempt was made to measure the final oxygen concentration in the samples, no significance is attached to the differences between the

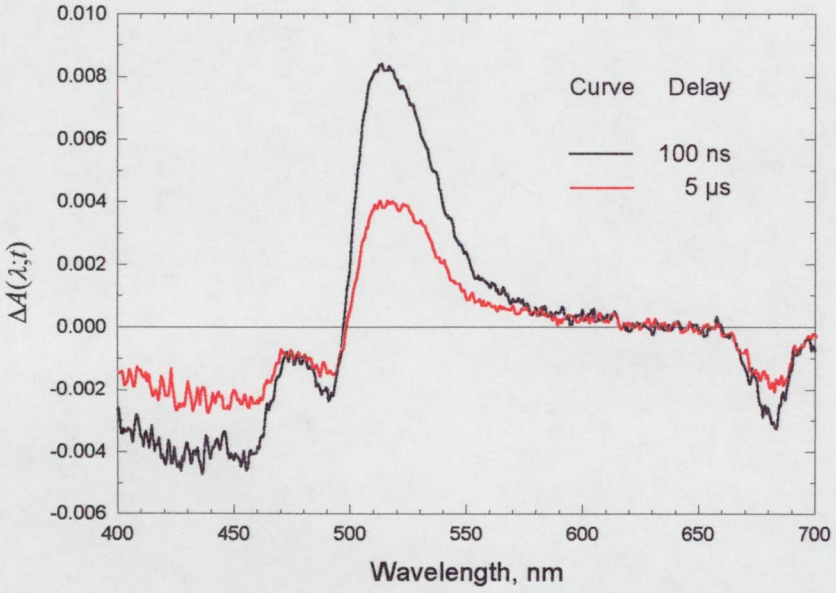

Fig. 31. *TmS spectra of the suspension of chloroplasts at two different delays.*

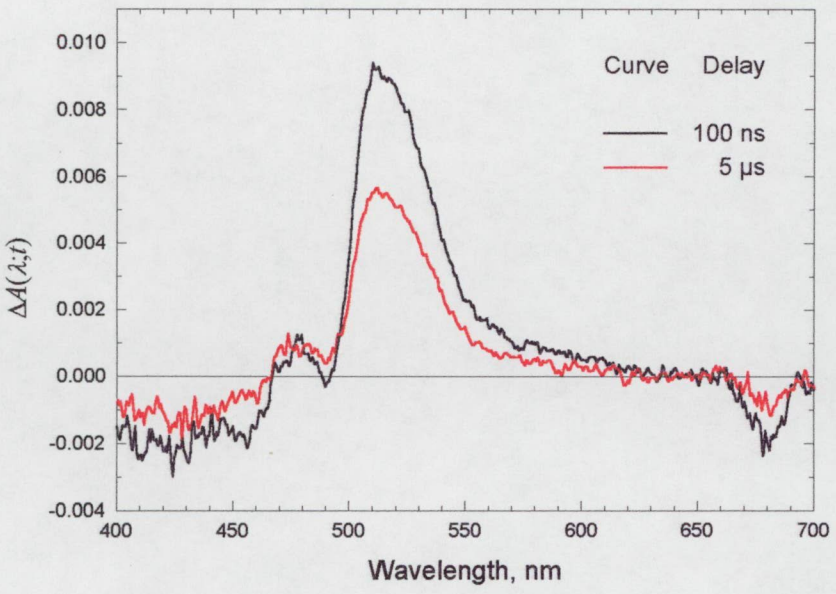

Fig. 32. *TmS spectra of the suspension of thylakoid membranes at two different delays.*

decay times in chloroplasts and thylakoids. Essentially the same spectra and lifetimes were obtained when DCMU or gramicidin was added to suspensions of thylakoids.

We conclude, on the basis of the spectra presented here and mentioned earlier, that the TmS spectrum of chloroplasts is similar to the TmS spectra of other natural and artificial systems where Car's and Pyr's are in intimate contact. This means that, in all the systems examined so far, a Car, which is situated so as to accept, within 100 ns or so, triplet excitation from a Pyr affects the singlet-singlet absorption spectrum of the latter. This effect, which was observed as a bleaching signal in the Q_y region of Pyr, imply that a proper description of the electronic states of a Pyr:Car pair can be obtained only by allowing the mixing of the zero-order states of the pair (Naqvi, 1998b). Such a treatment would also imply the mechanism of catalysed internal conversion via virtual transitions to and from intermediate states. On the basis of our observations we can conclude that the mechanism of catalysed internal conversion operates also in chloroplasts, providing a channel for the dissipation of excess excitation energy in green plants.

CONCLUSIONS

Our investigations on the interactions between Car's and Chl's (or Chl-like molecules) in LHCII (at different level of molecular organization), in caroteno-pheophorbide dyads and in chloroplasts have led us to the following conclusions:

- When allowance is made for scattering and sieving, the absorption spectrum of LHCII aggregates turns out to be almost identical with that of the trimers. Intertrimer interactions due to aggregation exert little influence on the absorption spectrum of the trimers. It implies that the rate constant for radiative relaxation of Chl*a** is not affected by aggregation. As a byproduct of our investigations we have the possibility to estimate the size of the aggregates. Our analysis of the trimer–aggregate system provides the first experimental evidence for the applicability of Duysens' method for the correction of the absorption spectra of turbid samples (Naqvi *et al.*, 1997a).
- Our data have revealed that, when aggregates disassemble into trimers, the peripheral Xan's cease to contribute to the TmS spectrum, thereby narrowing the positive absorption band associated with Car†. Consequently, the bleaching signal in the Q_y region of Chl*a* — due to an adjacent Car† — is less pronounced in isolated trimers than that in the aggregates. Although the 100% efficiency of triplet ET from Chl*a* to Car and the lifetime of Car† are not affected by aggregation, the triplet formation yield decreases significantly. Taking into account the parallel decrease of the fluorescence yield we hypothesize that Car's enhance the internal conversion rate of the nearby Chl*a* molecules. The process of Car-mediated catalysed internal conversion (CIC) provides a channel for the non-photochemical dissipation of excitation energy of Chl*a* (Naqvi *et al.*, 1997c).
- Detergent induced perturbation of the chromophoric organization of the complex severs the contact between the chromophores to such an extent that Chl*b*† starts to form, as a deactivation product of Chl*b**, competing with singlet ET from Chl*b* to Chl*a*. The triplet yield of Chl*a* continues to increase and the efficiency of triplet ET from Chl*a* to Car decreases. These results can be grasped if we assume, as we did in the case of intact trimers, that the internal conversion in Chl*a** is faster (slower) in the presence (absence) of a Car neighbour (Naqvi *et al.*, 1999).

- Triplet absorption spectra of some Car's revealed only one vibronic progression in the 250-900 nm region, which belongs to the same electronic transition. The 0-0 peak was found to be the largest in contrast with the singlet absorption spectrum, where the 1-0 peak is the most intense. It overlaps but is red-shifted with respect to the singlet absorption progression and the two spectra move by almost the same amount, as the solvent changes (Jhutti *et al.*, 1998; Jávorfi & Naqvi, 1999). These results do not coincide with the previously proposed assignments of the location of Xan triplet absorption peaks in LHCII.
- In caroteno-pyropheophorbide dyads, where the relative energy levels are not favourable for singlet ET back to the Car moiety, quenching in the pheophorbide fluorescence was observed. Depending on the Car moiety and the solvent, the dyad adopts different conformations. Though fluorescence quenching was observed regardless of the conformation, $Car^{\dagger}$-induced bleaching signal in the Q_y region of the partner molecule is present only if the conformation of the dyad allows fast (within about 100 ns) transfer of triplet excitation, i.e. considerable overlap of the π-electrons between the chromophores. These results indicate that the mechanism of catalysed internal conversion may still provide a relaxation channel even if the energy levels are not suitable for transfer of excitation energy. It supports our previous hypothesis that one should consider indirect effects, such as the catalysed internal conversion, when trying to explain non-photochemical quenching in natural antenna systems (Osuka *et al.*, 1999).
- Our investigation on the TmS spectra of intact chloroplasts and thylakoid membranes revealed — in contrast what was published earlier — a bleaching signal in the Q_y region of Chl*a*, similar to those found in a wide variety of natural antenna complexes as well as in artificial systems, where a Chl (or a Chl-like molecule) and a Car was in intimate contact (Jávorfi *et al.* 1999). This result implies that the mechanism of catalysed internal conversion also operates in green plants.

ACKNOWLEDGEMENTS

I wish to thank Dr. Győző Garab, who initiated this work, for his great support and help during the past few years.

I am very grateful to Prof. K. Razi Naqvi for giving me the opportunity to work in his laboratory and for the excellent guidance and motivating conversations during the time I spent in Norway.

Thanks are due to Prof. Dénes Dudits, general director of the Biological Research Center (former director of Institute of Plant Biology) and to Dr. Imre Vass, director of Plant Biology, for supporting our work in Szeged.

I would like to thank to all my colleagues from the Biological Research Center as well as from the Norwegian University of Science and Technology for their support, cooperation and patience.

The warmest thanks to my parents and to all those friends and acquaintances who helped me during all this time and gave me moral support.

I would like to acknowledge the financial support I received from various foundations and organizations (European Science Foundation Programme of Biophysics of Photosynthesis, The Research Council of Norway, Magyar Ösztöndíj Bizottság). The work described here was supported by The Research Council of Norway (NFR) and by grants (T 017827 and T 019226) awarded by the Hungarian Research Fund (OTKA).

SUMMARY OF THE THESIS

Photosynthesis is undoubtedly one of the most important processes on planet Earth. Almost all of the life-forms rely on the products of photosynthetic organisms such as algae, higher plants and certain bacteria. These organisms are able to capture energy directly from the solar radiation and utilize it for the synthesis of energy-rich chemical compounds, which can serve as food for other life-forms. The whole course of photosynthesis can be divided into two distinct parts. The initial steps, which require the presence of light, involve the process of water splitting (oxygen evolution) and the production of energy-rich ATP and NADPH. These compounds are utilized in the second part of photosynthesis, which consists of a series of biochemical processes such as carbon fixation, and can be performed without the presence of light. We focussed our interest to the beginning of photosynthesis, which starts with the absorption of a photon in the antenna complexes, and the capability of higher plants to safely and efficiently utilize the excitation energy created in such a way.

The chlorophyll *a/b* containing light-harvesting pigment-protein complex (LHCII) associated with photosystem II in the chloroplasts of higher plants is one of the most abundant proteins in the biosphere. It alone binds roughly half the total amount of chlorophyll (Chl) content of plants. *In vitro* LHCII appears to be aggregates of trimeric complexes of 25-27 kDa monomers, whose structure has been resolved to 3.4 Å with the aid of electron crystallography of two-dimensional crystals (Kühlbrandt *et al.*, 1994). Within each monomer subunit 12-14 Chl's and 2-4 xanthophylls (Xan's) are non-covalently bound to the LHCII polypeptide. Seven Chl's which are in van der Waals contact with the two central Xan's — identified as luteins (Lut's) — were tentatively assigned as chlorophyll *a* (Chl*a*) molecules to allow efficient triplet transfer from Chl*a* to Xan.

In LHCII any excited Xan or chlorophyll *b* (Chl*b*) molecule can transfer its (singlet) excitation to a Chl*a* pigment — all the other, unimolecular decay processes being too slow to compete with energy transfer (ET). From a Chl*a* molecule the excitation can be forwarded to the reaction center, where the primary charge separation takes place, or, when the reaction center is already occupied, it can be dissipated in three different ways: (*i*) by internal conversion to the ground state; (*ii*) by emitting a light quantum (fluorescence); or (*iii*) by undergoing intersystem crossing to the triplet manifold. The formation of triplet Chl*a* ($Chla^{\dagger}$), however, should be

avoided because it can react with ground state (triplet) oxygen creating deleterious singlet oxygen. Xan's, having a low lying triplet state, can efficiently prevent this process either directly, accepting triplet excitation from Chl*a*, or indirectly, by quenching singlet oxygen. The excitation from a triplet state of a Xan is harmlessly dissipated to the environment as heat.

Apart from light-harvesting and quenching of Chl$a^{\dagger}$, Xan's are thought to have two other important roles, namely (*i*) stabilizing the structure of LHCII (Plumley & Schmidt, 1987) and (*ii*) quenching of singlet excited Chl*a* (Chla^{*}) when the reaction center is closed (under excess illumination) (Horton *et al.*, 1996). Two mechanisms were proposed to explain this latter process. Owens and his co-workers (1992) assumed that the S_1 state of Xan's, which has a very weak oscillator strength and does not manifest itself in the absorption spectrum, might be the key in quenching of Chla^{*} molecules. Based on model calculations on polyenes, they suggested that, under excess illumination, the reversible de-epoxidation of violaxanthin (Vio) to zeaxanthin (Zea) lowers the S_1 energy level of the latter below that of Chl*a* allowing a back transfer from Chl*a* to Zea, where the excitation is dissipated through internal conversion. Recent results (Polivka *et al.*, 1999), however, do not support this "molecular gear-shift" model. The other explanation does not involve the S_1 level of different Xan's but, instead, suggests that ΔpH throughout the thylakoid membrane and the xanthophyll cycle can induce structural alterations in LHCII, which result the quenching of Chla^{*} (Horton *et al.*, 1996). It is proposed that high ΔpH or the interconversion of Vio to Zea enhances the formation of quenching centers through, hitherto unidentified, Chl-Chl or Chl-Zea interaction while Vio inhibits that. In thylakoid membranes, due to its high self-aggregation capability, LHCII has been shown to be found in large ordered arrays (Garab *et al.*, 1988a). Thylakoids and lamellar aggregates of LHCII when exposed to excess illumination have also been shown to be capable of undergoing reversible structural changes and quenching of Chla^{*} (Garab *et al.*, 1988b; Barzda *et al.*, 1994).

The present study was undertaken to investigate the disparate photophysical behaviour of LHCII at different levels of molecular organization, in suspensions of (*i*) isolated aggregates, (*ii*) intact trimers, and (*iii*) perturbed trimers, as well as (*iv*) in native thylakoid membranes. The different state of aggregation can be achieved by using non-ionic detergent (Ide *et al.* 1987). It cannot be ruled out, and indeed seems likely, that as monomers assemble into trimers, and these go on to form oligomers, additional interactions, intra-trimer (involving exterior pigments of one monomer and the interior pigments of another monomer within the same trimer) as well as extra-

trimer (entailing the peripheral pigments belonging to different trimers) come into play. Our main goal was to find a connection between the extent of quenching and the changing interactions between the chromophores in LHCII and to find clues for the physical mechanism of quenching.

The formation of LHCII aggregates brings about a noticeable change in the absorption spectrum compared to that of the trimers. For one thing the Q_y peak shifts to the red, and for another, the ratio of the peak absorbance in the blue region to that in the red region becomes smaller, a phenomenon known as absorption flattening. Since the few results which bear on this issue (Jennings *et al.*, 1991; Horton *et al.*, 1991) are of a qualitative nature, we decided to perform a thorough analysis taking into account the effects of selective scattering and the non-random distribution of trimers in the sample. We adopted a method from Latimer and Eubanks (1962) to correct the measured absorption spectrum of the aggregates for selective scattering and from Duysens (1956) for the mutual shadowing of trimers within a single aggregate. We found that the absorption spectrum of LHCII aggregates, when corrected for these distortions, turns out to be almost superposable on the absorption spectrum recorded after disrupting the aggregates by the addition of a detergent at a characteristic concentration (C_C). Since earlier attempts on unicellular organisms were handicapped by the fact that disintegration of the scattering sample, using organic solvents, destroyed the pigment–protein interactions (Duysens, 1956) or by the failure of rupturing the cells into fragments by mechanical agitation (Das *et al.*, 1967), our results on the trimer–aggregate system provides the first experimental evidence for the applicability of Duysens' method. Our analysis also provides a painless method for estimating the size of the aggregates. The spectral similarity of the trimers and aggregates also implies that the radiative lifetime of Chl*a* does not change with aggregation.

Aggregation affects not only the absorption spectrum but also the fluorescence quantum yield, ϕ_F. It is known that ϕ_F decreases upon the formation of aggregates, but the quenching mechanism remains, despite a fair deal of effort, obscure. We carried out nanosecond laser photolysis experiments on trimeric and aggregated forms of LHCII to look for implications whether the formation of Chl$a^\dagger$ has some bearings on the non-photochemical dissipation of excess energy. We found that the triplet-minus-singlet (TmS) spectra of aggregated LHCII differ from the corresponding spectra of trimers on two counts: (*i*) in the aggregates, the large positive band around 508 nm, which is associated to Car triplet absorption, is red shifted and broader; and

(*ii*) the features attributable to the perturbation of the Q_y region of Chl*a* by a nearby $Car^{\dagger}$ are more pronounced, than in trimers. We also found that, parallel to ϕ_F, aggregation decreases the triplet formation yield (ϕ_T) of Chl*a*, while on the other hand the efficiency of triplet transfer from Chl*a* to Car (100%) and the lifetime of $Car^{\dagger}$ (9.3 μs) is not affected by aggregation. Similar results were observed earlier in artificial caroteno-porphyrin dyads (Bensasson *et al.*, 1981; Moore *et al.*, 1982; Gust *et al.*, 1992), which was explained by suggesting that Car's are able to enhance the internal conversion rate of a nearby Chl-like molecule. Based on this similarity, we put forward the hypothesis that the same process, which had been termed as 'catalysed internal conversion' (CIC), also operates in natural antenna complexes. This process provides an alternative physical mechanism for quenching of Chl*a* fluorescence.

Further increasing the detergent concentration in the sample (above C_C, when it starts to affect the molecular organization of the monomers) we probed the interactions between Chl*a* and Chl*b* and between Chl*a* and Lut. Once the detergent concentration exceeds C_C the TmS spectrum becomes sensitive to the wavelength of excitation and to the delay between excitation and observation. The efficiency of triplet–triplet transfer from Chl*a* to Car decreases while the fluorescence and triplet yields (ϕ_F and ϕ_T) of Chl*a* increases. At the same time the efficiency of singlet–singlet transfer from Chl*b* to Chl*a* drops down to such an extent that $Chlb^{\dagger}$ starts to form as a deactivation product of $Chlb^{*}$. We explained our observations by assuming that the detergent severs contact between adjacent molecules and the internal conversion rate of $Chla^{*}$ is faster in the presence of a Xan neighbour than in the absence of such a partner.

In order to find more evidence to support our hypothesis that Car's can quench $Chla^{*}$ through a process other than ET we wanted to show the generality of this phenomenon, i.e. when the energy levels are known to be unfavourable for ET. For this purpose we used two artificial systems, where a Chl*a*-like molecule, a pyropheophorbide *a* (Pyr) was attached to a Car (fucoxanthin or peridinin), the S_1 level of which lies above that of its partner. Apart from ϕ_F we investigated the quenching of Pyr triplets by the attached Car and the transfer of singlet excitation from Car to Pyr in order to assess these dyads as a model of a photosynthetic antenna system. Our results revealed that both the efficiency of singlet energy transfer from Car to Pyr and that of triplet energy transfer from Pyr to Car depend markedly on the solvent and also on the dyad. We also observed that the Car moiety is able to quench the fluorescence of its Pyr

partner. Such indirect quenching must entail a process other than ET; we suggested, that Pyr fluorescence is quenched via the process of catalysed internal conversion.

Nanosecond laser-kinetic spectroscopy of LHCII revealed that Chl*a*† decays rapidly, transferring its triplet excitation to a neighbouring Car. This means that the Car† formation yield equals the corresponding yield of Chl*a*†. In order to determine the latter yield, one must know ε and $\varepsilon^{\dagger}$, the extinction coefficients of the singlet ($S_2 \leftarrow S_0$) and triplet absorption ($T_n \leftarrow T_1$) of Car. The values of ε are well documented for a large number of Car's (Britton, 1995), but the determination of $\varepsilon^{\dagger}$ has lagged behind. We recorded the triplet absorption spectra of a handful of Car's, the three LHCII Xan's among them, in three different organic solvents. Since intersystem crossing from the singlet to the triplet manifold in Car's is negligible we used triplet ET from Chl*a* to populate the triplet states of Car's. We found only one vibronic progression in the 250-900 nm region, which overlaps, but is red-shifted with respect to the $S_2 \leftarrow S_0$ absorption progression. The 0-0 peak in the triplet spectrum is the most intense one in contrast with the singlet spectrum, where the 1-0 peak is the largest. The solvent-induced shift in the singlet and triplet peaks of Xan's may also give us a clue to the location of these bands in LHCII.

Studying the TmS spectra of LHCII or the caroteno-pheophorbide dyads revealed, apart from a peak attributable to a Car†, a sizeable bleaching signal in the Q_y region of Chl*a* or Pyr. This was first observed in LHCII by van der Vos and his co-workers (1991), who explained it—since Car's do not absorb in that region—by a perturbation in the Q_y band of Chl*a* by a contagious Car†. Later on similar signals were reported in a wide range of photosynthetic complexes (Angerhofer *et al.*, 1995; Peterman *et al.*, 1995; Büchel *et al.*, 1998) as well as in artificial systems (Osuka *et al.*, 1999), where a Car is in close contact with a Chl*a* or a Chl*a*-like partner molecule. However, Wolff and Witt (1969) emphasized the absence of such a signal in isolated chloroplasts. This result, if reproducible, would imply that the TmS signal in chloroplasts originates from a group of Car's whose photophysical behaviour is appreciably different from the Car's which give rise to the TmS spectrum of LHCII. Accordingly, we decided to reinvestigate the TmS spectrum of chloroplasts under the same experimental conditions as those employed earlier for recording the TmS spectra of Chl *a/b*–LHCII, Chl *a/c*–LHCII, and caroteno-pheophorbide dyads, where the Q_y bleaching signal was observed. Our results revealed a prominent bleaching signal in the Q_y region and the triplet decay time was found to be comparable to that of LHCII triplets. Such a bleaching signal cannot be explained

without allowing the admixture of the zero-order states of a Chl*a*:Car pair (Naqvi, 1998b). This would also imply the mechanism of catalysed internal conversion via virtual transitions to and from intermediate states. On the basis of our observations we can conclude that the mechanism of catalysed internal conversion operates also in chloroplasts, providing a channel for the dissipation of excess excitation energy *in vivo*.

A DOLGOZAT ÖSSZEFOGLALÁSA

A fotoszintézis kétségtelenül az egyik legfontosabb biológiai folyamat a Földön. Szinte valamennyi élőlény létfenntartásához nélkülözhetetlen anyagok a fotoszintézis során keletkeznek. Csak a növények, algák és egyes baktériumok képesek a Napból érkező fényt kémiai energiává alakítani, ami azután a többi élőlény energiaforrásául szolgál. A fotoszintézis folyamata két jól szétválasztható szakaszra bontható. Az első szakasz a növényekben a vízbontástól (oxigénfejlesztés) az ATP ill. NADPH szintéziséig tart, csak fény jelenlétében megy végbe, míg a második szakasz, ami biokémiai folyamatok sorozata, sötétben is lejátszódhat. Dolgozatomban a fotoszintézis kezdeti szakaszával foglalkoztam, azon belül is a fénybegyűjtő antenna komplexben elnyelt fényenergia hasznosításával.

A második fotokémiai rendszer (PSII) klorofill *a/b* kötő fénybegyűjtő pigment-protein komplexe, ami a magasabbrendű növények kloroplasztiszaiban található, az egyik legnagyobb mennyiségben előforduló protein a bioszférában. A növényekben található klorofill kb. 50%-a ehhez a proteinhez kötődik. Izolált állapotban az LHCII trimerek aggregátumaként fordul elő. A 25-27 kDa-os monomerek szerkezete elektron-krisztallográfiai vizsgálatokból 3,4 Å felbontással ismert (Kühlbrandt és mtsi., 1994). Az egyes monomereken belül 12-14 klorofill és 2-4 xantofill molekula nem-kovalensen kötődik az LHCII polipeptidhez. Fotofizikai megfontolások alapján 7 klorofill molekulát, amelyek van der Waals kapcsolatban vannak a két centrális helyzetű luteinnel, klorofill *a* (kl*a*) molekulaként jelöltek meg, mivel így lehetőség nyílik a hatékony triplett energiaátadásra a kl*a*-ról a xantofillokra.

Az LHCII-ben a fény elnyelésének következtében az abszorbeáló molekula magasabb gerjesztettségi állapotba kerül. A pigmentek proteinváz által biztosított elhelyezkedésének következtében a kisegítő pigmentekről (kl*b*, xantofillok) a gerjesztési energia 100%-os hatásfokkal átadódik a kl*a* molekuláknak. A kl*a* molekulákról a gerjesztési energia a reakciócentrumokba továbbítódik, ahol elsődleges töltésszétválasztás jön létre. Ha azonban a reakciócentrum éppen foglalt, akkor a szingulett gerjesztési állapotban lévő kl*a* molekulák (kla^*) energiájának lecsengésére háromféle lehetőség kínálkozik: (*i*) sugárzás nélküli átmenet, melynek során a molekula lehűl, energiáját hő formájában adva át a környezetének; (*ii*) fluoreszcencia, ami egy foton kibocsátásával jár; illetve (*iii*) szigulett-triplett átmenet, amikor a molekula triplett multiplicitású gerjesztett állapotba kerül át. A triplett állapotú kl*a* (kl$a^\dagger$) képződése azonban

nemkívánatos jelenség, mivel ezek a molekulák reakcióba tudnak lépni az alapállapotban triplett oxigénnel, aminek következtében káros szingulett oxigén keletkezik. A xantofillok azonban, alacsony triplett energiaszintjük következtében, hatékonyan képesek megakadályozni ezt a káros folyamatot vagy közvetlenül, átvéve a triplett gerjesztési energiát a kl*a*-tól, vagy közvetve, deaktiválva a szingulett állapotba került oxigén molekulákat. A triplett állapotba került xantofillok ezután gerjesztési energiájukat hő formájában adják le a környezetüknek.

A fény elnyelésén és a gerjesztési energia továbbításán, valamint a kl$a^{\dagger}$ molekulák deaktiválásán kívül a xantofilloknak még két fontos szerepe van. Az egyik az LHCII szerkezetének stabilizálása (Plumley és Schmidt, 1987), a másik pedig a kla^{*} molekulák deaktiválása és ezen keresztül az elnyelt fényenergia hasznosításának szabályozása (Horton és mtsi., 1996). Ez utóbbi regulációs mechanizmusra kétféle magyarázat található az irodalomban. Az egyik elképzelés szerint a xantofillok S_1 állapotán keresztül, energiaátadás útján deaktiválódhatnak a kla^{*} molekulák. Xantofillokban az $S_1 \leftarrow S_0$ átmenet optikailag tiltott, így közvetlen spektroszkópiai meghatározása nem lehetséges. Poliéneken végzett modellszámítások alapján azonban Owens és mtsi. (1992) feltételezik, hogy a xantofill-ciklusban a violaxantin (vio) fény hatására bekövetkező de-epoxidációja során keletkező zeaxantin (zea) S_1 energiaszintje a kl*a* S_1 szintje alá süllyed, és így lehetővé válik a gerjesztési energia átadása a zea-ra, ahol az sugárzás nélküli átmenet révén disszipálódik. Újabb eredmények (Polivka és mtsi., 1999) azonban nem támasztják alá ezt, az energiaáramlás irányát megfordító molekuláris mechanizmust. A másik magyarázat szerint a xantofillok S_1 energiaszintjének nincsen közvetlen szerepe a reguláló folyamatban. Horton és mtsi. szerint (1996) a fény hatására a tilakoid membrán két oldala között kialakuló ΔpH és a xantofill-ciklus aktivitása szerkezeti változásokat indukál az LHCII-ben, ami a kla^{*} kioltásához vezet. (Horton és mtsi., 1996). Elképzelésük szerint a nagy ΔpH és a zea képződése elősegíti a kioltást a kl-kl vagy kl-zea kölcsönhatáson keresztül, míg a vio meggátolja azt. A jelenség fizikai magyarázata azonban még tisztázatlan. Tilakoid membránokban kimutatták, hogy az LHCII (nagyfokú önaggregációs tulajdonságának köszönhetően) hosszú távú rendezettséget mutató struktúrákba szerveződik (Garab és mtsi., 1988a). Kimutatták továbbá, hogy tilakoid membránokban és izolált LHCII lamelláris aggregátumaiban erős megvilágítás hatására reverzibilis szerkezetváltozások lépnek fel, és ezzel párhuzamosan fluoreszcencia kioltás is megfigyelhető (Garab és mtsi., 1988b; Barzda és mtsi., 1996).

Dolgozatomban az LHCII fotofizikai sajátságait vizsgáltam különböző szerveződési szinteken: (*i*) aggregátumokban; (*ii*) intakt trimerekben; és (*iii*) perturbált trimerekben. A különböző aggregáltsági állapotokat detergens hozzáadásával érhetjük el (Ide és mtsi. 1987). Egy, a detergensre jellemző karakterisztikus koncentráció (C_C) elérésekor túlnyomórészt trimerekből álló mintát kapunk, míg további detergens hozzáadásával az arány a monomerek felé tolódik el, illetve a trimerekben szerkezeti változások állnak be. Valószínűnek látszik, hogy az aggregátumok trimerekké illetve még tovább, monomerekké történő szétválasztása során megváltoznak a trimereken belüli kölcsönhatások (pl. az egyik monomer külső pigmentje és a trimer egy másik monomerjének belső pigmentjei között) illetve a trimerek közötti kölcsönhatások (pl. különböző trimerek külső pigmentjei között) is. Elsődleges célunk az volt, hogy kapcsolatot találjunk a kl*a* fluoreszcencia kioltása és a változó pigment-pigment kölcsönhatások között, valamint kerestük a magyarázatot a kioltás fizikai mechanizmusára is.

Az LHCII aggregátumok abszorpciós spektruma jelentősen eltér a trimerek spektrumától. Egyrészt a Q_y sáv a vörös hullámhossz felé tolódik el, másrészt a kék tartományba eső abszorpciós sáv nagysága jelentősen lecsökken a vörös tartományba eső sáv nagyságához képest. Ez utóbbi jelenséget abszorpciós szűrőhatásnak (*sieving*) hívják és az egyes aggregátumokon belüli trimerek egymást leárnyékoló hatásának tudható be. Mivel az irodalomban fellelhető közlemények inkább minőségi elemzéssel foglalkoztak (Jennings és mtsi., 1991; Horton és mtsi., 1991), ezért elhatároztuk a két spektrum összehasonlítását a szelektív fényszórás és az abszorpciós laposodás figyelembevétele mellett. Az aggregátumokon a detektor nyílásszögén kívülre szóródó fényt a spektrométer abszorpcióként értelmezi, ami meghamisítja a valós abszorpciós spektrumot. Ennek kiküszöbölésére egy analitikai eljárást alkalmaztunk (Latimer és Eubanks, 1962), míg az abszorpciós szűrőhatást Duysens (1956) által levezetett matematikai formulával vettük figyelembe. A korrekciós eljárások alkalmazása után úgy találtuk, hogy az aggregátumok abszorpciós spektruma gyakorlatilag megegyezik a trimerek spektrumával. Mivel az eljárás igazolására irányuló korábbi törekvéseket hátráltatta az a tény, hogy az egysejtűeken végzett kísérletek során a szerves oldószer alkalmazása megváltoztatta a pigment–protein kölcsönhatásokat (Duysens, 1956), illetve a sejtek mechanikus szétzúzása is sikertelen volt (Das és mtsi., 1967), így az LHCII trimer–aggregátum rendszeren végzett vizsgálatunk a korrekciós eljárás első kísérleti bizonyítékának tekinthető. A korrekciós eljárás alkalmazása során lehetőség nyílik az aggregátumok méretének közelítő meghatározására is. A trimerek és aggregátumok

abszorpciós spektrumának hasonlóságából arra is következtethetünk, hogy az aggregáció nem befolyásolja a kl*a* molekulák radiatív élettartamát.

Az aggregáció hatására nem csak az abszorpciós spektrum változik meg, hanem a fluoreszcencia hatásfok (ϕ_F) is lecsökken, bár ez utóbbi jelenség molekuláris magyarázata az eddigi próbálkozások ellenére (pl. Horton és mtsi., 1996) sem kielégítő. Nanoszekundumos lézerimpulzus által indukált abszorpcióváltozás-mérésekkel arra kerestük a választ, hogy az LHCII trimerekben és aggregátumokban a triplett állapotú kl*a* kialakulásának lehet-e szerepe a fölösleges gerjesztési energia levezetésében. Kísérleti eredményeink szerint az LHCII aggregátumok triplett-mínusz-szingulett (TmS) spektruma két lényeges pontban különbözik a trimerek TmS spektrumától: (*i*) aggregátumokban a karotinoidok triplett abszorpciójának tulajdonítható, 508 nm körül található pozitív sáv szélesebb és a vörös hullámhosszak felé eltolódott; illetve (*ii*) a kl*a* molekulák Q_y sávjában bekövetkező abszorpcióváltozás, amit a triplett állapotú karotinoidok indukálnak, jelentősebb, mint a trimer LHCII esetében. Kimutattuk, hogy a triplett állapotú kl*a* kialakulása a fluoreszcencia hatásfokhoz hasonlóan csökken. Azonban a triplett energiaátadás hatásfoka (100%) a kl*a*-ról a karotinoidokra, illetve a karotinoid triplett állapotok élettartama (9.3 μs) nem változik meg az aggregációval. Hasonló eredményeket figyeltek meg korábban mesterséges karotino-porfirin rendszerekben is, amit azzal magyaráztak, hogy a karotinoid képes befolyásolni a partner molekula sugárzásnélküli átmenetének valószínűségét (Bensasson és mtsi., 1981; Moore és mtsi., 1982; Gust és mtsi., 1992). Hipotézisünk szerint hasonló mechanizmus működik természetes antenna komplexekben is, ahol a két központi helyzetű lutein, illetve a perifériás xantofillok (violaxantin ill. neoxantin) a kl*a** molekulák sugárzás nélküli átmenetét katalizálják, ezáltal csökkentve a fluoreszcencia és a szingulett–triplett átmenet valószínűségét. Ez a jelenség (angol nevével *catalysed internal conversion*, vagy röviden CIC) egy alternatív lehetőséget kínál a kl*a* fluoreszcencia kioltás magyarázatára, vagyis a fotoszintézis során nem hasznosítható (túlzott) gerjesztési energia disszipálására.

A detergens koncentráció további növelésével (C_C fölé) a kl*a* és kl*b*, illetve a kl*a* és lutein molekulák közötti kölcsönhatások megváltozását vizsgáltuk. Ha a detergens koncentrációja túllépi a C_C értéket, akkor a TmS spektrumot a gerjesztési lézerimpulzus hullámhossza illetve a gerjesztés és a detektálás közötti késleltetési idő is befolyásolja. A kl*a*-ról a karotinoidokra történő triplett energia átadás hatásfoka lecsökken, míg a kl*a* fluoreszcencia hatásfoka és triplett

hozama (ϕ_F ill. ϕ_T) megnő. Mindemellett a kl*b*-ről kl*a*-ra történő szingulett energia átadás hatásfoka annyira lecsökken, hogy triplett állapotú kl*b* is megjelenik, mint a kl*b** egyik deaktivációs formája. Megfigyeléseinket azzal magyarázzuk, hogy a detergens megváltoztatja a pigmentek közötti kölcsönhatást, aminek következtében a kl*a** sugárzás nélküli átmenetének valószínűsége megnő a szomszédos xantofill jelenlétében, illetve lecsökken annak hiányában. Hipotézisünk szerint a karotinoidok képesek a kl*a** állapotok kioltására a gerjesztési energia átvétele nélkül, megnövelve annak sugárzás nélküli átmeneti valószínűségét (CIC).

Fenti elképzelésünket bizonyítandó vizsgálatokat végeztünk olyan mesterséges rendszereken, ahol a karotinoidok S_1 energiaszintje kizárja a gerjesztési energia átvételét a partner molekulától. Kísérleti rendszerünkben egy kl*a* típusú molekulához (pirofeoforbid *a*) kovalensen kapcsolódott egy karotinoid molekula (fukoxantin ill. peridinin), aminek az S_1 energianívója bizonyítottan magasabban van, mint a partner molekuláé. Kísérleteinkkel arra is kerestük a választ, hogy ez a mindössze két pigmentből álló rendszer, ún. diád, vajon használható-e a fotoszintetikus antennák tulajdonságainak modellezésére. Ennek eldöntésére a fluoreszcencia hozamon kívül vizsgáltuk még a triplett energiaátadást a pirofeoforbidról a karotinoidra (triplett kioltás), illetve a szingulett energia átadását a karotinoidról a pirofeoforbidra (fénybegyűjtés). Azt tapasztaltuk, hogy mind a szingulett, mind pedig a triplett energiaátadás hatékonysága jelentősen függ a használt oldószertől, illetve a diád karotinoidjától. Eredményeink szerint ezen bimolekuláris rendszerekben a karotinoid képes volt a pirofeoforbid szingulett gerjesztési állapotának a kioltására, ami szükségképpen a sugárzás nélküli átmeneti valószínűség megnövekedésével (CIC) magyarázható. Ez a jelenség tehát más, természetes antenna rendszerekben is magyarázatot adhat a fotoszintézis számára már nem hasznosítható gerjesztési energia disszipálására.

Az LHCII TmS spektrumainak tanúsága szerint a kl*a* kb. 20 ns-on belül átadja triplett gerjesztési energiáját a szomszédos karotinoidnak. Ebből következik, hogy a karotinoidok triplett hozama megegyezik a kl*a* triplett hozamával. Ahhoz azonban, hogy ez utóbbi mennyiséget meghatározhassuk, ismernünk kellene a karotinoidok szingulett ($S_2 \leftarrow S_0$) és triplett ($T_n \leftarrow T_1$) abszorpcióhoz tartozó extinkciós koefficiensét (ε és $\varepsilon^\dagger$). Az ε értékek a legtöbb karotinoidra ismertek (Britton, 1995), azonban az $\varepsilon^\dagger$-ról viszonylag kevés adat lelhető fel az irodalomban. Ezt a hiányt pótlandó meghatároztuk néhány, a fotoszintézis szempontjából fontosabb karotinoid triplett spektrumát három különböző szerves oldószerben. Mivel a karotinoidokban a szingulett–

triplett átmenet valószínűsége igen csekély, így a karotinoid triplett állapotokat kl*a*-ról triplett energiaátadás révén alakítottuk ki. A 250-900 nm-es tartományban talált abszorpciós sávok mind egyazon elektronikus átmenethez tartoztak, ami bár a vörös hullámhossz felé tolódott, de átfed a szingulett ($S_2 \leftarrow S_0$) abszorpciós sávokkal. A triplett spektrumban a 0-0 vibrációs átmenethez tartozó sáv a legintenzívebb, ellentétben a szingulett spektrummal, ahol a 1-0 átmenethez tartozó sáv a legnagyobb. A szingulett és triplett abszorpciós sávok oldószertől függő eltolódása lehetőséget kínálhat a xantofillok abszorpciós sávjainak a behatárolására az LHCII-ben is.

Az LHCII és a karotino-feoforbid diádok TmS spektrumának tanulmányozása során láthatjuk, hogy a karotinoid tripletteknek betudható sáv mellett a kl*a* illetve a pirofeoforbid Q_y tartományában egy nem elhanyagolható negatív sáv is jelentkezik. Ezt először LHCII-ben van der Vos és mtsi. mutatták ki (1991). Mivel a karotinoidok abszorpciója elhanyagolható ebben a tartományban ezért megfigyelésüket a karotinoid triplettek által a kl*a* Q_y sávjában okozott abszorpcióváltozással magyarázták. A későbbiekben ezt a jelenséget sikerült kimutatni különböző fotoszintetikus komplexekben (Angerhofer és mtsi., 1995; Peterman és mtsi., 1995; Büchel és mtsi., 1998) illetve mesterséges rendszerekben is (Osuka és mtsi., 1999), ahol karotinoidok szoros kölcsönhatásban álltak kl*a* vagy kl*a*-szerű molekulákkal. Kloroplasztiszok vizsgálata során azonban Wolff és Witt (1969) nem találtak semmiféle abszorpcióváltozást a Q_y tartományban. Ez az eredmény azt jelentené, hogy a karotinoidok fotofizikai tulajdonságai kloroplasztiszokban különböznek az LHCII-ben tapasztaltaktól, ami egyben az általunk javasolt kioltási mechanizmus (CIC) működését is megkérdőjelezné *in vivo* rendszerekben. Ezt eldöntendő elhatároztuk a kloroplasztiszok TmS spektrumának újbóli vizsgálatát ugyanazon kísérleti körülmények között, mint korábban, kl *a/b*–LHCII, kl *a/c*–LHCII, illetve karotino-feoforbideok tanulmányozásakor, amikor a Q_y tartományban a negatív abszorpciós sávot sikerült kimutatnunk. Eredményeink igazolták várakozásainkat, miszerint a kloroplasztiszok TmS spektrumában is megtalálható a Q_y perturbációs sáv, illetve a spektrum egésze, valamint a triplett állapotok élettartama nagyban hasonlatos az LHCII esetében tapasztaltakkal.

LIST OF PUBLICATIONS

Naqvi K. R., Melø T. B. Bangar Raju B. **Jávorfi T.**& Garab G.: Comparison of the absorption spectra of trimers and aggregates of chlorophyll *a/b* light-harvesting complex LHCII. *Spectrochim. Acta Part A* **53** (1997) 1925-1936

Naqvi K. R., Melø T. B. Bangar Raju B. **Jávorfi T.**, Simidjiev I. & Garab G.: Quenching of chlorophyll *a* singlets and triplets by carotenoids in light-harvesting complex of photosystem II: comparison of aggregates with trimers. *Spectrochim. Acta Part A* **53** (1997) 2659-2667

Naqvi K. R., **Jávorfi T.**, Melø T. B. & Garab G.: More on the catalysis of internal conversion in chlorophyll *a* by an adjacent carotenoid in light-harvesting complex (Chla/b LHCII) of higher plants: time-resolved triplet-minus-singlet spectra of detergent perturbed complexes. *Spectrochim. Acta Part A* **55** (1999) 193-204

Jávorfi T., Garab G. & Naqvi K. R.: Reinvestigation of the triplet-minus-singlet spectra of chloroplasts. *Spectrochim. Acta Part A* **56** (1999) 211-214

Osuka A., Kume T., Haggquist G. W., **Jávorfi T.**, Lima J. C., Melo E. & Naqvi K. R.: Photophysical characteristics of two model antenna systems: a fucoxanthin-pyropheoporbide dyad and its peridinin analogue. *Chem. Phys. Lett.* **313/3-4** (1999) 499-504

Jávorfi T. & Naqvi K. R.: Solvatochromism gives a clue to the locations of the $S_2 \leftarrow S_0$ and $T_n \leftarrow T_1$ peaks of LHCII xanthophylls. *In Spectroscopy of Biological Molecules: New Directions 8th* Editors: J. Greve, G.J. Puppels, C. Otto (1999) 159-160.

- Simidjiev I., Stoylova S., Amenitsch H., **Jávorfi T.**, Mustárdy L., Laggner P., Holzenburg A. & Garab G.: Self-assembly of large, ordered lamellae from non-bilayer lipids and integral membrane proteins *in vitro*. *PNAS* **97** 4 (2000) 1473-1476

Conference proceedings:

Jhutti C.S., **Jávorfi T.**, Merzlyak M.N., Naqvi K.R.: Triplet-triplet absorption spectra and extinction coefficients of lutein, neoxanthin and violaxanthin. *In Photosynthesis: Mechanisms and Effects (Ed.: G.Garab; Kluwer Acad. Publ., Dordrecht) 1998* 491-494 (Vol. I)

- **Jávorfi T.**, Amenitsch H., Laggner P., Cseh Z., Mustárdy L., Borbély S., Rosta L., Garab G.: Nature of irreversible structural changes induced by intense light in thylakoids. Small angle X-ray and neutron scattering of magnetically aligned chloroplasts. *In Photosynthesis: Mechanisms and Effects (Ed.: G.Garab; Kluwer Acad. Publ., Dordrecht) 1998* 349-352 (Vol. I)

- Simidjiev I., Stoylova S., Holzenburg A., Amenitsch H., Laggner P., **Jávorfi T.**, Mustárdy L., Garab G.: Reconstition of membranes using non-bilayer forming lipids and plant LHCII. *In Photosynthesis: Mechanisms and Effects (Ed.: G.Garab; Kluwer Acad. Publ., Dordrecht) 1998* 1799-1802 (Vol. III)

- The results published under these titles have not been included in the Thesis.

REFERENCES

Andersson, P. O., Gillbro, T., Ferguson, L. & Cogdell, R. J. 1991, *Photochem. Photobiol.* **54**: 353.

Angerhofer, A., Bornhäuser, F., Gall, A. & Cogdell, R. J. 1995, *Chem. Phys.* **194**: 259.

Barzda, V., Mustárdy, L. & Garab, G. 1994, *Biochemistry* **33**: 10837.

Barzda, V., Garab, G., Gulbinas, V. & Valkunas, L. 1995, in *Photosynthesis: from Light to Biosphere* (Mathis, P. ed.), Vol. I, pp. 319-322, Kluwer Academic Publishers, The Netherlands.

Barzda, V., Istokovics, A., Simidjiev, I. & Garab, G. 1996, *Biochemistry* **35**: 8981.

Barzda, V., Peterman, E. J. G., van Grondelle, R. & van Amerongen, H. 1998, *Biochemistry* **37**: 546.

Barzda, V., Jennings, R. C., Zucchelli, G. & Garab, G. 1999, *Photochem. Photobiol.* **70**: 751.

Bassi, R., Silversti, M., Dainese, P., Moya, I. & Giacometti, M. 1991, *J. Photochem. Photobiol. B: Biol.* **9**: 335.

Bassi, R., Pineau, B., Dainese, P. & Marquardt, J. 1993, *Eur. J. Biochem.* **212**: 297.

Bensasson, R. V., Land, E. J., Moore, A. L., Crouch, R. L., Dirks, G., Moore T. A. & Gust, D. 1981, *Nature* **290**: 329.

Berberan-Santos, M. N. 1990, *J. Chem. Educ.* **67**: 757.

Britton, G. 1995, in *Carotenoids* (Britton, G., Liaaen-Jensen, S. & Pfander, H. eds.), Vol. 1B: Spectroscopy, pp. 13-62, Birkhäuser Verlag, Basel, Switzerland.

Butler, P. J. G. & Kühlbrandt, W. 1988, *Proc. Natl. Acad Sci. USA*, **85**: 3797.

Büchel, C., Naqvi, K. R. & Melø, T. B. 1998, *Spectrochim. Acta Part A* **54**: 719.

Carbonera, D., Giacometti, G. & Segre, U. 1996, *J. Chem. Soc. Faraday Trans.* **92**: 989.

Carmichael, I. & Hug, G. L. 1986, *J. Phys. Chem. Ref. Data* **15**: 1.

Connelly, J. P., Müller, M. G., Hucke, M., Gatzen, G., Mullineaux, C. W., Ruban, A. V., Horton, P. & Holzwarth, A. R 1997, *J. Phys. Chem.* **101:** 1902.

Das, M., Rabinowitch, E., Szalay, L. & Papageorgiou, G. 1967, *J. Phys. Chem.* **71**: 3543.

Demmig B., Winter, K., Kruger, A. & Czygan, F. C. 1987, *Plant Physiol.* **84**: 218.

Demmig-Adams B. 1990, *Biochim. Biophys. Acta* **1020**: 1.

Demmig-Adams, B. & Adams III, W. W. 1996. *Trends in Plant Sci.* **1**: 21.

Demmig-Adams, B. & Adams III, W. W. 2000, *Nature* **403**: 371.

Duysens, L. N. M. 1956, *Biochim. Biophys. Acta*, **19**: 1.

Englman, R. & Jortner, J. 1970, *Mol. Phys.* **18**(2): 145.

Finzi, L., Bustamante, C., Garab, G. & Juang, C-B. 1989, *Proc. Natl. Acad. Sci. USA* **86**: 8748.

Förster, Th. 1965 in *Modern Quantum Chemistry*, Vol. **3**. (Sinanoglu, O. ed.) pp. 93-137, Academic Press, New York

Frank, H. A., Farhoosh, R., Gebhard, R., Lugtenburg, J., Gosztola, D. & Wasielewski, M. R. 1993, *Chem. Phys. Lett.* **207**: 88.

Frank, H. A., Cua, A., Chynwat, V., Young, A., Gosztola, D. & Wasielewski, M. R. 1994, *Photosynth. Res.* **41**: 389.

Frank, H. A. & Cogdell, R. J. 1996, *Photochem. Photobiol.* **63**: 257.

Fujimori, E. & Livingston, R. 1957, *Nature* **180**: 1036.

Garab, G., Faludi-Dániel, Á., Sutherland, J. C. & Hind, G. 1988a, *Biochemistry* **27**: 2425.

Garab, G., Leegood, R. C., Walker, D. A., Sutherland, J. C. & Hind, G. 1988b, *Biochemistry* **27**: 2430.

Garab, G., Wells, K. S., Finzi, L. & Bustamante, C. 1988c, *Biochemistry* **27**: 5839.

Garab, G. 1996, in *Biophysical Techniques in Photosynthesis* (Amesz, J. & Hoff, A. eds.), pp. 11-40, Kluwer Academic Publishers, The Netherlands.

Gilbert, A. & Baggott, J. 1991, in *Essentials of Molecular Photochemistry*, 97-98, Blackwell Scientific Publications, Great Britain.

Gregory, R. P. F. & Raps, S. 1974, *Biochem J.* **142**: 193.

Gruszecki, W. I., Matula, M., Mysliwa-Kurdziel, B., Kernen, P., Krupa Z. & Strzalka, K. *J.* 1997, *Photochem. Photobiol. B: Biol.* **37**: 84.

Gussakovsky, E. E., Barzda, V., Shahak, Y. & Garab, G. 1997, *Photosynth. Res.* **51**: 119.

Gust, D., Moore, T. A., Moore, A. L., Devadoss, C., Liddell, P. A., Hermant, R., Nieman, R. A., Demanche, L. J., DeGraziano, J. M. & Gouni, I. 1992, *J. Am. Chem. Soc.* **114**: 3590.

Horton, P., Ruban, A. V., Rees, D., Pascal, A. A., Noctor, G. & Young, A. J. 1991, *FEBS Lett.* **292**: 1.

Horton P. & Ruban, A. V. 1992, *Photosynth. Res.* **34**: 375.

Horton, P., Ruban, A. V. & Walters, R. G. 1996, *Annu. Rev. Plant Physiol. Plant Mol. Biol.* **47**: 655.

Ide, J. P., Klug, D. R., Kühlbrandt, W., Giorgi, L. B. & Porter, G. 1987, *Biochim. Biophys. Acta*, **839**: 349.

Jansson, S. & Gustaffson, P. 1990, *Plant Mol. Biol.* **14**: 287.

Jansson, S. 1994, *Biochim. Biophys. Acta* **1184**: 1.

Jávorfi, T., Garab, G. & Naqvi, K. R. 1999, *Spectrochim. Acta A* **56**: 211.

Jávorfi, T. & Naqvi, K. R. 1999, in *Spectroscopy of Biological Molecules: New Directions* (Greve, J., Puppels, G.J. & Otto C. eds.), pp. 159-160, Kluwer Academic Publishers, The Netherlands.

Jennings, R. C., Garlaschi, F. M. & Zucchelli, G. 1991, *Photosynth. Res.* **27**: 57.

Jennings, R. C., Zucchelli, G., Bassi, R., Vianelli, P. & Garlaschi, F. M. 1994, *Biochim. Biophys. Acta* **1184**: 279.

Jhutti, C. S., **Jávorfi, T.**, Merzlyak, M. N. & Naqvi, K. R. 1998b, in *Photosynthesis: Mechanisms and Effects* (Garab, G. ed.), Vol. 1, pp. 491-494, Kluwer Academic Publishers, The Netherlands.

Keller, D. & Bustamante C. 1986, *J. Chem. Phys.* **84**: 2961.

Kleima, F. J. 1999, PhD Thesis, Vrije Universiteit, Amsterdam, The Netherlands.

Krinsky, N. I. 1979, *Pure and Appl. Chem.* **51**: 649.

Krueger, B. P., Scholes, G. D., Gould, I. R. & Fleming, G. R. 1999, *Phys. Chem. Comm.* 8 (http://www.rsc.org/ej/QU/1999/C9903172/index.htm).

Krupa, Z., Huner, N. P. A., Williams, J. P., Maissan, E. & James, D. R. 1987, *Plant. Physiol.* **84**: 19.

Kühlbrandt, W., Wang, D. N. & Fujiyoshi, Y. 1994, *Nature* **367**: 614.

Kühlbrandt, W. 1994, *Curr. Opin. Struct. Biol.* **4**: 519.

Larsson, U.K., Anderson, J.M. &. Andersson, B. 1987, *Biochim. Biophys. Acta* **894**: 59-68, and 69-75.

Latimer, P. & Rabinowitch, E. 1959, *Arch. Biochem. Biophys.* **84**: 428.

Latimer, P. & Eubanks, C. A. H. 1962, *Arch. Biochem. Biophys.* **98**: 274.

Li, X.-P., Björkman, O., Shih, C., Grossman, A. R., Rosenquist, M., Jansson, S. & Niyogi, K. K. 2000, *Nature* **403**: 391.

Lichtenthaler, H. K. 1987, *Methods in Enzymol.* **148**: 350.

Liddell, P. A., Nemeth, G. A., Lehman, W. R., Joy, A. M., Moore, A. L., Bensasson, R. V., Moore, T. A. & Gust, D. 1982, *Photochem. Photobiol.* **36**: 641.

Mathis, P., Butler, W. L. & Satoh, K. 1979, *Photochem. Photobiol.* **30**: 603.

Melø, T. B., Frigaard, N.-U., Matsuura, K. & Naqvi, K. R. 2000, *Spectrochim. Acta A* **56**: 2001.

Merzlyak, M. N., Kovrizhnikh, V. A. & Kaurov Yu. N. 1983, *J. Chromatog.* **262**: 331.

Merzlyak, M. N. & Naqvi, K. R. 2000, *Photochem. Photobiol., B: Biology* (in press)

Mimuro, M., Nagashima, U., Takaichi, S., Nishimura, Y., Yamazaki, I. & Kato, T. 1992, *Biochim. Biophys. Acta* **1098**: 271.

Moore, A. L., Joy, A., Tom, R., Gust, D., Moore, T. A., Bensasson, R. V. & Land, E. J. 1982, *Science* **216**: 982.

Naqvi, K. R. 1980, *Photochem. Photobiol.***31**: 523.

Naqvi, K. R., Melø, T. B., Bangar Raju, B., **Jávorfi, T.** & Garab, G. 1997a, *Spectrochim. Acta A* **53**: 1925.

Naqvi, K. R., Melø, T. B. & Bangar Raju, B. 1997b, *Spectrochim. Acta A* **53**: 2229.

Naqvi, K. R., Melø, T. B., Bangar Raju, B., **Jávorfi, T.**, Simidjiev, I. & Garab, G. 1997c, *Spectrochim. Acta A* **53**: 2659.

Naqvi, K. R. 1998a, *Spectrosc. Lett.* **31**: 147.

Naqvi, K. R. 1998b, in *Photosynthesis: Mechanisms and Effects* (Garab, G., ed.), Vol. 1, pp. 265–270 Kluwer Academic Publishers, The Netherlands.

Naqvi, K. R., **Jávorfi, T.**, Melø, T. B. & Garab, G. 1999, *Spectrochim. Acta A* **55**: 193.

Nechustai, R., Thornber, J. P. Patterson, L. K. Fessenden, R. W. & Levanon, H. 1988, *J. Phys. Chem.* **92**: 1165.

Noctor G. et al. 1991, *Biochim. Biophys. Acta* **1057**: 320.

Nussberger, S., Dörr, K., Wang, D. N. & Kühlbrandt, W. 1993, *J. Mol. Biol.* **234**: 347.

Osuka, A. & Kume,T. 1998, *Tetrahedron Lett.* **39**: 655.

Osuka, A., Kume, T., Haggquist, G., **Jávorfi, T.**, Lima, J. C., Melo, E. & Naqvi, K. R. 1999, *Chem. Phys. Lett.* **313**: 499.

Owens, T. G., Shreve, A. P. & Albrecht, A. C. 1992, in *Research in Photosynthesis* (Murata, N. ed.), Vol. I, pp. 179-186, Kluwer Academic Publishers, The Netherlands.

Paulsen, H., Rümler, U. & Rüdiger, W. 1990, *Planta* **181**: 204.

Peterman, E. J. G., Dukker, F. M., van Grondelle, R. & van Amerongen, H. 1995, *Biophys. J.* **69**: 2670.

Peterman, E. J. G., Gradinaru, C. C., Calkoen, F., Borst, J.C., van Grondelle, R. & van Amerongen, H. 1997, *Biochemistry* **36**: 12208.

Phillip D., Ruban, A. V., Horton, P., Asato, A. & Young, A. J. 1996, *Proc. Natl. Acad. Sci. USA* 93: 1492.

Plumley, F. G. & Schmidt, G. W. 1987, *Proc. Natl. Acad. Sci. USA* **84**: 146.

Polivka, T., Herek, J., Zigmantas, D., Åkerlund, H.-E. & Sundström V. 1999, *Proc. Natl. Acad. Sci. USA* **96**: 4914.

Ruban, A. V. & Horton, P. 1992, *Biochim. Biophys. Acta* **1102**: 30.

Salisbury, F. B. & Ross, C. W. 1992, in *Plant Physiology* (fourth edition) 218. Wadsworth Publishing Company, USA

Siefermann-Harms, D. & Ninnemann, H. 1982, *Photochem. Photobiol.* **35**: 719.

Siefermann-Harms, D. 1985, *Biochim. Biophys. Acta* **811**: 325.

Simidjiev, I., Barzda, V., Mustárdy, L. & Garab, G. 1997, *Anal. Biochem.* **250**: 169.

Simidjiev, I. 1998. PhD Thesis, József Attila University, Szeged, Hungary.

Simidjiev, I., Stoylova, S., Amenitsch, H., **Jávorfi, T.**, Mustárdy, L., Laggner, P., Holzenburg, A. & Garab, G. 2000, *Proc. Natl. Acad. Sci. USA* **97**: 1473.

Slovacek, R. E. & Hind, G. 1977 *Plant Physiol.* **60**: 538.

Strickler, S. J. & Berg, R. A. 1962, *J. Chem. Phys.* **37**: 814.

Tosic, J. & Moore, T. 1945, *Biochem. J.* **39**: 498.

Trinkunas, G., Connelly, J. P., Müller, M. G., Valkunas, L. & Holzwarth, A. R. 1997, *J. Phys. Chem.* **101**: 1902.

van der Vos, R., Carbonera, D. & Hoff, A. J. 1991, *Appl. Magn. Res.* **2**: 179.

van der Vos et al., R., Franken, E. M.. & Hoff, A. J. 1994, *Biochim. Biophys. Acta* **1188**: 243.

Walters R. G. & Horton, P. 1991, *Photosynth. Res.* **27**: 121.

Wolff, Ch. & Witt, H. T. 1969, *Z. Naturfor.* **24b**: 1031.

Yamamoto H. Y. 1979, *Pure Appl. Chem.* **51**: 639.

Young, A. J. & Frank, H. A. 1996, *J. Photochem. Photobiol. B: Biol.* **36**: 3.